Evolution of the Tyrone ophiolite, Northern Ireland, during the Grampian-Taconic orogeny: A correlative of the Annieopsquotch Ophiolite Belt of central Newfoundland?

S. P. Hollis[1,2], M. R. Cooper[3], S. Roberts[1], G. Earls[4], R. Herrington[5], D. J. Condon[6] and J. S. Daly[7]

[1]*Ocean and Earth Science, National Oceanography Centre Southampton, University of Southampton, Waterfront Campus, European Way, Southampton, SO14 3ZH, UK*

[2]*CSIRO Earth Science and Resource Engineering, 26 Dick Perry Avenue, Kensington, Western Australia, 6151 (email steven.hollis@csiro.au)*

[3]*Geological Survey of Northern Ireland, Colby House, Stranmillis Court, Malone Lower, Belfast, BT9 5BJ, UK*

[4]*16 Mill Road, Ballygowan, Newtownards, Co. Down, BT23 6NG, UK*

[5]*Department of Mineralogy, Natural History Museum, London, SW7 5BD, UK*

[6]*NERC Isotope Geosciences Laboratory, British Geological Survey, Kingsley Dunham Centre, Keyworth, Nottingham, NG12 5GG, UK*

[7]*UCD School of Geological Sciences, University College Dublin, Belfield, Dublin 4, Ireland*

Keywords: Obduction, Caledonian - Appalachian, Grampian – Taconic, ophiolite

ABSTRACT

The Tyrone Plutonic Group of Northern Ireland represents the upper portions of a tectonically dissected suprasubduction zone ophiolite accreted to the composite Laurentian margin during the Middle Ordovician. Understanding its development and relationship to the Tyrone Central Inlier, an outboard fragment of relatively high-grade, peri-Laurentian continental crust, is essential for reconstructing the closure of the Iapetus Ocean. The Tyrone Plutonic Group is composed of tectonised layered, isotropic and pegmatitic gabbros, sheeted dolerite dykes and rare pillow lavas. New U-Pb zircon TIMS geochronology has yielded an date of 483.68 ± 0.81 Ma from pegmatitic gabbro. Geochemical characteristics, Nd and Sr isotope systematics, and zircon inheritance indicate the Tyrone Plutonic Group formed above a N-dipping subduction zone, by the propagation of a spreading centre into a microcontinental block. Syn-kinematic, calc-alkaline tonalitic to granitic material preserved in the contact zone between the Tyrone Plutonic Group and the Tyrone Central Inlier has produced pressure estimates of 2.3-4.0 ± 0.6 kbar and temperatures of 525-610 °C. Coeval arc-ophiolite accretion at *ca.* 470 Ma may explain how sillimanite-grade metamorphic conditions were reached locally in the underlying Tyrone Central Inlier. Strong temporal, geochemical and lithological similarities exist with the Annieopsquotch Ophiolite Belt of Newfoundland.

INTRODUCTION

Ophiolites represent fragments of upper mantle and oceanic crust incorporated into continental margins during continent-continent and arc-continent collisions, ridge-trench interactions and/or subduction-accretion events (references in Dilek & Furnes 2011). Following the Penrose definition (Anonymous 1972) and establishment of the plate tectonic theory, a paradigm shift occurred for ophiolite genesis between the early 1970s and mid 1980s, when it was recognized that most have geochemical similarities to island-arcs (e.g. Miyashiro 1973; Harper 1984). Consequently, the ophiolite concept moved toward a magmatic origin in subduction zone settings (suprasubduction zone ophiolites; e.g. Pearce *et al.* 1984). Suprasubduction zone ophiolites are interpreted to form in arc-forearc or backarc settings at convergent margins shortly before orogenesis (Dilek & Furnes 2011). Common within many Early Palaeozoic orogens, such as the Caledonian, Appalachian, and Uralian belts, suprasubduction zone ophiolites often mark the location of subduction sutures within short-lived collision zones and can therefore provide essential information on the closure of ancient ocean basins and their temporal evolution (e.g. Dewey 2005).

The Grampian-Taconic phase (*ca.* 475-465 Ma) of the Caledonian-Appalachian orogen (Fig. 1) resulted from the progressive accretion of a diverse set of arc terranes, ribbon-shaped microcontinental blocks and oceanic tracts to the Laurentian margin during the Early Palaeozoic closure of the Iapetus Ocean (Draut *et al.* 2004; van Staal *et al.* 2007; Cooper *et al.* 2011). In the British and Irish Caledonides, deformed and metamorphosed Neoproterozoic to Early Palaeozoic rocks of the Dalradian Supergroup represent cover sequences of the Laurentian margin (Chew 2009). Recent advances, including new fieldwork, geochemistry, U-Pb zircon and Ar-Ar geochronology (e.g. Chew *et al.* 2008, 2010; Flowerdew *et al.* 2009; Cooper *et al.* 2008, 2011; Hollis *et al.* 2012, companion publication), revealed that the Grampian orogeny was more complex than previously thought. Three main episodes of arc-ophiolite emplacement are recognized within the Newfoundland Appalachians, during the equivalent Taconic orogeny (van Staal *et al.* 2007). Although potential correlatives to each of the *ca.* 510-500 Ma Lushs Bight Oceanic Tract, *ca.* 490-470 Ma Baie Verte Oceanic Tract/Snooks Arm arc, and *ca.* 480-460 Ma Annieopsquotch Accretionary Tract of the Newfoundland Appalachians have been suggested in the British and Irish Caledonides (e.g. van Staal *et al.* 1998; Chew *et al.* 2010; Cooper *et al.* 2011; Hollis *et al.* 2012), a number of specific terrane correlations remain contentious.

In the Newfoundland Appalachians, the presence of outriding microcontinental blocks was invoked to explain both: (i) discrepancies between the timing of syntectonic sedimentation and tectonic loading on the passive continental margin at *ca.* 475 Ma and ophiolite emplacement prior to *ca.* 488 Ma (see Waldron & van Staal 2001); and (ii) the range of ages for Iapetan ophiolites accreted to the Laurentian margin (van Staal *et al.* 2007). Recent work from the British and Irish Caledonides has similarly demonstrated that subduction and the onset of obduction occurred at least *ca.* 15 Ma before the Grampian orogeny (Chew *et al.* 2010). Consequently, understanding the relationship between suprasubduction zone ophiolites and any peri-Laurentian microcontinental blocks within the Caledonides (such as the Tyrone Central Inlier and Slishwood Division; Flowerdew *et al.* 2009, Chew *et al.* 2010; Hollis *et al.* 2012) is vital for reconstructing the progressive closure of the Iapetus Ocean.

The Tyrone Plutonic Group of Northern Ireland (Fig. 2) represents the upper parts of a tectonically dissected ophiolite sequence (Hutton *et al.* 1985) accreted onto an outboard segment of Laurentia, the Tyrone Central Inlier, during the Ordovician (Cooper & Mitchell 2004). Opinions on the timing of its formation, emplacement and relationship to both the Tyrone Volcanic Group (a peri-Laurentian island arc) and the Tyrone Central Inlier (a peri-Laurentian microcontinental block; Chew *et al.* 2008, 2010) have varied (e.g. Angus 1970; GSNI 1879; Hutton *et al.* 1985; Cooper & Mitchell 2004; Cooper *et al.* 2008; Chew *et al.* 2008; Draut *et al.* 2009; Cooper *et al.* 2011; Hollis *et al.* 2012). Recent U-Pb zircon geochronology has dated LREE-depleted layered olivine gabbro from the Tyrone Plutonic Group to 479.6 ± 1.1 Ma (Cooper *et al.* 2011), which is significantly younger than previous geochronology from the ophiolite (493 ± 2 Ma: Draut *et al.* 2009) and other ophiolites preserved in the British and Irish Caledonides. For example, the Deer Park Complex of western Ireland, the Scottish Highland Border Ophiolite and the Shetland Ophiolite have yielded considerably older ages of 514 ± 3 Ma, 499 ± 8 Ma and 492 ± 3 Ma respectively (Spray & Dunning 1991; Chew *et al.* 2010). Only the Ballantrae Ophiolite Complex of Scotland has produced a similar U-Pb zircon age of 483 ± 4 Ma (Bluck *et al.* 1980).

Here we present the interpreted results of high-resolution airborne geophysics, whole rock and mineral geochemistry (including new Nd- and Sr-isotope constraints), and key field relationships across the region, in addition to a new U-Pb zircon age for a pegmatitic gabbro from the Tyrone Plutonic Group. These new data suggest that the *ca.* 484-479 Ma Tyrone Plutonic Group was emplaced relatively late in the Grampian orogeny at *ca.* 470 Ma, coeval

with the accretion of the Tyrone arc (=Tyrone Volcanic Group, see Cooper *et al.* 2011), and is therefore broadly equivalent to the Annieopsquotch Ophiolite Belt of Newfoundland. The relations between the accretion of oceanic rocks and sillimanite-grade metamorphism in the underlying Tyrone Central Inlier will be discussed.

FIELD RELATIONSHIPS

The Tyrone Plutonic Group is exposed across approximately 95 km^2 of counties Tyrone and Londonderry, Northern Ireland. It crops out predominantly SE of the Tyrone Central Inlier, and to a lesser extent to the NW around Davagh Forest in faulted contact with the Tyrone Volcanic Group (Fig 2). The Tyrone Plutonic Group consists mainly of variably tectonised and metamorphosed, layered, isotropic and pegmatitic gabbros, sheeted dolerite dykes and rare pillow lavas which were thrust over the Tyrone Central Inlier during the Middle Ordovician (Hutton *et al.* 1985; Cooper & Mitchell 2004) (Fig. 2). Primary mineral assemblages in the Tyrone Plutonic Group have been altered to epidote-amphibolite metamorphic assemblages (Merriman & Hards 2000). Mafic minerals have been replaced by hornblende, epidote, actinolite and/or chlorite, with feldspars variably sericitised. Groundmass often comprises a mixture of quartz, amphibole, actinolite, chlorite and epidote, as well as less abundant zircon, titanite, sericite, biotite, and locally carbonate. Although the Tyrone Plutonic Group is tectonically dissected and poorly exposed, several key localities preserve a relatively complete upper crustal ophiolite sequence (Hutton *et al.* 1985). The following zones have been recognised (adapted after GSNI 1879; Hutton *et al.* 1985).

Layered and isotropic gabbros: Layered and isotropic gabbros comprise the majority of the Tyrone Plutonic Group and are best exposed at Scalp Hill and eastwards through Cregganconroe and Craignagore (Fig. 2). Olivine gabbros at Scalp Hill display cumulate layering, locally differentiated into compositionally distinct bands (cm to m scale) (Cobbing, 1969; GSNI 1879). Locally gabbro may be deformed to hornblende schist, with schistosity parallel to mineral layering in surrounding rocks (Cooper & Mitchell 2004). Cooper *et al.* (2011) reported a U-Pb zircon age of 479.6 ± 1.1 Ma for layered gabbro from Scalp Hill. Layered magnetite gabbro is common around Scalp and immediately NW of the Craigballyharky Complex (GSNI 1879).

Layered and isotropic gabbros at several localities appear to be younger than an early suite of dolerites ('Early Dolerites and Gabbros': BGS 1986). At Craignagore, a central gabbro

intrudes early, fine to medium grained amphibolite-facies dolerite (Angus 1970). Exposures of dolerite surrounding the gabbro are generally foliated or schistose amphibolites; with a finely crystalline relic of pyroxene-hornfels exposed at one locality (Angus 1970). The gabbro is largely uniform and porphyritic adjacent to its southern contact, and is itself cut by a later series of dolerite dykes (equivalent to the 'Ophitic Dolerites of Carrickmore' of BGS 1986).

Transition Zone: At Black Rock (Fig. 2), coarse-grained hornblende gabbro intrudes, and contains xenoliths of, an early-formed suite of dolerite (the 'Early Dolerites and Gabbros' of BGS 1986). This sequence is in turn intruded by younger 1-2 m wide, basalt and dolerite dykes (Cooper & Mitchell 2004) (Fig. 3a-b). Early basaltic and dolerite dykes are deformed, locally schistose and extensively altered with fine stringers of epidote. Gabbro is extremely coarse grained, ranging from equigranular in nature to pegmatitic. Irregular veins of pegmatitic gabbro contain large hornblende and plagioclase crystals often exceeding 2 cm in diameter (rarely > 8 cm). The youngest suite of basaltic and doleritic dykes at Black Rock are relatively undeformed and less extensively altered. Porphyritic varieties contain 1-2 mm rounded and angular laths of plagioclase in a fine-grained, ophitic or intergranular matrix.

At Oritor (Fig. 2), dolerite dykes intrude gabbro, which contain xenoliths of an earlier foliated dolerite. Dolerite dykes typically trend NW-SE and can be distinguished from Palaeogene olivine-bearing dykes by their composition and state of alteration; the former always being extensive uralitised (Hartley 1933). At Slaghtfreeden (Fig. 2), isotropic and pegmatitic gabbro, microgabbro and dolerite also contain xenoliths of foliated basalt. These are intruded by, and present as xenoliths in, late intrusive rocks of quartz and hornblende porphyritic diorite (Fig. 3c). Late ophitic dolerite dykes are also present at Carrickmore, Cregganconroe and Craignagore (Fig. 2) which cut olivine gabbro and/or poikiloblastic hornblende gabbro.

Sheeted Dykes: Although the presence of ophitic dolerite at Carrickmore was recognized by Hartley (1933), it was Hutton *et al.* (1985) who first reported the presence of parallel sheeted dolerite dykes in Carrickmore Quarry (Fig. 2). The sheeted dykes typically average 1 m in thickness, intrude one another forming two-sided chilled margins and more commonly one sided chilled margins and can locally constitute 100 % of the exposure (Hutton *et al.* 1985). Dolerite at Carrickmore appears aphanitic in hand specimen, though may be either

intergranular or ophitic in thin section. In Craigballyharky Quarry, dolerite dykes display rare chilled margins and are intruded by relatively undeformed plagiogranite and aplite (Fig. 3d).

Pillow basalts and volcaniclastic rocks: Pillow lavas are scarce within the Tyrone Plutonic Group, and are best exposed as a series of roof-pendants within the Craigballyharky complex (Cobbing *et al.* 1965). Pillow structures at Craigballyharky typically range between 30 and 75 cm in diameter (Fig. 3e). These lavas are aphanitic, subalkaline, tholeiitic, LILE and LREE-depleted and of suprasubduction affinity (Draut *et al.* 2009; Cooper *et al.* 2011, see geochemistry). Intermediate and basic lavas have also been reported to occur at Scalp and Oritor (Hartley 1933), with amygdaloidal lavas present SW of Scalp Hill. At Slaghtfreeden, Hartley (1933) noted a sheet of gabbro intruding lavas overlain by coarse breccias and tuffs. This sequence was subsequently intruded by a dolerite dyke that contains xenocrysts of hornblende derived from the gabbro.

Craigballyharky complex: The Craigballyharky complex (Cobbing *et al.* 1965; GSNI 1879) is exposed across approximately 3.5 km^2 (Fig. 2) and is composed of three major units: an intrusion of tonalite representing the summit of Craigballyharky (472 $^{+2}/_{-4}$ Ma of Hutton *et al.* 1985; 470.3 ± 1.9 Ma of Cooper *et al.* 2011), an intrusion of biotite-granodiorite representing the summit of Craigbardahessiagh (464.9 ±1.5 Ma of Cooper *et al.* 2011), and quartz-diorite (see Angus 1962, 1977). A series of roof pendants exposed across the complex include siliceous ironstone possibly derived from the Tyrone Volcanic Group, and isotropic gabbros, dolerites and pillow lavas from the Tyrone Plutonic Group (Cobbing *et al.* 1965). Siliceous ironstone xenoliths have been recorded in both the Craigbardahessiagh granodiorite and Craigballyharky tonalite (GSNI 1879). Together, these roof pendants, coupled with xenocrystic Proterozoic zircons, imply both the Tyrone Volcanic Group and Tyrone Plutonic Group were in their present structural position above the Tyrone Central Inlier prior to *ca.* 470 Ma (Cooper *et al.* 2011). Occurrences of agglomerate, limestone and silicified metasedimentary rocks have also been reported (Cobbing *et al.* 1965; GSNI 1879), though were not observed during recent fieldwork.

Quartz diorite is widely regarded to be hybrid in origin (Angus 1962, 1977), produced by magma mixing and mingling between arc-related gabbro and *ca.* 470 Ma tonalite at Craigballyharky (Hutton *et al.* 1985; Cooper *et al.* 2011). Although recent dating reported an age of 493 ± 2 Ma for Craigballyharky gabbro (Draut *et al.* 2009), Cooper *et al.* (2011)

presented a recalculated mean $^{206}Pb/^{238}U$ age of 473.2 ±1.6 Ma for this unit, significantly younger and in agreement with field-relations and its relatively unaltered and undeformed nature. Consequently, the Craigballyharky gabbro is attributed to the younger *ca.* 470-464 Ma arc related intrusive suite (see following), consistent with its LILE and LREE-enriched geochemical characteristics (figure 5 of Draut *et al.* 2009; Cooper *et al.* 2011). Late arc-related gabbro also intrudes the c. 475-469 Ma Tyrone Volcanic Group at Beaghbeg and Mweenascallagh (Fig. 2), although the latter is of eMORB affinity (Hollis *et al.* 2012). At Craigballyharky, magma mixing and mingling within a hybrid quartz diorite is seen in outcrop where large quartz ocelli are observed to have migrated from the tonalite into gabbro. Contacts are typically diffuse and irregular, though may locally be sharp (Fig. 3f).

Arc-related intrusive suite: The arc-related intrusive suite includes a series of high-level plutons, sills and dykes of various compositions, which intrude all levels of the Tyrone Igneous Complex (Fig. 2). Large intrusions of diorite, granodiorite, tonalite, biotite- and hornblende-bearing granite, and quartz ± feldspar porphyry are the most frequent; although minor occurrences of arc-related gabbro and dolerite also occur (Hollis *et al.* 2012). Field relationships and published U-Pb geochronology (Cooper *et al.* 2011) are consistent with the intrusions being significantly younger than the Tyrone Plutonic Group (*ca.* 470-464 Ma). For example, diorite at Lough Lily (Fig. 2) contains angular xenoliths of ophiolite-derived dolerite and intrudes the latter as veins (Hartley 1933). At Scalp, coarsely crystalline, pink and grey hornblende-rich tonalite (equivalent to the Golan Burn tonalite of Cooper *et al.* 2011: 469.9 ± 2.9 Ma) contains xenoliths of gabbro which show all stages of assimilation and the development of hybrid granite (GSNI 1879). At Black Rock, xenoliths of amphibolite-facies gabbro are present within LREE-enriched arc-related quartz ± biotite ± hornblende porphyry. Diorite at Crooked Bridge displays a magma mixing-mingling relationship with hornblende-granite and has produced an age of 469.58 ± 0.77 Ma (see Hollis *et al.* companion publication).

Tremoge Glen: Medium to coarse grained and pale-grey to pink granite exposed at Tremoge Glen is unusual within the Tyrone Igneous Complex as it is extensively altered, intensely sheared and muscovite-bearing. Geological mapping reveals the granite intrudes gabbros of the Tyrone Plutonic Group and is itself intruded by NE and NW trending late Fe-Ti enriched basaltic/doleritic dykes with ophitic textures (GSNI 1879; Fig. 2). The Tremoge Glen intrusion occurs as a NE-SW orientated wedge of granite bound on its eastern side by the

Tempo – Sixmilecross Fault (Fig. 2). These dykes appear to be related to the younger *ca*. 475-469 Ma Tyrone Volcanic Group (see following).

OPHIOLITE CONTACT: BLAEBERRY ROCK

A high strain zone of mylonitic metamorphosed igneous rocks E of Davagh Forest was discovered at the mapped contact between the Tyrone Central Inlier and Tyrone Plutonic Group (Fig. 2). The exposure, known locally as Blaeberry Rock, consists of a 7 x 6 x 3 m block and several smaller boulders (Fig. 4a). The main exposure comprises cm- to dm-sized blocks of amphibolite-facies gabbroic to doleritic material within an intimate mixture of mm- to cm- scale banded and isoclinally folded syn-kinematic tonalitic to granitic material, amphibolite and possible Dalradian metasedimentary rocks (Fig. 4b-e). Nearby exposures include smaller angular blocks of gabbro and dolerite which display preserved chilled margins and patchy outcrops of quartzofeldspathic paragneisses of the Tyrone Central Inlier invaded by tonalitic intrusive sheets, leucosomes and pegmatite. Younger moderately deformed tonalitic to granitic veins cut the sheared rocks and are themselves often folded and boudinaged.

Preferential localization of strain appears to be confined to the intrusive sheets, with gabbroic inclusions relatively undeformed except for some alignment of amphibole crystals. Large amphibole crystals up to 3.5cm in length occur within the melt network and appear to be derived from brecciated bodies of gabbro cut by thin veins. These crystals, along with minor drag folds, show evidence for sinistral shearing (Fig. 4f). Paler grey andesitic (?) clasts (~10 x 20 cm) also contain a well-developed mineral stretching lineation. Narrow shear zones and late veins of epidote cut the exposure.

Gabbroic and doleritic blocks exposed within the Blaeberry Rock contact are petrologically and geochemically (see following) similar to those from the Tyrone Plutonic Group. These ophiolite-derived lithologies have experienced amphibolite facies metamorphism and are composed of actinolite (after pyroxene) and plagioclase replaced by white-mica, chlorite and epidote (Supplementary Material: Fig. 4g-j). Syn-kinematic and late tonalitic to granitic veins are composed of quartz, orthoclase, sericitised labradorite with minor muscovite, trace biotite and accessory phases (fluorapatite and sphene). Plagioclase may be internally altered to chlorite, epidote and muscovite (Supplementary Material: Fig. 4g-j).

TELLUS AIRBORNE GEOPHYSICS

During 2005-2006 the Tellus airborne geophysical survey, part of the Tellus Project (see GSNI 2007), was flown across the entirety of Northern Ireland. Magnetic, radiometric and electromagnetic (EM) data were acquired. Further detail on survey specification and geophysical data processing are provided within Gunn *et al.* (2008). Interpreted EM and total magnetic intensity (analytic signal) maps over the Tyrone Plutonic Group are shown in Figure 5. Lithologies of the Tyrone Plutonic Group are clearly distinguishable from the non-magnetic units of the Tyrone Central Inlier. Faulted contacts between the Tyrone Plutonic Group, Tyrone Volcanic Group, Tyrone Central Inlier and post-Ordovician cover sequences are best discriminated by EM imagery, (Fig. 5a) with boundaries corresponding well to previous mapping (GSNI 1879, 1995). The Tyrone Plutonic Group is characterised by short-wavelength magnetic anomalies (Gunn *et al.* 2008), with magnetic highs corresponding to areas of magnetite-bearing dolerite and gabbro. Magnetic imagery reveals the Tyrone Plutonic Group to be dissected into thin slices by a series of NE-SW orientated Caledonian faults (Fig. 5b). Magnetic lows within the Tyrone Plutonic Group are associated with deep seated granitic plutons of the *ca.* 470-464 Ma arc-related intrusive suite (e.g. Pomeroy granite) and demagnetized zones associated with faulting (e.g. Tempo-Sixmilecross; Fig. 2). Tonalitic and granodioritic plutons at Craigballyharky and Craigbardahessiagh, may represent thin laccoliths underlain by highly magnetic material. Along the eastern side of the Tyrone Central Inlier where gneissose psammites and semipelites crop out, highly-magnetic lithologies appear to be present. Although it is possible a portion of the Tyrone Plutonic Group structurally underlies the Tyrone Central Inlier, these magnetic rocks may also represent mafic volcanics associated with the rifting of the Tyrone Central Inlier from the Laurentian margin or buried basement material.

WHOLE ROCK GEOCHEMISTRY

Sampling and Analytical Techniques

Eighteen samples were collected from key localities across the Tyrone Plutonic Group and Blaeberry Rock for whole-rock geochemical analysis. Major-elements and trace-elements were determined for powdered whole-rock samples on fused glass beads and powder pellets by X-ray fluorescence at the University of Southampton. Rare earth-elements (plus Nb, Hf, Ta, Th, U) were determined by inductively coupled plasma mass spectrometry (ICP-MS) on the same samples using HF/HNO_3 digest. Further detail is provided in Hollis *et al.* (2012).

311 Geochemical analyses of Draut *et al.* (2009) and Cooper *et al.* (2011) are also included.
312 Results are presented as Supplementary Material (Table 1).
313
314 Two samples were analysed at Southampton for Sr isotopes (Supplementary Material Table
315 1). Strontium was separated using approximately 80µl columns containing Sr-Spec resin and
316 elution with 3M HNO_3 to remove interfering elements. The purified Sr samples were
317 collected with water and loaded onto a single Ta filament using a Ta activator solution.
318 Samples were run using a multi dynamic peak jumping routine on a VG Micromass Sector 54
319 thermal ionization mass spectrometer (TIMS) at the University of Southampton. Rb and Sr
320 concentrations were obtained by ICP-MS. The ratios were corrected using an exponential
321 fractionation correction relative to $^{86}Sr/^{88}Sr$ of 0.1194. NIST-987 was run and its long term
322 average $^{87}Sr/^{86}Sr$ value was 0.710243 ± 18 (2sd n=93). An age correction was performed to
323 account for radioactive decay and ingrowth of ^{87}Sr; values for that time are reported as
324 $^{87}Sr/^{86}Sr_i$. Modern CHUR was taken to be 0.7045 and 0.0827 for $^{87}Sr/^{86}Sr$ and $^{87}Rb/^{86}Sr$
325 respectively. The decay constant of ^{87}Sr is 1.42×10^{-11} yr^{-1}.
326
327 Four samples were analysed for Sm-Nd and Rb-Sr by isotope dilution thermal ionisation mass
328 spectrometry at University College Dublin (Supplementary Material Table 1). Samples were
329 weighed and spiked prior to digestion in HF-NNO_3 in teflon bombs at temperatures up to
330 180°C, following initial treatment with cold, followed by hot, HCl, to remove any carbonates
331 present. Standard ion chromatography separation procedures used Eichrom ion specific
332 resins (Sr Resin for Sr, TRU Resin SPS for the REE as nitrates) and a Biorad cation exchange
333 resin (AG 50W-X12 for Rb as chloride). Sm and Nd were separated from one another as
334 chlorides using Eichrom Ln Resin SPS. Sm, Nd and Sr isotopic analyses were carried out on
335 a ThermoScientific Triton multiple collector thermal ionization mass spectrometer. Analyses
336 were carried out in static multicollection mode, with switching of amplifiers between Faraday
337 collectors to correct for differential amplifier responses. All Nd peaks were measured, along
338 with ^{149}Sm and ^{152}Sm to correct for isobaric interference from Sm. In practice, this correction
339 was negligible (for example <2 ppm on $^{143}Nd/^{144}Nd$ ratios). The La Jolla standard yielded a
340 value of $^{143}Nd/^{144}Nd = 0.511842 \pm 5$ (2sd, n=24) during the period of this work. The
341 uncertainty in $^{147}Sm/^{144}Nd$ is estimated to be 0.1%. Sr aliquots were measured on single Ta
342 filaments using a Ta activator solution. At UCD, the SRM987 standard yielded a value of
343 $^{87}Sr/^{86}Sr = 0.710247 \pm 11$ (2sd, n= 25), indistinguishable from that obtained at Southampton.
344 $^{87}Rb/^{85}Rb$ ratios were measured on a ThermoScientific Neptune multiple collector inductively

coupled plasma mass spectrometer on solutions doped with zirconium and corrected for mass bias using the measured $^{90}Zr/^{91}Zr$ ratio, assuming a natural $^{90}Zr/^{91}Zr$ ratio of 4.588, following Nebel et al. (2005).

Element Mobility

Various studies have demonstrated that most of the major elements (e.g. SiO_2, Na_2O, K_2O, CaO, MgO) and the low field strength elements (LFSE: Cs, Rb, Ba, Sr, except Th) are mobile during metamorphism and hydrothermal alteration (references in Dilek & Furnes 2011). As primary mineral assemblages within the Tyrone Plutonic Group have been metamorphosed to amphibolite facies conditions only elements demonstrated to be immobile are used to elucidate petrogenesis and tectonic affinities. Comparison of the major and trace element data from the Tyrone Plutonic Group to Zr (assumed immobile) confirms this mobility, with considerable scatter for Na_2O, K_2O, Sr and Ba in particular (Hollis 2013). TiO_2, MgO, P_2O_5, Th, Nb, V, Cr, Co, Sc Y, U and the REEs appear to have remained immobile. SiO_2 appears to have remained relatively immobile, apart from minor silicification in some samples. Al_2O_3/Na_2O ratios vary between 2.3 and 23.9 (Fig. 6a). Sampled lithologies show carbonate-chlorite-pyrite index (CCPI: see Large *et al.* 2001) values typical of mafic volcanics (41.1-95.4, most >80 Fig. 6b) and Hashimoto alteration index (AI: Ishikawa *et al.* 1976) values (22.6-51.5) typical of weakly altered rocks. Sericite index values (Saeki & Date 1980; K_2O/K_2O+Na_2O) vary between 0.07 and 0.49. Analyses show a weak negative correlation between Na_2O and LOI, suggesting that lower Na_2O contents are due to losses associated with alteration (e.g. sericitisation).

Petrochemistry

Tyrone Plutonic Group: Immobile element ratios within the Tyrone Plutonic Group are predominantly subalkaline (Nb/Y <0.06) and tholeiitic (Zr/Y 0.7-3.8) (Fig. 6c). On multi-element variation diagrams sampled lithologies display slight LREE depletion (La/Sm 0.6-1.2, Fig. 7a) and flat HREE profiles (Gd/Lu 0.7-1.1, most 1.0-1.1). Th concentrations (i.e. LILE) are similarly low (Th_{CN} 0.76-15.88; Fig. 6d). Aphanitic basaltic rocks classify as island-arc tholeiitic basalts according to Pearce and Cann (1973), Pearce and Norry (1979), Wood (1980), and Meschede (1986). Positive Pb, negative Nb and modest Ti anomalies across the Tyrone Plutonic Group are consistent with formation in a suprasubduction environment (as in Draut *et al.* 2009; Cooper *et al.* 2011) (Fig. 6e-f; 7a). Gabbro and pegmatitic gabbro from Black Rock, Carrickmore and Bonnety Bush display slightly lower

379 Th_{CN}, LREE and HREE concentrations than others sampled from the Tyrone Plutonic Group.
380 Plagiogranite that cuts sheeted dykes at Craigballyharky Quarry is borderline calc-alkaline,
381 and strongly LILE and LREE-enriched (Zr/Y 7.5, La/Yb 6.8, Th_{CN} 166.55) relative to the
382 HREE (Fig. 7).
383
384 Initial $^{87}Sr/^{86}Sr$ ratios were calculated for five samples from the Tyrone Plutonic Group at an
385 age of 480 Ma (after Cooper *et al.* 2011). These yielded $^{87}Sr/^{86}Sr_i$ ratios ranging from
386 0.71064 to 0.70851, and included dolerite dykes from Craigballyharky Quarry (0.71019),
387 Black Rock (0.71064), Carrickmore Quarry (fine-grained dolerite = 0.70874 and coarse-
388 grained dolerite = 0.70851) and a pillowed basalt at Craigballyharky (0.70908). Mobility of
389 Rb and Sr is well documented during seafloor hydrothermal alteration, metamorphism and
390 subsequent weathering (e.g. Jacobsen & Wasserburg 1979). $^{87}Sr/^{86}Sr_i$ ratios obtained from
391 the Tyrone Plutonic Group are comparable to the $^{87}Sr/^{86}Sr$ isotopic composition of Lower to
392 Middle Ordovician seawater (0.7087-0.7090, Young *et al.* 2009), although they range up to
393 slightly more radiogenic values. These slightly higher $^{87}Sr/^{86}Sr_i$ values may suggest the
394 incorporation of some continental material into the source region, which is supported by the
395 presence of inherited zircons in layered gabbros from Scalp (Cooper *et al.* 2011) and Sm-Nd
396 constraints (see following). By contrast, gabbro from Scalp (Fig. 2) has a less radiogenic
397 $^{87}Sr/^{86}Sr_i$ value of 0.70391, suggesting somewhat lesser interaction with seawater, consistent
398 with its likely deeper original position within the ophiolite.
399
400 Previous Nd isotope geochemistry from the Tyrone Plutonic Group is restricted to three
401 samples of Draut *et al.* (2009). Recalculated εNd_t values for an age of 480 Ma (Cooper et al.
402 2011) are: +4.40 (gabbro from Scalp), +5.85 (dolerite from Carrickmore) and +7.43 (gabbro
403 from Carrickmore). New analyses (Table 1) are consistent with these previously published
404 values, and include: +5.30 and +5.33 for fine-grained and coarse-grained dolerite respectively
405 from Carrickmore Quarry, +6.12 from gabbro at Scalp Hill; and +5.33 from pillowed basalt at
406 Craigballyharky. Most of these values are lower than calculated values from the depleted
407 mantle growth curve at 480 Ma (+7.0; DePaolo 1988), suggesting some contamination from
408 continentally-derived material occurred during the formation of the Tyrone Plutonic Group.
409
410 **Blaeberry Rock:** A fine to medium grained doleritic clast collected from Blaeberry Rock is
411 subalkaline (Nb/Y 0.27) and tholeiitic (Zr/Y 0.94; Fig. 6c), relatively LILE-depleted (Th_{CN}
412 15.8) and slightly LREE-depleted relative to the HREE (La/Yb_{CN} 0.93; Fig. 6d-e; 7b). These

geochemical characteristics, in addition to low Ti/V (1.2), and Zr/TiO_2 (91.9), moderate AI (53.2), and high CCPI (94.5), Al_2O_3/Na_2O (12.9) and Gd/Lu ~1 are consistent with derivation from the Tyrone Plutonic Group. Th/Yb-Nb/Yb systematics classifies the clast as similar to eMORB (Fig. 6f). This sample displays a positive Nb anomaly relative to Th and La (Fig. 7b), and a higher Nb/Y ratio than samples typical from the Tyrone Plutonic Group (Fig. 6c). Nb enrichment may be associated with increased alteration (e.g. CCPI).

Samples of tonalitic to granitic intrusive material collected from Blaeberry Rock (SiO_2 59.6-64.4 wt%, Zr/TiO_2 227.9-318.5) are calc-alkaline (Zr/Y 5.8-16.2), strongly LILE-enriched (Th_{CN} 34.7-174.0, Fig. 8c), and display steep LREE profiles (La/Sm 3.3-6.5) relative to the HREE (La/Yb 4.2-16.4) and strong negative Nb anomalies (0.11-0.48) on multi-element variation diagrams (Fig. 7d). These samples geochemically resemble the *ca.* 470-465 Ma tonalites of the Tyrone Igneous Complex (see Cooper *et al.* 2011) which are characterized by high Zr/TiO_2 (154.5-583.8), Zr/Y (5.6-10.5) and La/Sm (4.5-6.8) ratios, Th_{CN} values (154.2-297.0) and pronounced negative Nb anomalies (0.17-0.27, Fig. 7c) (values from Cooper *et al.* 2011; Hollis *et al.* 2012; Hollis 2013). Sampled Dalradian-affinity metasedimentary rocks of the Tyrone Central Inlier from Corvanaghan Quarry and Fir Mountain Quarry (adjacent to Blaeberry Rock: Fig. 2) similarly have steep REE profiles (La/Sm to 7.2, La/Yb to 28.7) and can display pronounced negative Nb anomalies (often due to the presence of melt), but have significantly higher Zr, Rb, Ba, Th_{CN} and REE_{Total} concentrations, and higher Ti/V and Nb/Y ratios (to 0.9) (Hollis 2013).

Tremoge Glen: S-type muscovite granite from Tremoge Glen shows calc-alkaline characteristics (Zr/Y 13.3) is strongly LREE enriched relative to the HREE (La/Yb 18.2), and strongly LILE enriched (Th_{CN} ~325). Samples analyzed have high $K_2O/(K_2O+Na_2O)$ ratios of ~0.6 and are strongly peraluminous (after Shand 1943). The S-type geochemical characteristics suggest it may have been intruded shortly after the emplacement of the Tyrone Plutonic Group from the melting of metasedimentary material of the Tyrone Central Inlier. This is consistent with its high Th_{CN} and LREE enrichment.

A single sample (MRC129) was analysed from the basaltic-doleritic dykes at Tremoge Glen which cut the S-type muscovite granite. This sample is Fe-Ti-enriched (Fe_2O_{3T} 15.4, TiO_2 2.7), lacks a prominent negative Nb anomaly characteristic of island-arc tholeiites (Nb anom 0.82) and is of 'within-plate' or eMORB affinity (e.g. Wood, 1980, Fig. 6b). MRC129 is

subalkaline, calc-alkalic, and LILE and LREE enriched (Nb/Y 0.55, Zr/Y 7.2, La/Yb 4.7, Th_{CN} 107.83). Low Cr (~50ppm) and Ni (~14ppm) confirms the relatively evolved nature of this sample. High LOI (7.06 wt.%), CCPI (87.4), SI (0.31) and AI (50.9) values are consistent with extensive alteration. The small negative Nb anomaly is indicative of a weak subduction signature or may reflect minor crustal contamination.

MINERAL CHEMISTRY

Electron microprobe analyses were completed at the Natural History Museum, London, to determine mineral compositions and establish P-T conditions from the Tyrone Plutonic Group and its contact with the underlying Tyrone Central Inlier. Three samples were analysed; one from pegmatitic gabbro from Black Rock within the 'transition zone' of the Tyrone Plutonic Group (SPH34); and two from Blaeberry Rock (SPH210: gabbroic clast; and SPH215: tonalitic material in the contact). SPH34 from Black Rock is dominated by plagioclase and amphibole (Fig. 4j). Plagioclase is extensively altered along grain boundaries to secondary minerals: epidote, carbonate, white mica, chlorite and residual albite. Amphibole occurs as large anhedral grains of hornblende intergrown with actinolite. Sample SPH210 (gabbroic clast) is similar to SPH34 (collected from Black Rock) and contains amphibole closely associated with epidote and muscovite, and is believed to represent ophiolite-derived material based on mineral chemical and whole rock geochemistry. By contrast, sample SPH215 comprises a mixture of hornblende, quartz, orthoclase, plagioclase, chlorite, epidote and accessory phases (sphene and fluorapatite) from tonalitic layers in the contact (Fig. 4g-h). Spot analyses were performed on a Cameca SX-50 electron microprobe equipped with a wavelength dispersive system, and were conducted at 20 keV and 20 nA. Counting times ranged from 10 to 50 seconds for spot analysis. Data are presented as Supplementary Material (Table 2).

Amphiboles analysed from SPH34 (Black Rock) and SPH210 (Blaeberry Rock clast) chemically classify as tremolitic actinolite and magnesio-hornblende, whereas those analysed from syn-kinematic tonalitic intrusive sheets at Blaeberry Rock (SPH215) classify as magnesio-hornblende with significantly lower Mg/(Mg+Fe) ratios and Si contents, and higher Ti, Fe and Mn concentrations (Fig. 8a). Low TiO_2 (0-0.45 wt.%) and Al_2O_3 (1.74-4.79 wt.%) in amphiboles from Black Rock (SPH34) and from the ophiolite-derived clast at Blaeberry rock (SPH210) plot predominantly just off the geothermometer of Ernst and Liu (1998), producing temperature estimates of c. <500 to 570 °C. Spot analyses from SPH215

amphiboles (tonalite) contain higher TiO_2 (0.35-0.65 wt.%) and Al_2O_3 (6.51-8.54 wt.%) indicating slightly higher temperatures of 525-610 °C. Hammarstrom and Zen (1986) first proposed that solidus pressures of intermediate calc-alkaline plutons can be estimated from the Al content of hornblende. Rocks should be near-solidus with the magmatic assemblage: hornblende + biotite + plagioclase + quartz + sanidine + sphene + magnetite or ilmenite ± epidote. The Al-in-hornblende geobarometer experimentally calibrated by Schmidt (1992) produces pressure estimates of *ca.* 2.3 to 4.0 ± 0.6 kbar for tonalite from Blaeberry Rock.

Epidotes from the Tyrone Plutonic Group typically have lower Fe and Ca, and higher Al, contents than those from Blaeberry Rock. Samples SPH210 and SPH215 are chemically similar, except for higher Si content in SPH215.

Alkali feldspar compositions from Blaeberry Rock sample SPH215 are restricted to a relatively narrow range between $Or_{82.6}Ab_{16.1}An_{1.3}$ and $Or_{96.7}Ab_{3.3}An_0$ (Fig. 8b). BaO and Ce_2O_3 concentrations range between 0.46 and 1.4 wt% and 0.17 and 0.53 wt% respectively. FeO_T concentrations vary between 0.03 and 0.43 wt%. The composition of plagioclase from SPH215 varies from andesine to labradorite ($Or_{0.9}Ab_{59.6}An_{39.4}$ to $Or_{0.7}Ab_{48.0}An_{51.3}$) (Fig. 8b). FeO_T concentrations range between 0.11 and 0.17 wt%.

Chlorites from the Tyrone Plutonic Group are relatively Mg-rich and classify as pycnochlorite (SPH34), whereas those analysed from Blaeberry Rock (SPH215) classify as both pycnochlore and ripidolite and have lower Mg# numbers (Fig. 8c-d). Si concentrations are similar and range between 5.6 and 5.8 apfu (based on 22 oxygens). Fe/(Fe+Mg+Mn) ratios are approximately 0.4 from Blaeberry Rock and 0.25 from the Tyrone Plutonic Group. Al_{IV} concentrations vary between 2.15 and 2.41 apfu. Chlorite geothermometers of Zhang and Fyfe (1995) and Kranidiotis and MacLean (1987) produce temperature estimates of *ca.* 261-274°C and 289-302°C respectively for chlorites from Blaeberry Rock sample SPH215. Similar, temperature estimates were produced from chlorites of Black Rock (SPH34: 261-281°C and 265-288°C respectively). Chlorite temperature estimates most likely reflect retrogression.

U-PB GEOCHRONOLOGY

Analytical Methods: A sample of pegmatitic gabbro from Black Rock was selected for U-Pb zircon geochronology at the NERC Isotope Geosciences Laboratory (NIGL). Zircons were isolated using conventional mineral separation techniques. Prior to isotope dilution thermal ionization mass spectrometry (ID-TIMS) analyses zircons were subject to a modified version of the chemical abrasion technique (Mattinson 2005). Methods are identical to those reported in Hollis *et al.* (2012). Data are presented as Supplementary Material (Table 3). Errors for U-Pb dates are reported in the following format: ±X(Y)[Z], where X is the internal or analytical uncertainty in the absence of systematic errors (tracer calibration and decay constants), Y includes the quadratic addition of tracer calibration error (using a conservative estimate of the standard deviation of 0.1% for the Pb/U ratio in the tracer), and Z includes the quadratic addition of both the tracer calibration error and additional ^{238}U decay constant errors of Jaffey *et al.* (1971).

Results: Six fractions (single grains) were analyzed from the Black Rock sample MRC344 (pegmatitic gabbro). All six analyses are concordant when their systematic $\lambda^{238}U$ and $\lambda^{235}U$ decay constant errors are considered with five analyses forming a coherent single population yielding a weighted mean $^{206}Pb/^{238}U$ date of 483.68 ± 0.36 (0.60)[0.81] Ma (MSWD = 1.8) (Fig. 9). We interpret this as being the best estimate for the age of this sample. This age is slightly older than that produced for layered gabbro from Scalp (479.6 ± 1.1 Ma: Cooper *et al.* 2011). No inherited Proterozoic ages were derived from any of the dated zircon fractions, although zircon selection was biased to avoid morphologies that may have contained inherited cores.

DISCUSSION

Evolution of the Tyrone Plutonic Group

The Tyrone Plutonic Group is composed primarily of layered, isotropic and pegmatitic gabbros, sheeted dolerite dykes and rare pillow lavas (Angus 1970; Hutton *et al.* 1985; Cooper & Mitchell 2004). Geochemical evidence and field relations presented herein are consistent with the Hutton *et al.* (1985) interpretation that the Tyrone Plutonic Group represents the upper portions of a tectonically dissected ophiolite which was accreted to the Laurentian margin during the Grampian orogeny. Multi-element profiles and Nd-isotope compositions are consistent for basalts generated at an oceanic spreading centre above a subduction zone (Draut *et al.* 2009). The new U-Pb zircon geochronology presented here

(483.68 ± 0.81 Ma) is similar to that of Cooper *et al.* (2011: 479.6 ± 1.1 Ma) constraining the formation of the Tyrone Plutonic Group to *ca.* 484-479 Ma. The slightly older age presented here for pegmatitic gabbro from Black Rock is in agreement with its more primitive geochemical characteristics. Pegmatitic gabbro from Black Rock is more LILE, LREE and HREE depleted than layered gabbro from Scalp. It is entirely possible that multiple slices of Iapetan ocean floor of slightly varying age occur within the Tyrone Plutonic Group, as the ophiolite is tectonically dissected.

Field relationships across the ophiolite are consistent with several phases of intrusive activity typical of oceanic spreading centres. Poor preservation of the sheeted dyke complex is typical of suprasubduction zone ophiolites in general; with large well-developed complexes requiring an appropriate balance between spreading and magma supply rates (references in Robinson *et al.* 2008). In contrast to fast-spreading Mid Ocean Ridges, where these conditions are maintained, suprasubduction zone spreading rates are not directly controlled by magma supply but are ultimately dependent on slab rollback, which is related to the angle of subduction and the rate of convergence (Robinson *et al.* 2008). The absence of a thick ultramafic section within the Tyrone Plutonic Group may be explained by post-tectonic excision or more likely by delamination and subduction of the lower crust during ophiolite emplacement (e.g. Annieopsquotch Ophiolite Belt; Zagorevski *et al.* 2009). Limited occurrences of ultramafic material may be present around Davagh Forest, where "basic and ultrabasic rocks, often pyroxenitic" have been described (see Gunn *et al.* 2008), closely associated with elevated PGE, Cr and Ni soil anomalies.

Fe-Ti enriched basaltic dykes which intrude S-type muscovite granite at Tremoge Glen have a within-plate affinity and lack a pronounced island-arc geochemical signature. High LILE and LREE-enrichment, coupled with low Cr and Ni, is indicative of their more evolved nature compared to other samples from the Tyrone Plutonic Group. Fe-Ti-enriched basalts are defined by >12 wt% FeO_T and >2 wt% TiO_2 (e.g. Sinton *et al.* 1983), and typically display lower concentrations of MgO, CaO and Al_2O_3 than normal MORB. Fe-Ti basalts are common in propagating rifts, and occur at several stratigraphic horizons in the structurally overlying *ca.* 475-469 Ma Tyrone Volcanic Group, a peri-Laurentian island arc/backarc (Hollis *et al.* 2012). Geochemically identical Fe-Ti basalts of eMORB affinity with slight negative Nb anomalies occur in the upper Tyrone Volcanic Group as the *ca.* 469 Ma Mountfield Basalts of the Broughderg formation (see Hollis *et al.* 2012; companion

582 publication). U-Pb zircon TIMS geochronology has also directly dated a geochemically
583 similar unit from Sruhanleanantawey Burn (Fig. 2) to 469.36 ± 0.34 Ma (Hollis *et al.*
584 companion publication). We suggest the Tremoge Glen Fe-Ti enriched dykes were emplaced
585 at *ca.* 469 Ma, and may be part of an extensive swarm which fed the Mountfield Basalts (see
586 Hollis *et al.* companion publication).
587
588 Incorporation of Palaeoproterozoic and Mesoproterozoic xenocrystic zircons (*ca.* 1015 and
589 2100 Ma) into the Scalp layered gabbros (Cooper *et al.* 2011) suggests that the Tyrone
590 Plutonic Group formed above a north-dipping subduction zone by the propagation of a
591 spreading centre into a microcontinental block (=Tyrone Central Inlier, see below) (Fig. 10).
592 A similar tectonic scenario was presented for the formation of the *ca.* 480 Ma
593 Annieopsquotch Ophiolite Belt of Newfoundland (Zagorevski *et al.* 2006; also see Cutts *et al.*
594 2012 and following section). The presence of propagating rifts is consistent with the
595 occurrence of: Fe-Ti-P enriched 'within-plate' basalt across the Tyrone Igneous Complex
596 from at least *ca.* 475 Ma to 469 Ma; minor continental contamination in the Tyrone Plutonic
597 Group according to Nd- and Sr-isotope systematics; and zircon inheritance at Scalp. This
598 tectonic scenario may also explain the strong LILE, LREE and negative εNd_t values in the *ca.*
599 475-469 Ma Tyrone Volcanic Group (Hollis *et al.* 2012). The Tyrone Volcanic Group is
600 believed to have formed above a north-dipping subduction zone immediately outboard of the
601 Tyrone Central Inlier (Hollis *et al.* 2012). These geochemical characteristics may be
602 explained if the arc was in part founded upon a fragment of microcontinental crust which was
603 rifted off the Tyrone Central Inlier during the formation of the Tyrone Plutonic Group (Fig.
604 10; Hollis *et al.* companion publication). A similar situation has been envisaged for the
605 evolution of the analogous Buchans-Robert's Arm arc of Newfoundland (Zagorevski *et al.*
606 2006; Zagorevski *et al.* 2012). *In situ* Hf isotope analysis of zircon rims from *ca.* 470 Ma
607 granitoid rocks that cut the Tyrone Central Inlier paragneisses yield negative εHf_{470} values of
608 *ca.* -39 (Flowerdew *et al.* 2009). This isotopic signature requires an Archaean source,
609 suggesting that rocks similar to the Lewisian Complex of Scotland occur at depth beneath the
610 Tyrone Central Inlier (Flowerdew *et al.* 2009).
611
612 **Accretion to the Tyrone Central Inlier**
613 The Tyrone Central Inlier is composed of a thick sequence of psammitic and semi-pelitic
614 paragneisses (Hartley 1933) exposed within the central regions of the Tyrone Igneous
615 Complex (Fig. 2), and is cut by a variety of acidic intrusive rocks. A prograde assemblage of

biotite + plagioclase + sillimanite + quartz ± muscovite ± garnet is observed in pelitic lithologies (Chew *et al.* 2010), with cordierite locally observed (Hartley 1933). The high-grade nature of the Tyrone Central Inlier (*ca.* 670 ± 113 °C, 6.8 ± 1.7 kbar; Chew *et al.* 2008) and its position SE of the Fair Head - Clew Bay Line (Fig. 1) has led recent workers (e.g. Chew *et al.* 2008; Flowerdew *et al.* 2009; Chew *et al.* 2010; Cooper *et al.* 2011) to suggest the Tyrone Central Inlier may represent part of an outboard segment of Laurentia, which detached as a microcontinent during the opening of Iapetus (*ca.* 570 Ma?) and subsequently reattached during the Grampian orogeny (*ca.* 470 Ma). Geochronology of syn-tectonic leucosomes (^{207}Pb-^{206}Pb zircon age of 467 ± 12 Ma; main fabric ^{40}Ar-^{39}Ar biotite cooling age of 468 ± 11.4 Ma) and post-tectonic muscovite-bearing pegmatites (^{40}Ar-^{39}Ar step heating plateaux ages of 466 and 468 ± 1 Ma) suggest a Grampian age (*ca.* 475-465 Ma) for the deformation and metamorphism of the Tyrone Central Inlier (Chew *et al.* 2008).

Obduction of the Tyrone Plutonic Group onto the Tyrone Central Inlier must have occurred prior to the intrusion of the Craigballyharky tonalite (470.3 ± 1.9 Ma) which contains inherited Proterozoic zircons and roof pendants of ophiolitic and arc-related material (Cooper *et al.* 2011). All rocks of the arc related intrusive suite are LILE and LREE-enriched with strongly negative εNd_t values (to -11.8: Hollis *et al.* 2012 and unpublished data) implying that interaction with continental crust was an integral part of their petrogenesis (Draut *et al.* 2009). Xenocrystic zircons are consistent with derivation from the structurally underlying Tyrone Central Inlier (Cooper *et al.* 2011), although the source of the *ca.* 2100 Ma inheritance remains elusive (Hutton *et al.* 1985; Cooper *et al.* 2011). Interestingly, plutons of the Notre Dame Arc in Newfoundland, built on an along strike equivalent of the Tyrone Central Inlier, termed the Dashwoods block (see following), have also yielded xenocrystic components of Palaeoproterozoic age (e.g. upper intercept of 2090 ± 75 Ma: Whalen *et al.* 1987).

The muscovite granite which cuts layered gabbro at Tremoge Glen is unusual within the arc related intrusive suite; its S-type geochemical characteristics, high Th_{CN} and LREE enrichment suggest it may have been intruded shortly after the emplacement of the Tyrone Plutonic Group from the melting of underthrust peri-Laurentian metasedimentary material (i.e. Tyrone Central Inlier). Attempts to date the Tremoge Glen muscovite granite using U-Pb zircon were not successful and produced large errors (Noble *et al.* 2004). Although apparently core-free zircons were picked, two analyses showed very significant inheritance,

649 with upper intercepts of *ca.* 1560 Ma and 2351 Ma (Noble *et al.* 2004). A second attempt to
650 date this unit is in progress.
651
652 Although the Tyrone Plutonic Group was emplaced between *ca.* 479 and 470 Ma, the exact
653 timing of this event has remained elusive. At Blaeberry Rock the presence of ophiolite-
654 derived blocks in abundant syn-kinematic tonalitic to granitic material and amphibolite
655 suggests the Tyrone ophiolite may have been accreted to the Tyrone Central Inlier at the same
656 time as the Tyrone Volcanic Group at *ca.* 470 Ma. Tonalite intrusions are abundant
657 throughout the Tyrone Igneous Complex and four occurrences have produced U-Pb zircon
658 ages: 470.3 ± 1.9 Ma at Craigballyharky (Cooper *et al.* 2011), 465.6 ± 1.1. Ma from Laght
659 Hill (Cooper *et al.* 2011: also 475 ± 10 Ma: Draut *et al.* 2009), 469.9 ± 2.9 Ma from Golan
660 Burn (Cooper *et al.* 2011), and 469.29 ± 0.33 Ma from Cashel Rock (Hollis *et al.* 2012).
661 Emplacement at *ca.* 470 Ma, synchronous with the Tyrone arc (=Tyrone Volcanic Group),
662 may explain how the metamorphic conditions evident within the Tyrone Central Inlier (*ca.*
663 670 ± 113 °C, 6.8 ± 1.7 kbar; Chew *et al.* 2008) were generated prior to *ca.* 468 Ma. These
664 conditions cannot have been solely the result of the obduction of the Tyrone Plutonic Group,
665 as it is tectonically dissected, thin and lacks an ultramafic section. The coeval emplacement
666 of both the arc and the ophiolite would provide a >10-15 km thick, hot crustal sequence,
667 enough to produce the required P-T conditions in the Tyrone Central Inlier.
668
669 Amphiboles from syn-kinematic tonalitic material within the Blaeberry contact (SPH210; Fig.
670 8a) produced temperature estimates of 525-610 °C, slightly lower (but within error) than
671 those produced by Chew *et al.* (2008) from the Tyrone Central Inlier (670 ± 113 °C).
672 Pressure estimates (after Schmidt, 1992) up to 4.0 ± 0.6 kbar for tonalitic melt from Blaeberry
673 Rock (SPH210) are again lower than those produced by Chew *et al.* (2008), however Hartley
674 (1933) noted that the presence of sillimanite in the Tyrone Central Inlier is restricted to its SE
675 side. As the Tyrone Igneous Complex was emplaced from this direction, the higher
676 temperatures and pressures from Corvanaghan Quarry may simply be restricted to that region,
677 where the accreted succession was thickest. Sillimanite-bearing paragneisses are also
678 preserved across the Notre Dame and Dashwoods subzones of the equivalent Newfoundland
679 Appalachians associated with arc-ophiolite accretion (e.g. Brem *et al.* 2007; van Staal *et al.*
680 2007; 2009; Fig. 1b). In the Dashwoods subzone, large bodies and screens of variably
681 migmatized sillimanite-bearing paragneisses are exposed (see van Staal *et al.* 2007). Lesser

682 exposures further north in the Notre Dame subzone (e.g. as screens in the Hungry Mountain
683 Complex: Waldron & van Staal 2001) is due to the level of denudation (van Staal *et al.* 2007).
684
685 Another possible fragment of microcontinental crust in the Irish Caledonides is the Slishwood
686 Division (Flowerdew *et al.* 2005; Chew *et al.* 2010) (Fig. 1a). This metasedimentary
687 sequence is exposed in three inliers of NW Ireland (NE Ox Mountains, Lough Derg and
688 Rosses Point) and is composed predominantly of migmatitic psammitic gneisses with minor
689 pelites, semipelites, calc-silicates, metabasites and serpentinites (Sanders 1979; Flowerdew &
690 Daly 2005; Daly 2009). All three inliers have been suggested on the basis of magnetic and
691 gravity data to form one basement block which acted as a rigid indenter during the Grampian
692 orogeny (Fig. 1a; references in Daly 2009). The Grampian histories of the Slishwood
693 Division and the Tyrone Central Inlier are very similar, both having undergone leucosome
694 generation during orogenesis, and subsequently intruded by pegmatites that cut the high level
695 fabrics (Flowerdew *et al.* 2005; Chew *et al.* 2008). The NE Ox Mountains Inlier was also
696 intruded by several tonalite and granite bodies between *ca.* 471-467 Ma (Flowerdew *et al.*
697 2005) with magmas contaminated by the host rocks. This is identical to the late-Grampian
698 evolution of the Tyrone Central Inlier (see Cooper *et al.* 2011). Final imbrication of the
699 Slishwood Division with the Central Ox Mountains Dalradian Supergroup occurred during
700 D3 regional thrusting (between *c.* 476-463 Ma: Flowerdew *et al.* 2005), equivalent in Country
701 Tyrone to the emplacement of the Dalradian Supergroup above the Tyrone Igneous Complex
702 and Tyrone Central Inlier (Omagh Thrust; Fig. 2).
703
704 Clear differences between the Slishwood Division and Tyrone Central Inlier are primarily
705 related to their pre-Grampian histories. These include the presence of calc-silicates,
706 metabasites and serpentinites in the former (Daly 2009),
707 although possible metabasites have been recognized in the Tyrone Central Inlier during GSNI
708 fieldwork. Metabasites in the Slishwood Division record pre-Grampian high-pressure
709 granulite- and earlier eclogite-facies metamorphic events (Sanders *et al.* 1987; Flowerdew &
710 Daly 2005) not observed within the Dalradian Supergroup or Tyrone Central Inlier. Sm-Nd
711 garnet-plagioclase whole rock isochrons from the granulite-facies assemblages have yielded
712 ages ranging between 605 ± 37 Ma and 539 ± 11 Ma; with P-T estimates of *ca.* 15 kbar and
713 860 °C (Saunders *et al.* 1987; Flowerdew & Daly 2005; see discussion in Daly 2009).
714 Although this early history is pre-Grampian, Daly (2009) has suggested the metamorphism
715 cannot be much older as: U-Pb detrital zircon ages (Daly *et al.* 2004) demonstrate a post-

Grenville age of deposition of the protolith; and a pre-tectonic metabasite body which preserves original gabbroic textures has produced a Sm-Nd mineral isochron age of 580 ± 36 Ma. This Sm-Nd age is consistent with magmatism related to the opening of the Iapetus Ocean between *ca.* 570 and 535 Ma (Cawood *et al.* 2001). Detrital zircon analysis from the Slishwood Division has also revealed differences compared with the Tyrone Central Inlier. A significant population between *ca.* 2.5 and 2.7 Ga is present in the Appin, Argyll and Southern Highland groups of the Dalradian Supergroup (Cawood *et al.* 2003) and Tyrone Central Inlier (Chew *et al.* 2008), but is absent in the Slishwood Division (Daly *et al.* 2004 cited by Flowerdew *et al.* 2005) and the Grampian Group of the Dalradian (Cawood *et al.* 2003). T_{DM} model ages are also significantly younger in the Tyrone Central Inlier than in the Slishwood Division (references in Chew *et al.* 2008).

A correlative of the Annieopsquotch Ophiolite Belt of Newfoundland?

Recent fieldwork, U-Pb zircon geochronology and geochemistry from across the Tyrone Igneous Complex has highlighted the close similarities between: (i) the Tyrone Plutonic Group and the Annieopsquotch Ophiolite Belt of Newfoundland (Cooper *et al.* 2011), (ii) Tyrone Volcanic Group and the Buchans and Robert's Arm groups of central Newfoundland (Hollis *et al.* 2012); and (iii) a late suite of *ca.* 470-464 Ma calc-alkaline intrusive rocks with the second phase of the Notre Dame arc (van Staal *et al.* 2007), which also invade the Annieopsquotch Accretionary Tract (Lissenberg *et al.* 2005; Lissenberg & van Staal 2006). The work presented herein, adds further weight to these correlations, indicating that the Tyrone Igneous Complex represents the third stage of arc-ophiolite emplacement in the peri-Laurentian British and Irish Caledonides at *ca*. 470 Ma, following the accretion of early *ca.* 510-500 Ma oceanic tracts (Chew *et al.* 2010), and the Lough Nafooey arc at *ca.* 480 Ma (see Hollis *et al.* 2012).

The Annieopsquotch Ophiolite Belt of central Newfoundland comprises several suprasubduction zone ophiolite complexes (e.g., King George IV, Annieopsquotch, Star Lake), which formed during west-directed subduction outboard of the Dashwoods peri-Laurentian microcontinent (Dunning *et al.* 1987; Whalen *et al.* 1997; Lissenberg *et al.* 2005; Zagorevski *et al.* 2006). Two U-Pb zircon ages from a pegmatitic and medium-grained trondhjemite (481.4 $^{+4.0}/_{-1.9}$ Ma and 477.5 $^{+2.6}/_{-2.0}$ Ma) constrain the age of the Annieopsquotch Ophiolite Belt to *ca.* 481-478 Ma (Dunning & Krogh 1985). The Annieopsquotch Ophiolite Complex is the largest and most studied ophiolite within the belt; and consists of

suprasubduction zone affinity layered to isotropic gabbros, sheeted dykes and pillow basalts (Lissenberg *et al.* 2005). The lower gabbro zone contains enclaves of troctolite inferred to have formed from boninitic melts (Lissenberg *et al.* 2004). The youngest basalts are of MORB-type affinity and are cut by sheeted dykes with back-arc geochemical characteristics (Lissenberg *et al.* 2005). εNd_t values within the Anniopsquotch Ophiolite Belt range from +7.6 to +8.4 (Zagorevski *et al.* 2006). The ophiolite lacks an upper mantle section apart from rare occurrences of dunite and pyroxenite (Lissenberg & van Staal 2006).

The age of formation for the Tyrone Plutonic Group between 484 and 479 Ma (including the new date of 483.68 ± 0.81 Ma for the pegmatitic gabbro at Black Rock, Table 3), primitive εNd_t values ranging from +4.40 to +7.73 (Draut et al., 2009; Cooper et al., 2011; Table 1), tholeiitic suprasubduction geochemical signatures (Table 1), preserved ophiolite sequences, and development outboard of a possible microcontinental block (i.e. Tyrone Central Inlier) support both a correlation with the Annieopsquotch Ophiolite Belt and formation at an oceanic spreading centre above a subduction zone (see Draut *et al.* 2009; Cooper *et al.* 2011). Xenocrystic Mesoproterozoic zircons present within the Tyrone Plutonic Group are consistent with T_{DM} ages of 1200-1800 Ma from felsic intrusive rocks of the Moretons Harbour Group (part of the Annieopsquotch Ophiolite Belt of Newfoundland; Cutts *et al.* 2012) indicating a significant amount of contamination from Mesoproterozoic or older continental crust.

Furthermore, the Lloyds River Fault Zone which separates the Annieopsquotch Ophiolite Belt from the Dashwoods microcontinental block bears a striking resemblance to Blaeberry Rock (Lissenberg & van Staal 2002). The Lloyds River Fault at its type locality is a complex shear zone having a central high-strain zone (mainly characterized by mafic and felsic tectonites), which is bounded by less-strained moderately foliated amphibolite and orthogneiss dissected by narrow shear zones (Lissenberg & van Staal 2002). The central high strain zone is composed of an intimate mixture of banded amphibolite and metapyroxenite (probably of ophiolitic origin) and strongly foliated quartz-diorite and tonalite. Moderately deformed, late-kinematic, folded and boudinaged tonalitic to granodioritic veins that cut sheared rocks suggests that these arc magmas were intruded syn-kinematically (Lissenberg & van Staal 2006). The outer zone of the Lloyds River Fault consists of gabbro and diabase cut by diorite and tonalite, with weakly deformed mafic rocks alternating with strongly sheared amphibolite and orthogneiss. Preferential localization of shear zones occurs in intrusive sheets rather than the ophiolite-derived gabbro, as at Blaeberry Rock. Shear sense indicators imply both the

784 Lloyds River Fault and Blaeberry Rock contacts accommodated oblique motion with a
785 sinistral component. Abundant metamorphic hornblende at both sites also suggests the fault
786 zones formed at amphibolite-facies conditions (with subsequent retrograde overprint)
787 (Lissenberg & van Staal 2006). Abundant syn-kinematic tonalitic material at Blaeberry
788 Rock implies that the Tyrone Plutonic Group was accreted at the same time as the Tyrone
789 Volcanic Group at *ca.* 470 Ma. This again is remarkably similar to that of the
790 Annieopsquotch Ophiolite Belt which occurred prior to *ca.* 468 Ma (Lissenberg *et al.* 2005;
791 Zagorevski *et al.* 2006).
792
793 In the Newfoundland Appalachians, three distinct phases of deformation and metamorphism
794 have been recognized during the Taconic orogeny, due to arc and ophiolite accretion (van
795 Staal *et al.* 2009). Early obduction of the Lushs Bight Oceanic Tract onto the peri-Laurentian
796 Dashwoods microcontinental block resulted in Taconic phase 1 at *ca.* 495 Ma (van Staal *et al.*
797 2009). Evidence for ductile deformation and metamorphism at this time is relatively cryptic
798 (van Staal *et al.* 2009) as in the British and Irish Caledonides (e.g. 514 ± 3 Ma ^{40}Ar-^{39}
799 hornblende age from Deer Park ophiolitic mélange: Chew *et al.* 2010). Taconic phase 2 is
800 largely regarded as the main orogenic phase of the Appalachians, and is broadly equivalent to
801 the main episode of Grampian deformation in the British and Irish Caledonides (*ca.* 475-465
802 Ma) (e.g. van Staal *et al.* 2009). In the Newfoundland Appalachians this resulted from the
803 dextral oblique collision of an Early Ordovician west-facing peri-Laurentian arc (containing
804 ensimatic and ensialic segments) with the passive Laurentian margin, and the obduction of
805 suprasubduction affinity crust of the intervening seaways (van Staal *et al.* 2007, 2009). It has
806 been suggested that choking of the A-subduction channel during Taconic 2 may have been
807 the main cause for the initiation of subduction at *ca.* 480 Ma immediately outboard of the
808 accreted Notre Dame arc/Dashwoods Block, which led to the formation of the
809 Annieospquotch Accretionary Tract (van Staal *et al.* 2009). This timing is identical to that in
810 the Irish Caledonides where the Lough Nafooey arc collided with the Laurentian margin
811 between *ca.* 484 and 476 Ma (Draut *et al.* 2004), coeval with the early development of the
812 Tyrone Igneous Complex outboard of the Tyrone Central Inlier (Hollis et al. companion
813 publication). The rapid accretion of the Tyrone and Buchans-Robert's Arm arc systems to the
814 composite Laurentian margin occurred at *ca.* 470-468 Ma during the peak of Taconic phase 2
815 deformation (van Staal *et al.* 2009; Cooper *et al.* 2011). It is presently unclear why the
816 Tyrone Igneous Complex was obducted whereas the Annieopsquotch Accretionary Tract was
817 underplated (Hollis *et al.* 2012). Late orogenesis in Newfoundland (Taconic phase 3) is

related to the accretion of a late peri-Gondwanan arc system to the leading edge of Laurentia along the Red Indian Line (Fig 1b) (van Staal *et al.* 2007).

Other potential correlatives?

The Ballantrae Ophiolite Complex of Scotland is a structurally imbricated assemblage of ophiolitic, ocean-island and island-arc rocks exposed over *ca.* 75km^2 immediately north of the Southern Uplands Fault (Fig. 1). A U-Pb zircon date of 483 ± 4 Ma from trondhjemite constrains the genesis of the ophiolite, and a K-Ar hornblende cooling age of 478 ± 4 Ma from its metamorphic sole constrains the timing of its emplacement (Bluck *et al.* 1980). While it is possible that the Ballantrae Ophiolite Complex is an along strike equivalent of the Tyrone Igneous Complex, current age constraints are not sufficient for reconstructing the petrochemical evolution of the exposed sequences across tectonic blocks (discussed in Hollis *et al.* 2012). Although graptolite-bearing sedimentary units are Early- to Late Arenig in age (Stone & Strachan 1981; Stone & Rushton 1983; Rushton *et al.* 1986), considerably older ages have also been produced from gabbro of within-plate affinity (K-Ar age of 487 ± 8 Ma: Harris *et al.* 1965), and island-arc lavas (e.g. whole-rock Sm-Nd age of 501 ± 12 Ma: Thirwall and Bluck, 1984). Post-obduction dykes of the Ballantrae Ophiolite Complex are similarly divisible into those of island-arc and within-plate affinity (Holub *et al.* 1984).

The Norwegian (Scandinavian) Caledonides consist of four major allochthonous nappe complexes, referred to as the Lower, Middle, Upper and Uppermost allochthons, which overlie parautochthonous and autochthonous Baltican rocks (Roberts & Gee 1985). The Uppermost Allochthon is of interest here as it is considered to represent an Ordovician Taconic orogenic event on the Laurentian margin, similar to that preserved in the British and Irish Caledonides (e.g. Slagstad *et al.* 2011). Although U-Pb ages similar to those from the Tyrone Plutonic Group have been obtained in the Norwegian Caledonides from trondhjemite of the Karmøy ophiolite (485 ± 2 Ma) and a cross-cutting arc related tonalite of the Gullfjellet ophiolite (482 $^{+6}_{-4}$ Ma), both ophiolites also record earlier magmatism at *ca.* 490 Ma (Dunning & Pedersen 1988). While it is clear ocean basin development occurred along the Laurentian margin at this time (published U-Pb ages summarized in Slagstad *et al.* 2011), it is not obvious how these units relate to those preserved in the Irish Caledonides.

CONCLUSIONS

852 The Tyrone Plutonic Group is composed of variably tectonised and metamorphosed, layered,
853 isotropic and pegmatitic gabbros, sheeted dolerite dykes and rare pillow lavas. New and
854 previously published geochronology constrains the formation of the Tyrone Plutonic Group to
855 *ca.* 484-479 Ma, within error of U-Pb zircon dating from the Annieopsquotch Ophiolite Belt
856 of Newfoundland. Whole rock Sr-isotopic constraints from the upper parts of the ophiolite
857 are comparable to the $^{87}Sr/^{86}Sr$ composition of Lower to Middle Ordovician seawater and
858 range to slightly more radiogenic values. By contrast, gabbro from Scalp yielded a
859 significantly less radiogenic $^{87}Sr/^{86}Sr_i$ value suggesting somewhat lesser interaction with
860 seawater, consistent with its likely deeper original position within the ophiolite. High
861 $^{87}Sr/^{86}Sr_i$ values in the upper ophiolite, Sm-Nd isotopic constraints (εNd_t +4.40 to +7.73) and
862 the presence of inherited zircons in layered gabbros are consistent with minor crustal
863 contamination into the source region. Together these data suggest that the Tyrone Plutonic
864 Group formed above a N-dipping subduction zone, by the propagation of a spreading centre
865 into a microcontinental block. S-type, peraluminous muscovite granite contains inherited
866 Proterozoic zircons, and appears to have been intruded shortly after ophiolite emplacement
867 generated from the partial melting of Laurentian-affinity metasedimentary material.
868 Ophiolite obduction onto the Tyrone Central Inlier must have occurred prior to the intrusion
869 of a *ca.* 470 Ma tonalite which contains roof pendants of ophiolitic and arc material and
870 xenocrystic Proterozoic zircons. Late Fe-Ti basaltic dykes of eMORB affinity are consistent
871 with formation at a propagating rift following obduction. Geochemically identical lavas are
872 present in the upper Tyrone Volcanic Group (Mountfield Basalts) and at Slieve Gallion
873 constrained by U-Pb zircon geochronology to *ca.* 469 Ma. The presence of syn-kinematic,
874 calc-alkaline tonalitic to granitic material within the contact between the Tyrone Central
875 Inlier and Tyrone Plutonic Group suggests that the latter may have been emplaced relatively
876 late within the orogen at *ca.* 470 Ma synchronous with the Tyrone arc. In the absence of an
877 ultramafic section, the coeval obduction of the ophiolite and volcanic arc may explain how
878 metamorphic conditions within the sillimanite-grade Tyrone Central Inlier were reached prior
879 to *ca.* 468 Ma.
880
881 Strong temporal, geochemical and lithological similarities to the Annieopsquotch Ophiolite
882 Belt of Newfoundland indicate that these ophiolites may have a shared origin and evolution.
883 This adds to a growing body of evidence that the Tyrone Igneous Complex represents the
884 third stage of arc-ophiolite emplacement in the peri-Laurentian British and Irish Caledonides

at *ca*. 470 Ma, following the accretion of early *ca.* 510-500 Ma ophiolites (Highland Border and Deer Park), and the Lough Nafooey arc at *ca.* 480 Ma.

ACKNOWLEDGEMENTS

The authors would like thank Ian Croudace, Matt Cooper and Andy Milton (University of Southampton) for XRF and ICP-MS analysis and Mick Murphy (University College Dublin) for assistance with isotopic analyses. John Dewey, Paul Ryan, Dick Glen, Jack Casey and many others are thanked for field discussions within the Tyrone Igneous Complex. John Spratt (Natural History Museum, London) is thanked for assistance using the electron microprobe. U-Pb zircon geochronology was made possible through a combination of Northern Ireland Department of Enterprise Trade and Investment and Northern Ireland Environment Agency funding. SPH gratefully acknowledge funding for this work from the British Geological Survey (BGS University Funding Initiative), Dalradian Resources, Geological Survey of Northern Ireland, University of Southampton, Metallum Resources and Natural History Museum, London. MRC publishes with permission of the Executive Director of the BGS (NERC). Reviewers Trond Slagstad and Cees van Staal, and subject editor Bernard Bingen are thanked for many constructive comments which improved this paper.

REFERENCES

ANGUS, N.S. 1962 Oscellar hybrids from the Tyrone Igneous Series, Ireland. *Geological Magazine,* **99**, 9-26.

ANGUS, N.S. 1970. A Pyroxene-Hornfels from the Basic Plutonic Complex, Co. Tyrone, Ireland. *Geological Magazine*, **107**, 277-287.

ANGUS, N.S. 1977. The Craigballyharky granitic complex within the Tyrone Igneous Series. *Proceedings of the Royal Irish Academy, Section B – Biological, Geological and Chemical Science*, **77**, 181-199.

ANONYMOUS. 1972. Penrose field conference on ophiolites. *Geotimes*, **17**, 24-55.

BICKLE, M.J. & TEAGLE, D.A.H. 1992. Strontium alteration in the Troodos ophiolite: implications for fluid fluxes and geochemical transport in mid-ocean ridge hydrothermal systems. *Earth and Planetary Science Letters*, **113**, 219-237.

BRITISH GEOLOGICAL SURVEY. 1986. Metamorphic Rocks – The crystalline Caledonides, in *British Regional Geology: Northern Ireland*, 5-17.

920 BLUCK, B.J., HALLIDAY, A.N., AFTALION, M. & MACINTYRE, R.M. 1980. Age and origin of
921 the Ballantrae ophiolite and its significance to the Caledonian orogeny and Ordovician
922 time scale. *Geology*, **8**, 492-495.
923 CAWOOD, P.A., MCCAUSLAND, P.J.A. & DUNNING, G. 2001. Opening Iapetus: Constraints
924 from the Laurentian margin in Newfoundland. *Geological Society of America Bulletin*,
925 **113**, 443-453.
926 CAWOOD, P.A., NEMCHIN, A.A., SMITH, M. & LOEWY, S. 2003. Source of the Dalradian
927 Supergroup constrained by U-Pb dating of detrital zircon and implications for the East
928 Laurentian margin. *Journal of the Geological Society,* **160**, 231-246.
929 CHEW, D.M. 2009. Grampian orogeny, in HOLLAND, C.H. & SANDERS, I.S. (eds) *The Geology*
930 *of Ireland. 2nd edition*, 69-93.
931 CHEW, D.M., FLOWERDEW, M.J., PAGE, L.M., CROWLEY, Q.G., DALY, J.S., COOPER, M. R., &
932 WHITEHOUSE, M.J. 2008. The tectonothermal evolution and provenance of the Tyrone
933 Central Inlier, Ireland: Grampian imbrication of an outboard Laurentian microcontinent?.
934 *Journal of the Geological Society, London*, **165**, 675-685.
935 CHEW, D.M., DALY, J.S., MAGNA, T., PAGE, L.M., KIRKLAND, C.L., WHITEHOUSE, M.J. &
936 LAM, R. 2010. Timing of ophiolite obduction in the Grampian orogen. *Geological Society*
937 *of America Bulletin*, **122**, 1787–1799.
938 CLIFT, P.D. & RYAN, P.D. 1994. Geochemical evolution of an Ordovician island arc, South
939 Mayo, Ireland. *Journal of the Geological Society, London*, **151**, 329-342.
940 COBBING, E.J. 1969. Schistosity and folding in a banded gabbro from Tyrone. *Bulletin of*
941 *the Geological Survey of Great Britain*, **30**, 89-97.
942 COBBING, E.J., MANNING, P.I. & GRIFFITH, A.E. 1965. Ordovician-Dalradian unconformity in
943 Tyrone. *Nature*, **206**, 1132-50.
944 COOPER, M.R. & MITCHELL, W.I. 2004. Midland Valley Terrane, in MITCHELL, W.I. (ed).,
945 *The Geology of Northern Ireland. Our Natural Foundation, second edition*. Geological
946 Survey of Northern Ireland.
947 COOPER, M.R., CROWLEY, Q.G. & RUSHTON, A.W.A. 2008. New age constraints for the
948 Ordovician Tyrone Volcanic Group, Northern Ireland. *Journal of the Geological Society,*
949 *London*, **165**, 333-339.
950 COOPER, M.R., CROWLEY, Q.G., HOLLIS, S.P., NOBLE, S.R., ROBERTS, S., CHEW, D., EARLS,
951 G., HERRINGTON, R. & MERRIMAN, R.J. 2011. Age constraints and geochemistry of the
952 Ordovician Tyrone Igneous Complex, Northern Ireland: implications for the Grampian
953 orogeny. *Journal of the Geological Society, London*, **168**, 837-850.

954 COOPER, M.R., ANDERSON, H., WALSH, J.J., VAN DAM, C.L., YOUNG, M.E., EARLS, G. &
955 WALKER, A. 2012. Palaeogene Alpine tectonics and Icelandic plume-related magmatism
956 and deformation in Northern Ireland. *Journal of the Geological Society, London*, **169**, 29-
957 36.
958 CUTTS, J.A., ZAGOREVSKI, A., MCNICOLL, V., & CARR, S.D. 2012. Tectono-stratigraphic
959 setting of the Moreton's Harbour Group and its implications for the evolution of the
960 Laurentian margin: Notre Dame Bay, Newfoundland. *Canadian Journal of Earth*
961 *Sciences*, **49**, 111-127.
962 DALY, J.S., FLOWERDEW, M.J. & WHITEHOUSE, M.J. 2004. The Slishwood Division really
963 does have a pre-Grampian high-grade history, but is it exotic to Laurentia? *Irish Journal*
964 *of Earth Sciences,* **22**, 59.
965 DALY, J.S. 2009. Precambrian, in HOLLAND, C.H. & SANDERS, I.S. (eds) *The Geology of*
966 *Ireland. 2nd edition*, 7-42.
967 DEPAOLO, D.J. 1988. *Neodymium Isotope Geology.* New York, Springer Verlag, p187.
968 DEWEY, J.F. 2005. Orogeny can be very short. *Proceedings of the National Academy of*
969 *Sciences of the United States of America*, **102**, 15286-15293.
970 DILEK, Y. & FURNES, H. 2011. Ophiolite genesis and global tectonics. Geochemical and
971 tectonic fingerprinting of ancient oceanic lithosphere. *Geological Society of America*
972 *Bulletin*, **123**, 387-411.
973 DRAUT, A.E., CLIFT, P.D., CHEW, D.M., COOPER, M.J., TAYLOR, R.N. & HANNIGAN, R.E.
974 2004. Laurentian crustal recycling in the Ordovician Grampian Orogeny: Nd isotopic
975 evidence from western Ireland. *Geological Magazine*, **114**, 195-207.
976 DRAUT, A.E., CLIFT, P.D., AMATO, J.M., BLUSZTAJN, J. & SCHOUTEN, H. 2009. Arc-continent
977 collision and the formation of continental crust: a new geochemical and isotopic record
978 from the Ordovician Tyrone Igneous Complex, Ireland. *Journal of the Geological Society,*
979 *London*, **166**, 485-500.
980 DUNNING, G.R. & KROGH, T.E. 1985. Geochronology of ophiolites in the Newfoundland
981 Appalachians. *Canadian Journal of Earth Sciences*, **22**, 1659-1670.
982 DUNNING, G.R., & PEDERSEN, R.B. 1988. U/Pb ages of ophiolites and arc-related plutons of
983 the Norweigan Caledonides: implications for the development of Iapetus. *Contributions to*
984 *Mineralogy and Petrology*, **98**, 13-23.
985 DUNNING, G.R., KEAN, B.F., THURLOW, J.G. & SWINDEN, H.S. 1987. Geochronology of the
986 Buchans, Roberts Arm, and Victoria Lake groups and Mansfield Cove Complex,
987 Newfoundland. *Canadian Journal of Earth Sciences*, **24**, 1175-1184.

ERNST, W.G. & LIU, J. 1998. Experimental phase equilibrium study of Al- and Ti-contents of calcic amphibole in MORB - A semiquantitative thermobarometer. *American Mineralogist*, **83**, 952-969.

FLOWERDEW, M.J. & DALY, J.S. 2005. Sm-Nd mineral ages and P-T constraints on the pre-Grampian high grade metamorphism of the Slishwood Division, north-west Ireland. *Irish Journal of Earth Sciences*, **23**, 107-123.

FLOWERDEW, M.J., DALY, J.S., & WHITEHOUSE M.J. 2005. 470 Ma granitoid magmatism associated with the Grampian Orogeny in the Slishwood Division, NW Ireland. *Journal of the Geological Society, London*, **162**, 563-575.

FLOWERDEW, M.J., CHEW, D.M., DALY, J.S. & MILLAR, I,L. 2009. Hidden Archeaen and Palaeoproterozoic crust in NW Ireland? Evidence from zircon Hf isotopic data from granitoid intrusions. *Geological Magazine*, **146**, 903-916.

GEOLOGICAL SURVEY OF NORTHERN IRELAND. 1979. Pomeroy, Northern Ireland Sheet 34. Solid. 1:50 000. *Ordnance Survey for the Geological Survey of Northern Ireland, Southampton.*

GEOLOGICAL SURVEY OF NORTHERN IRELAND. 1983. Cookstown, Northern Ireland Sheet 27. Solid. 1:50 000. *Ordnance Survey for the Geological Survey of Northern Ireland, Southampton.*

GEOLOGICAL SURVEY OF NORTHERN IRELAND. 1995. Draperstown. Northern Ireland Sheet 26. Solid and Drift Geology. 1:50 000. *British Geological Survey, Keyworth, Nottingham.*

GEOLOGICAL SURVEY OF NORTHERN IRELAND. 2007. The Tellus project: Proceedings of the end-of-project conference, Belfast, October 2007. See http://www.bgs.ac.uk/gsni/tellus/conference/index.html).

GUNN, A.G., LUSTY, P.A.J., MCDONNELL, P.M. & CHACKSFIELD, B.C. 2008. A preliminary assessment of the mineral potential of selected parts of Northern Ireland. *British Geological Survey, Economic Minerals Programme, Commissioned Report, CR/07/149, pp. 161.*

HAMMARSTROM, J.M. & ZEN, E-A. 1986. Aluminum in hornblende: An empirical igneous geobarometer. *American Mineralogist*, **71**, 1297-1313.

HARPER, G.D. 1984. The Josephine Ophiolite, northwestern California. *Geological Society of America Bulletin*, **95**, 1009-1026.

HARPER, G.D. 2003. Fe-Ti basalts and propagating-rift tectonics in the Josephine Ophiolite. *Geological Society of America Bulletin*, **115**, 771-787.

1021 HARRIS, P.M., FARRAR, E., MACINTYRE, R.M., MILLER, J.A. & YORK, D. 1965. Potassium-
1022 argon age measurements on two igneous rocks from the Ordovician system of Scotland.
1023 *Nature*, **205**, 352-353.
1024 HARTLEY, J.J. 1933. The geology of north-eastern Tyrone and the adjacent portions of County
1025 Londonderry. *Proceedings of the Royal Irish Academy, Section B- Biological, Geological*
1026 *and Chemical Science*, **41**, 218-285.
1027 HOLLIS, S.P., ROBERTS, S., COOPER, M.R., EARLS, G., HERRINGTON, R.J., CONDON, D.J.,
1028 COOPER, M.J., ARCHIBALD, S.M. & PIERCEY, S.J. 2012. Episodic-arc ophiolite
1029 emplacement and the growth of continental margins: Late accretion in the Northern Irish
1030 sector of the Grampian-Taconic orogeny. *Geological Society of America Bulletin*, **124**,
1031 1702-1723.
1032 HOLLIS, S.P., COOPER, M.R., ROBERTS, S., EARLS, G., HERRINGTON, R.J. & CONDON, D.J.
1033 Companion Publication. Stratigraphic, geochemical and U-Pb zircon constraints from
1034 Slieve Gallion, Northern Ireland: a correlation of the Irish Caledonian arcs. *Journal of the*
1035 *Geological Society, London*. NOTE: ARTICLE ACCEPTED – DOI NOT YET
1036 PROVIDED.
1037 HOLLIS, S.P. 2013. Evolution and mineralization of volcanic arc sequences: Tyrone Igneous
1038 Complex, Northern Ireland. Unpublished PhD thesis, University of Southampton, UK.
1039 262pp.
1040 HOLUB, F.V., KLAPOVA, H., BLUCK, B.J. & BOWES, D.R. 1984. Petrology and geochemistry
1041 of post-obduction dykes of the Ballantrae complex, SW Scotland. *Transactions of the*
1042 *Royal Society of Edinburgh: Earth Sciences,* **75**, 211-224.
1043 HUTTON, D.H.W., AFTALION, M. & HALLIDAY, A.N. 1985. An Ordovician ophiolite in County
1044 Tyrone, Ireland. *Nature*, **315**, 210-212.
1045 ISHIKAWA, Y., SAWAGUCHI, T., IWAYA, S. & HORIUCHI, M. 1976. Delineation of prospecting
1046 targets for Kuroko deposits based on modes of volcanism of underlying dacite and
1047 alteration halos. *Mining Geology*, **26**, 105-117.
1048 JACOBSEN, S.B. & WASSERBURG, G.J. 1979. Nd and Sr isotopic study of the Bay of Islands
1049 ophiolite complex and the evolution of the source of mid-ocean ridge basalts. *Journal of*
1050 *Geophysical Research*, **84**, 7429-7445.
1051 JAFFEY, A.H., FLYNN, K.F., GLENDENIN, L.E., BENTLEY, W.C. & ESSLING, A.M. 1971.
1052 Precision measurements of half-lives and specific activities of ^{235}U and ^{238}U. *Physics*
1053 *Press,* **C4**, 1889–1906.

KRANIDIOTIS, P. & MACLEAN, W.H. 1987. Systematics of chlorite alteration at the Phelps Dodge massive sulfide deposit, Matagami, Quebec. *Economic Geology*, **82**, 1898-1911.

LARGE, R.R., GEMMELL, J.B. & PAULICK, H. 2001. The alteration box plot: a simple approach to understanding the relationship between alteration mineralogy and lithogeochemistry associated with volcanic-hosted massive sulfide deposits. *Economic Geology*, **96**, 957-971.

LISSENBERG, C.J. & VAN STAAL, C.R. 2002. The relationships between the Annieopsquotch Ophiolite Belt, the Dashwoods Block and the Notre Dame Arc in southwestern Newfoundland. *Current Research, Newfoundland Department of Mines and Energy*, Report 02-1, 145-153.

LISSENBERG, C.J. & VAN STAAL, C.R. 2006. Feedback between deformation and magmatism in the Lloyds River Fault Zone, an example of episodic fault reactivation in an accretionary setting, Newfoundland Appalachians. *Tectonics*, **25**, TC4004

LISSENBERG, C.J., BEDARD, J.H. & VAN STAAL, C.R. 2004. The structure and geochemistry of the gabbro zone of the Annieopsquotch Ophiolite, Newfoundland: implications for lower crustal accretion at spreading ridges. *Earth and Planetary Science Letters*, **229**, 105-123.

LISSENBERG, C.J., ZAGOREVSKI, A., MCNICOLL, V.J., VAN STAAL, C.R. & WHALEN, J.B. 2005. Assembly of the Annieopsquotch Accretionary Tract, Newfoundland Appalachians: Age and Geodynamic Constraints from Syn-Kinematic Intrusions. *Journal of Geology*, **113**, 553-570.

MATTINSON, J.M. 2005. Zircon U–Pb chemical abrasion ('CA-TIMS') method: Combined annealing and multi-step partial dissolution analysis for improved precision and accuracy of zircon ages. *Chemical Geology*, **220**, 47–66.

MCDONOUGH, W.F. & SUN. S.-S. 1995. The composition of the Earth. *Chemical Geology*, **120**, 223-254.

MERRIMAN, R.J. & HARDS, V.L. 2000. Petrographic notes on igneous and metamorphic rocks from Northern Ireland. *British Geological Survey Short Report MPSR/00/7.*

MESCHEDE, M. 1986. A method of discriminating between different types of mid-ocean ridge basalts and continental tholeiites with the Nb-Zr-Y diagram. *Chemical Geology*, **56**, 207-218.

MIYASHIRO, A. 1973. The Troodos Complex was probably formed in an island arc. *Earth and Planetary Science Letters*, **73**, 217-222.

NEBEL, O., MEZGER, K., SCHERER, E.E. & MÜNKER, C. 2005. High precision determinations of $^{87}Rb/^{85}Rb$ in geologic materials by MC-ICP-MS *International Journal of Mass Spectrometry*, **246**, 10-18.

1088 NOBLE, S.R., DAVID, K., CROWLEY, Q. & STOREY, C. 2004. U-Pb geochronology of igneous
1089 rocks from the Midland Valley Terrane, Northern Ireland, part 2. *NERC Isotope*
1090 *Geosciences Laboratory, Report Series No. 201.*
1091 PEARCE, J.A. 1983. Role of the sub-continental lithosphere in magma genesis at active
1092 continental margins, in: HAWKESWORTH, C.J. (ed) *Continental basalts and mantle*
1093 *xenoliths*, 230-249
1094 PEARCE, J.A. & CANN, J.R. 1973. Tectonic setting of basic volcanic rocks determined using
1095 trace element analyses. *Earth and Planetary Science Letters*, **19**, 290-300.
1096 PEARCE, J.A. & NORRY, M.J. 1979. Petrogenetic implications of Ti, Zr, Y and Nb variations
1097 in volcanic rocks. *Contributions to Mineralogy and Petrology*, **69**, 33-47.
1098 PEACE, J.S., LIPPARD, S.J. & ROBERTS, S. 1984. Characteristics and tectonic significance of
1099 suprasubduction zone ophiolites, in GASS, I.G., LIPPARD., S.J. & SHELTON, A.W. (eds)
1100 *Ophiolites and Oceanic Lithosphere*: Geological Society, London, Special Publications,
1101 **16**, 77-94.
1102 POLLOCK, J.C., HIBBARD, J.P. & SYLVESTER, P.J. 2009. Early Ordovician rifting of Avalonia
1103 and birth of the Rheic Ocean: U–Pb detrital zircon constraints from Newfoundland.
1104 *Journal of the Geological Society, London*, **166**, 501–515.
1105 RAVEGGI, M., GILES, D., FODEN, J. & RAETZ, M. 2007. High Fe-Ti magmatism and tectonic
1106 setting of the Paleoproterozoic Broken Hill Block, NSW, Australia. *Precambrian*
1107 *Research*, **156**, 55-84.
1108 ROBERTS, D. & GEE, D.G. 1985. An introduction to the structure of the Scandinavian
1109 Caledonides, in GEE D.G. & STURT, B.A. (eds). *The Caledonide Orogen – Scandinavia*
1110 *and related areas.* Wiley, Chichester, 55-68.
1111 ROBINSON, P.T., MALPAS, J., DILEK, Y. & ZHOU, M-F. 2008. The significance of sheeted dike
1112 complexes in ophiolites. *GSA Today*, **18**, 4-10.
1113 RUSHTON, A.W.A., STONE, P.S., SMELLIE, J.L. & TUNNICLIFF, S.P. 1986. An Early Arenig
1114 age for the Pinbain sequence of the Ballantrae Complex. *Scottish Journal of Geology*, **22**,
1115 41-54.
1116 SAEKI, Y. & DATE, J. 1980. Computer application to the alteration data of the footwall dacite
1117 lava at the Ezuri Kuroko deposits, Akita prefecture. *Mining Geology*, **30**, 241-250.
1118 SANDERS, I.S. 1979. Observations on eclogite- and granulite-facies rocks in the basement of
1119 the Caledonides, in HARRIS, A.L., HOLLAND, C.H. & LEAKE, B.E. *The Caledonides of the*
1120 *British Isles: reviewed*. Geological Society, London, Special Publications, **8**, 97-100.

SANDERS, I.S., DALY, J.S. & DAVIES, G.R. 1987. Late Proterozoic high-pressure granulite facies metamorphism in the north-east Ox inlier, north-west Ireland. Journal of Metamorphic Geology, **5**, 69-85.

SCHMIDT, M.W. 1992. Amphibole composition in tonalite as a function of pressure: an experimental calibration of the Al-in-hornblende barometer. *Contributions to Mineralogy and Petrology*, **110**, 304-310.

SHAND, S.J. 1943. Eruptive Rocks. Their genesis, composition, classification, and their relation to ore-deposits with a chapter on meteorite. New York: John Wiley & Sons.

SINTON, J.M., WILSON, D.S., CHRISTIE, D.M., 948 HEY, R.N. & DELANEY, J.R. 1983. Petrologic consequences of rift propagation on oceanic spreading ridges. *Earth and Planetary Science Letters*, **62**, 193-207.

SLAGSTAD, T., DAVIDSEN, B. & DALY, J.S. 2011. Age and composition of crystalline basement rocks on the Norweigan continental margin: offshore extension and continuity of the Caledonian – Appalachian orogenic belt. *Journal of the Geological Society of London*, **168**, 1167-1185.

SPRAY, J.G. & DUNNING, G.R. 1991. A U/Pb age for the Shetland Islands oceanic fragment, Scottish Caledonides - evidence from anatectic plagiogranites in layer 3 shear zones. *Geological Magazine*, **128**, 667-671.

SPITZ, G. & DARLING, R. 1978. Major and minor element lithogeochemical anomalies surrounding the Louvem copper deposit, Val d'Or, Quebec. *Canadian Journal of Earth Sciences*, **15**, 1161-1169.

STONE, P. & RUSHTON, A.W.A. 1983. Graptolite faunas from the Ballantrae ophiolite complex and their structural implications. *Scottish Journal of Geology*, **19**, 297-310.

STONE, P. & STRACHAN, I. 1981. A fossiliferous borehole section within the Ballantrae ophiolite. *Nature*, **293**, 455-456.

THIRLWALL, M.F. & BLUCK, B.J. 1984. Sr-Nd isotope and geological evidence that the Ballantrae "ophiolite", SW Scotland, is polygenetic, in GASS, I.G., LIPPARD, S.J. & SHELTON, A.W. (eds). *Ophiolites and oceanic lithosphere.* Journal of the Geological Society of London Special Publications, **13**, 215-230.

VAN STAAL, C.R., WHALEN, J.B., MCNICOLL, V.J., PEHRSSON, S.J., LISSENBERG, C.J., ZAGOREVSKI, A., VAN BREEMAN, O. & JENNER, G.A. 2007. The Notre Dame arc and the Taconic Orogeny in Newfoundland, in HATCHER, J., CARLSON, M.P., MCBRIDE, J.H., AND MARTÍNEZ CATALÁN, J.R., (eds). *The 4D framework of continental crust*. Geological Society of America, Memoirs, **200**, 511-552.

VAN STAAL, C.R., WHALEN, .J.B., VALVERDE-VAQUERO, P., ZAGOREVSKI, A. & ROGERS, N. 2009. Pre-Carboniferous, episodic accretion-related, orogenesis along the Laurentian margin of the northern Appalachians, in MURPHY, J.B., KEPPIE, J.D. & HYNES, A.J. (eds). *Ancient Orogens and Modern Analogues.* Geological Society of London, Special Publications, **327**, 271-316.

WALDRON, J.W.F. & VAN STAAL, C.R. 2001. Taconian Orogeny and the accretion of the Dashwoods Block: a peri-Laurentian microcontinent in the Iapetus Ocean. *Geology*, **29**, 811-814.

WHALEN, J.B., CURRIE, K.L. & VAN BREEMEN, O. 1987. Episodic Ordovician – Silurian plutonism in the Topsails igneous terrane, western Newfoundland. *Transactions of the Royal Society of Edinbugh: Earth Sciences*, **78**, 17-28.

WHALEN, J.B., JENNER, G.A., LONGSTAFFE, F.J., GARIEPY, C. & FRYER, B.J. 1997. Implications of granitoid geochemical and isotopic (Nd, O, Pb) data from the Cambrian-Ordovician Notre Dame arc for the evolution of the Central Mobile Belt, Newfoundland Appalachians, in SINHA, A.K., WHALEN, J.B. & HOGAN, J.P. *The nature of magmatism in the Appalachian orogen*. Geological Society of America, Memoir, **191**, 367-395.

WOOD, D.A. 1980. The application of a Th-Hf-Ta diagram to problems of tectonomagmatic classification and to establishing the nature of crustal contamination of basaltic lavas of the British Tertiary volcanic province. *Earth and Planetary Science Letters*, **50**, 11-30.

YOUNG, S.A., SALTZMAN, M.R., FOLAND, K.A., LINDER, J.S. & KUMP, L.R. 2009. A major drop in seawater $^{87}Sr/^{86}Sr$ during the Middle Ordovician (Darriwilian): Links to volcanism and climate? *Geology*, **37**, 951-954.

ZAGOREVSKI, A. & VAN STAAL., C.R. 2011. The Record of Ordovician Arc-Arc and Arc-Continent Collisions in the Canadian Appalachians During the Closure of Iapetus: in BROWN, D., AND RYAN, P.D. (eds.). *Arc-Continent Collision*, Frontiers in Earth Sciences, 341-371.

ZAGOREVSKI, A., ROGERS, N., VAN STAAL, C.R., MCNICOLL, V., LISSENBERG, C.J. & VALVERDE-VAQUERO, P. 2006. Lower to Middle Ordovician evolution of peri-Laurentian arc and back-arc complexes in Iapetus: constraints from the Annieopsquotch Accretionary Tract, central Newfoundland. *Geological Society of America Bulletin*, **118**, 324-342.

ZAGOREVSKI, A., LISSENBERG, C.J. & VAN STAAL, C.R. 2009. Dynamics of accretion of arc and backarc crust to continental margins: Inferences from the Annieopsquotch accretionary tract, Newfoundland Appalachians. *Tectonophysics*, **479**, 150-164.

ZAGOREVSKI, A., VAN STAAL, C.R. & ROGERS, N. 2012. Making and breaking of an arc: recurring extensional magmatism in the Annieopsquotch Accretionary Tract, Newfoundland Appalachians. GAC-MAC-AGC-AMC Joint Annual Meeting, St. Johns 2012. Abstract Volume 35, p.154.

ZHANG, W. & FYFE, W. 1995. Chloritization of the hydrothermally altered bedrock at the Igarapé Bahia gold deposit, Carajás, Brazil. *Mineralium Deposita*, **30**, 30-38.

FIGURES

Fig. 1 (a) Setting of the Tyrone Igneous Complex and other comparable ophiolite and volcanic arc associations in Britain and Ireland. (b) Simplified regional geology of Newfoundland (c) Early Mesozoic restoration of North Atlantic region and Appalachian-Caledonian orogen. Figure after Cooper *et al.* (2001).

Fig. 2. Geological map of the Tyrone Igneous Complex (after GSNI 1879, 1983, 1995; Cooper *et al.* 2011; Hollis *et al.* 2012). For subdivision of the Tyrone Volcanic Group see Hollis *et al.* (2012). Stars refer to localities discussed in the text.

Fig. 3. ***FIGURE IN COLOUR IN PRINT*** Field photographs from across the Tyrone Plutonic Group. (A) Pegmatitic gabbros (light coloured rock above hammer head) intruding, and intruded by, dolerite/basaltic dykes (dark coloured rock) at Black Rock, (B) Angular xenoliths (right of hammer) of early foliated dolerite/gabbro in hornblende gabbro at Black Rock, (C) Dolerite intruded by a dyke of quartz and hornblende porphyryitic diorite at Slaghtfreeden (D) Dolerite cut by veins of aplite at Craigballyharky Quarry, (E) Pillow basalts at Craigballyharky, (F) Quartz ocelli migrating from tonalite into gabbro at Craigballyharky.

Fig. 4. ***FIGURE IN COLOUR IN PRINT*** Field photographs and petrography from Blaeberry Rock and the Tyrone Plutonic Group. (A) Main Blaeberry Rock exposure, (B) Blocks of amphibolite facies gabbro (right) and andesite(?) (left), (C) Angular block of amphibolite-facies basalt in granitic-tonalitic intrusive material, (D) Late stage granitic-tonalitic veins crosscutting main fabrics, (E) Isoclinally folded tonalitic to granitic melt and amphibolite, (F) Sinistrally rotated amphibole crystals in melt network.

Fig. 5. ***FIGURE IN COLOUR IN PRINT*** Results of the Tellus airborne geophysical survey of Northern Ireland. (a) EM low frequency (ApCond), (b) Total magnetic intensity, analytic signal (TMI-AS). All maps show original GSNI linework (GSNI 1879, 1983 and 1995). Grid references are according to Irish Grid. Dashed lines denote interpreted faults/unconformities. Heavier set lines show the boundaries between the Tyrone Volcanic Group, Tyrone Plutonic Group and Tyrone Central Inlier. Question marks show the position of magnetic material of unknown affinity underlying the Tyrone Central Inlier.

1234 Fig. 6. Geochemistry of the Tyrone Plutonic Group and associated rocks discussed herein.
1235 (A) Al_2O_3/Na_2O ratio of Spitz and Darling (1978) against SiO_2, (B) Carbonate-chlorite-pyrite
1236 Index of Large *et al.* (2001) against Zr/TiO_2, (C) Zr/Y against Nb/Y, (D) Th_{CN} against Ti/V,
1237 (E) La/Sm_{CN} against Nb anomaly (calculated from Th and La), (F) Th/Yb against Nb/Yb
1238 (after Pearce, 1983). Data of Draut *et al.* (2009) and Cooper *et al.* (2011) also included. CN
1239 refers to chondrite normalized (after McDonough and Sun 1995). Shaded and dashed fields
1240 reflect data for the Tyrone Plutonic Group and Annieopsquotch Ophiolite Belt respectively
1241 (from Lissenberg *et al.* 2004).
1242
1243 Fig. 7. Multi-element variation diagrams for samples from the Tyrone Plutonic Group,
1244 Blaeberry Rock and arc-related intrusive suite. Chondrite normalization values after
1245 McDonough and Sun (1995). Analyses of Draut *et al.* (2009), Cooper *et al.* (2011), and Hollis
1246 *et al.* (2012, companion publication) are also included. Shaded field represents data from the
1247 Annieopsquotch Ophiolite Belt (from Lissenberg *et al.* 2004).
1248
1249 Fig. 8. Mineral chemistry of samples from Black Rock (SPH34) and Blaeberry Rock
1250 (SPH210 and SPH215). (A) Amphibole mineral chemistry; (B) Feldspar mineral chemistry
1251 from Blaeberry Rock sample SPH215; (C) and (D) Chlorite mineral chemistry.
1252
1253 Fig. 9. U-Pb zircon concordia and summary of interpreted U-Pb zircon date for pegmatitic
1254 gabbro from Black Rock.
1255
1256 Fig. 10. Tectonic model for the evolution of the Tyrone Plutonic Group. After model for the
1257 development of the Annieopsquotch Ophiolite Belt (Zagorevski *et al.* 2006). eMORB,
1258 enriched Mid Ocean Ridge basalt; IAT, island arc tholeiite; OIB, ocean island basalt.
1259
1260 **SUPPLEMENTARY INFORMATION**
1261
1262 *Petrographic photographs, whole rock, isotopic and mineral geochemical data, and U-Th-Pb*
1263 *isotopic data.*
1264
1265 Petrography photographs: Figure 4g-h. SEM microphotographs of amphibolite-facies
1266 gabbroic material from Blaeberry Rock contact, (I) Thin section photograph of contact
1267 between amphibolite and tonalitic/granitic material at Blaeberry Rock (J) SEM
1268 microphotograph of Black Rock pegmatitic gabbro from the Tyrone Plutonic Group.
1269
1270 Table 1. Whole rock geochemistry, and Sm-Nd and Rb-Sr isotope data. Samples with MRC
1271 prefixes from Cooper *et al.* 2011.

1272
1273 Table 2(a-d). Mineral chemical data. (a) Chlorite (calculated after 28 oxygens). (b) Epidote
1274 (after 12.5 oxygens). All Fe calculated to Fe3+. (c) Amphibole (after 23 oxygens). (d)
1275 Feldspar.
1276
1277 Table 3. U-Th-Pb isotopic data for sample MRC344.

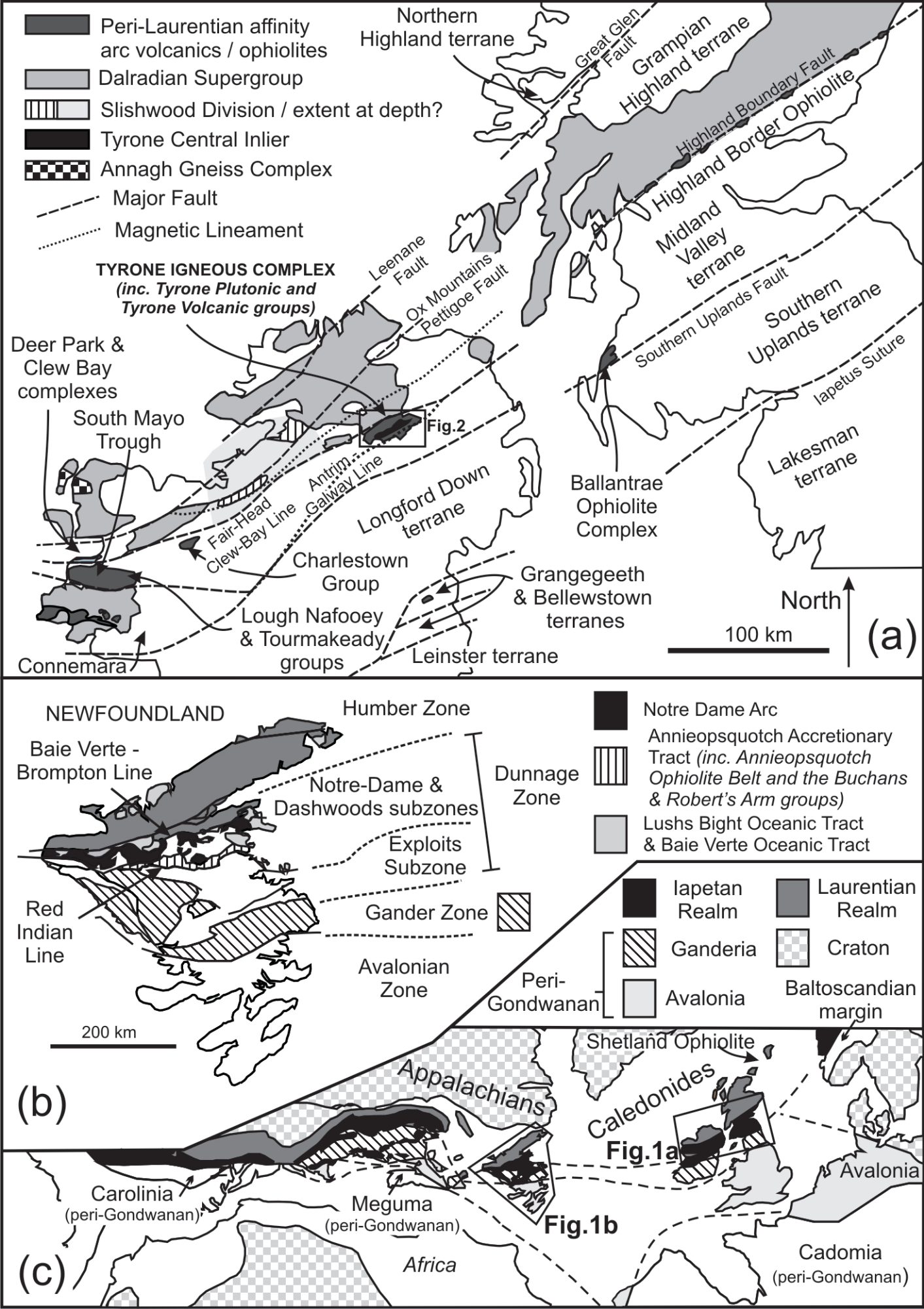
Peri-Laurentian affinity arc volcanics / ophiolites
Dalradian Supergroup
Slishwood Division / extent at depth?
Tyrone Central Inlier
Annagh Gneiss Complex
Major Fault
Magnetic Lineament
Northern Highland terrane
Great Glen Fault
Grampian Highland terrane
Highland Boundary Fault
Highland Border Ophiolite
Midland Valley terrane
Southern Uplands Fault
Southern Uplands terrane
Iapetus Suture
Lakesman terrane
Ballantrae Ophiolite Complex
TYRONE IGNEOUS COMPLEX
(inc. Tyrone Plutonic and Tyrone Volcanic groups)
Leenane Fault
Ox Mountains Pettigoe Fault
Deer Park & Clew Bay complexes
South Mayo Trough
Fig.2
Antrim - Galway Line
Fair-Head Clew-Bay Line
Longford Down terrane
Charlestown Group
Grangegeeth & Bellewstown terranes
Lough Nafooey & Tourmakeady groups
Leinster terrane
Connemara
North
100 km
(a)
NEWFOUNDLAND
Humber Zone
Baie Verte - Brompton Line
Notre-Dame & Dashwoods subzones
Dunnage Zone
Exploits Subzone
Red Indian Line
Gander Zone
Avalonian Zone
200 km
(b)
Notre Dame Arc
Annieopsquotch Accretionary Tract (inc. Annieopsquotch Ophiolite Belt and the Buchans & Robert's Arm groups)
Lushs Bight Oceanic Tract & Baie Verte Oceanic Tract
Iapetan Realm
Laurentian Realm
Ganderia
Craton
Peri-Gondwanan
Avalonia
Baltoscandian margin
Shetland Ophiolite
Appalachians
Caledonides
Fig.1a
Avalonia
Carolinia (peri-Gondwanan)
Meguma (peri-Gondwanan)
Fig.1b
Africa
Cadomia (peri-Gondwanan)
(c)

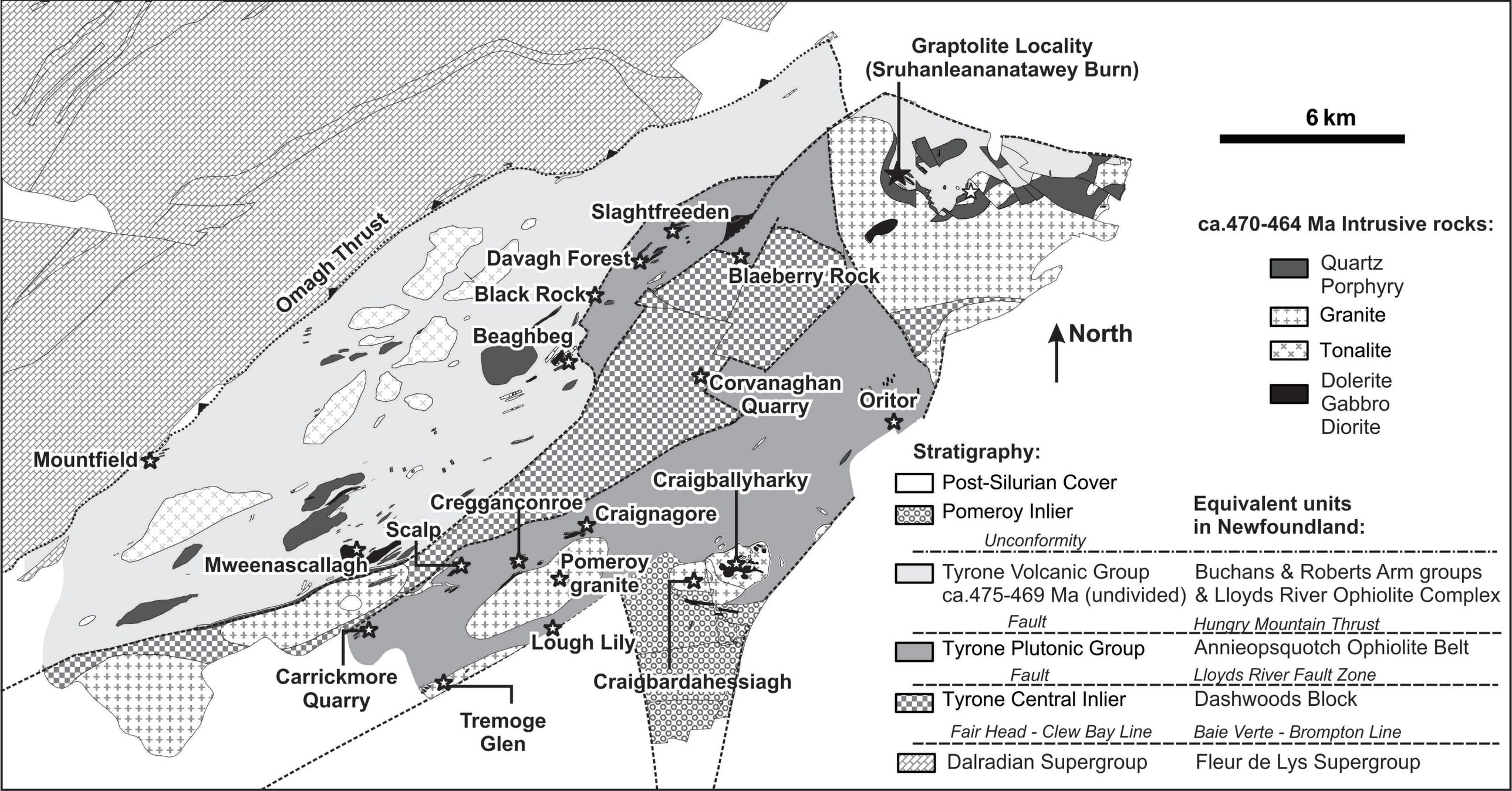
Graptolite Locality
(Sruhanleananatawey Burn)
6 km
Omagh Thrust
Slaghtfreeden
Davagh Forest
Blaeberry Rock
Black Rock
Beaghbeg
Corvanaghan
Quarry
Oritor
North
Mountfield
Craigballyharky
Cregganconroe
Craignagore
Scalp
Mweenascallagh
Pomeroy
granite
Lough Lily
Carrickmore
Quarry
Craigbardahessiagh
Tremoge
Glen
ca.470-464 Ma Intrusive rocks:
Quartz
Porphyry
Granite
Tonalite
Dolerite
Gabbro
Diorite
Stratigraphy:
Post-Silurian Cover
Pomeroy Inlier
Unconformity
Tyrone Volcanic Group
ca.475-469 Ma (undivided)
Fault
Tyrone Plutonic Group
Fault
Tyrone Central Inlier
Fair Head - Clew Bay Line
Dalradian Supergroup
Equivalent units
in Newfoundland:
Buchans & Roberts Arm groups
& Lloyds River Ophiolite Complex
Hungry Mountain Thrust
Annieopsquotch Ophiolite Belt
Lloyds River Fault Zone
Dashwoods Block
Baie Verte - Brompton Line
Fleur de Lys Supergroup

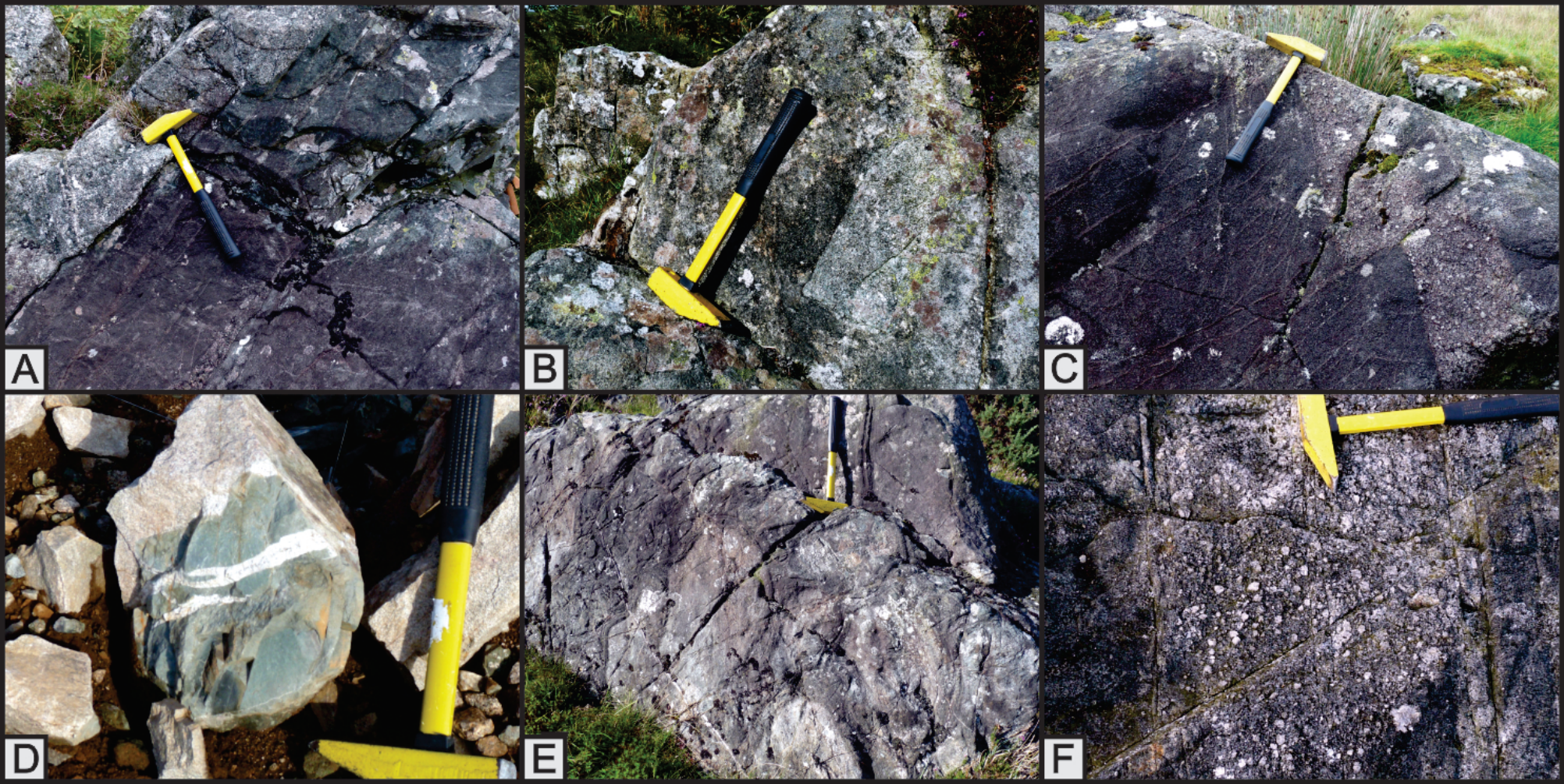
A
B
C
D
E
F

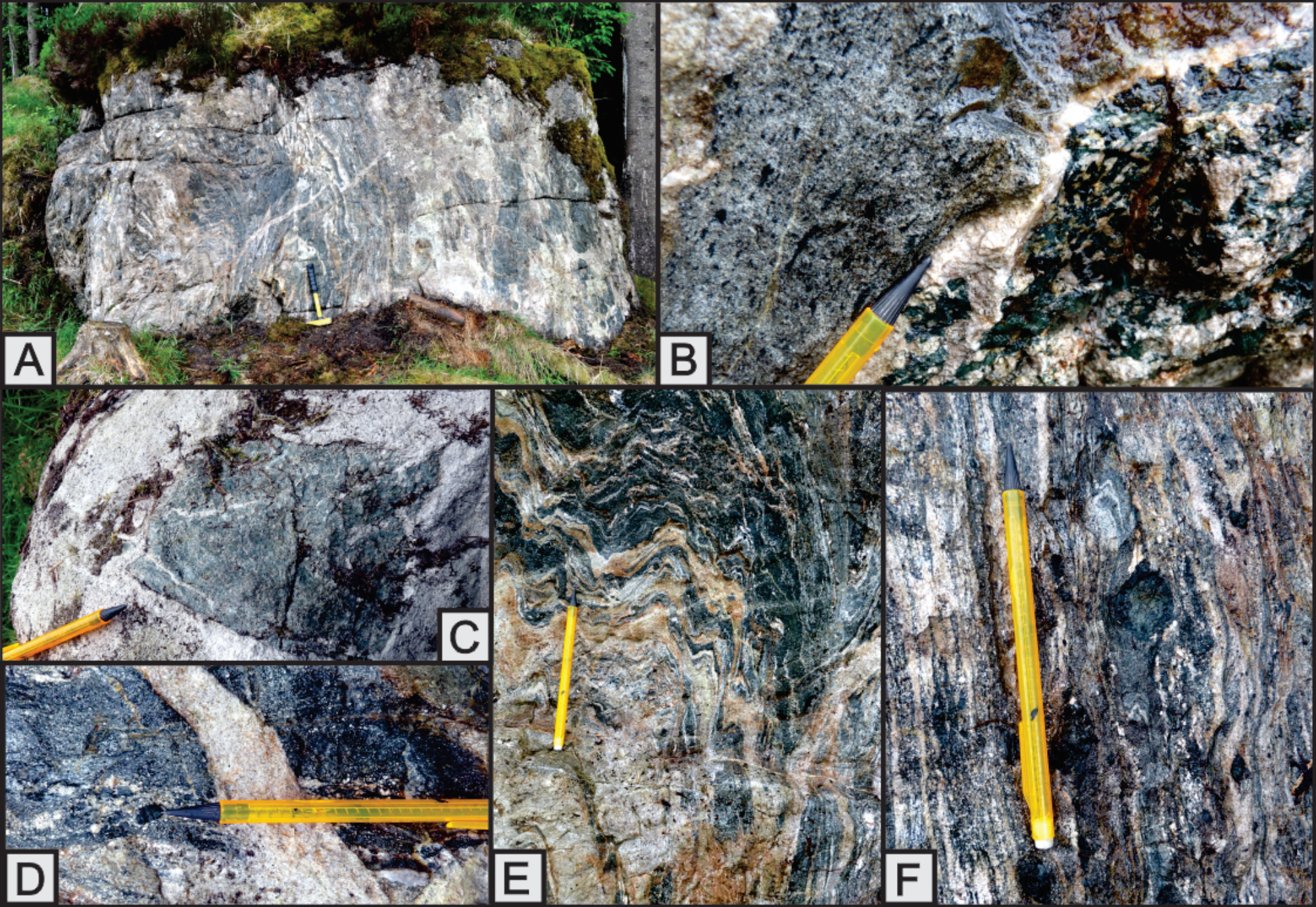
A
B
C
D
E
F

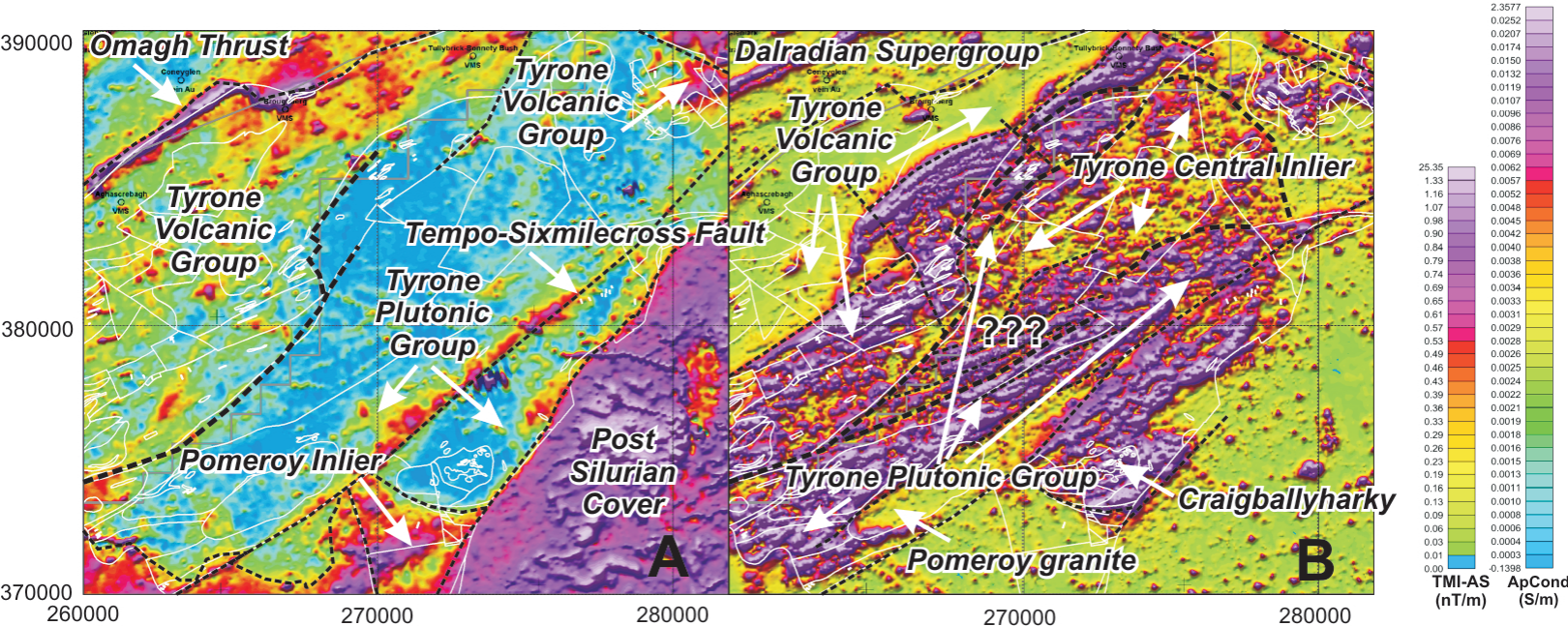
Omagh Thrust
Tyrone Volcanic Group
Tyrone Volcanic Group
Tempo-Sixmilecross Fault
Tyrone Plutonic Group
Pomeroy Inlier
Post Silurian Cover
A
Dalradian Supergroup
Tyrone Volcanic Group
Tyrone Central Inlier
???
Tyrone Plutonic Group
Craigballyharky
Pomeroy granite
B
390000
380000
370000
260000
270000
280000
270000
280000
TMI-AS (nT/m)
ApCond (S/m)

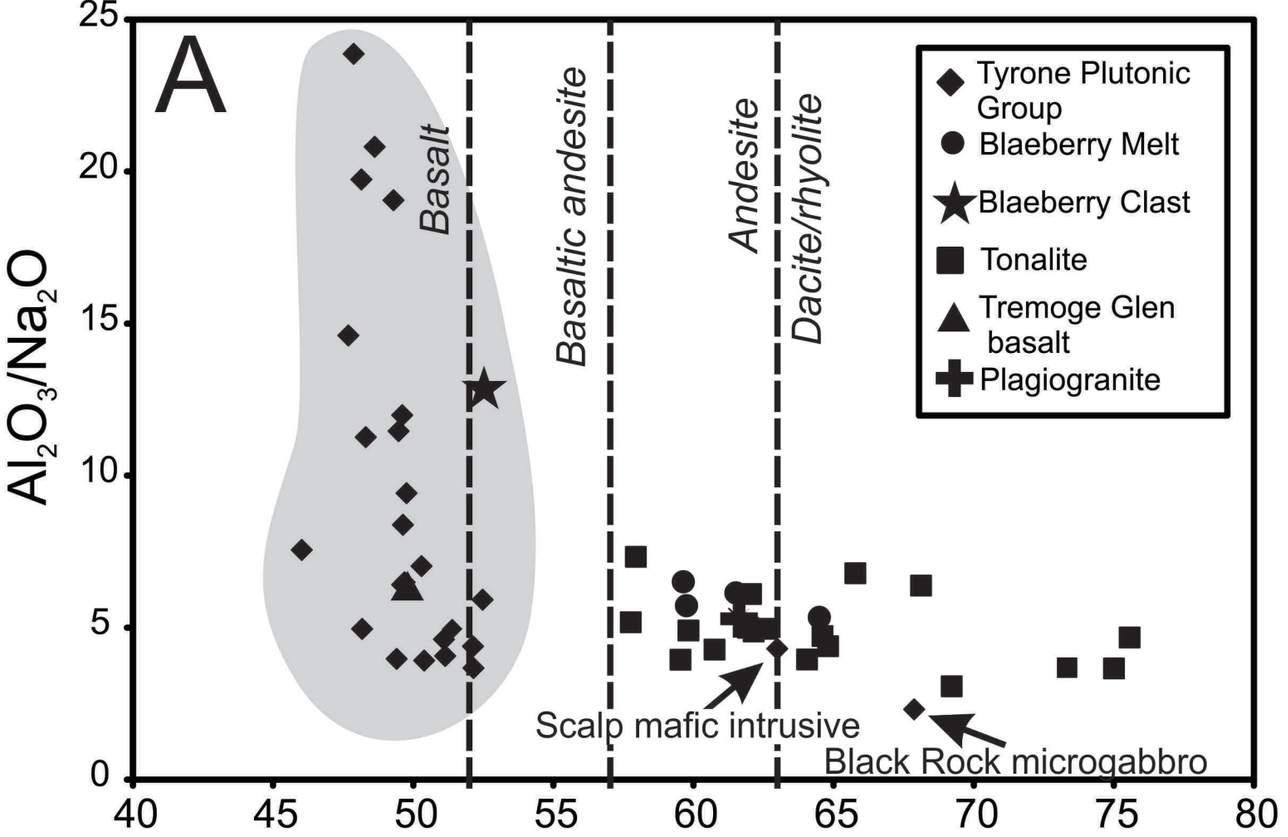
A
Basalt
Basaltic andesite
Andesite
Dacite/rhyolite
Tyrone Plutonic Group
Blaeberry Melt
Blaeberry Clast
Tonalite
Tremoge Glen basalt
Plagiogranite
Scalp mafic intrusive
Black Rock microgabbro
Al2O3/Na2O

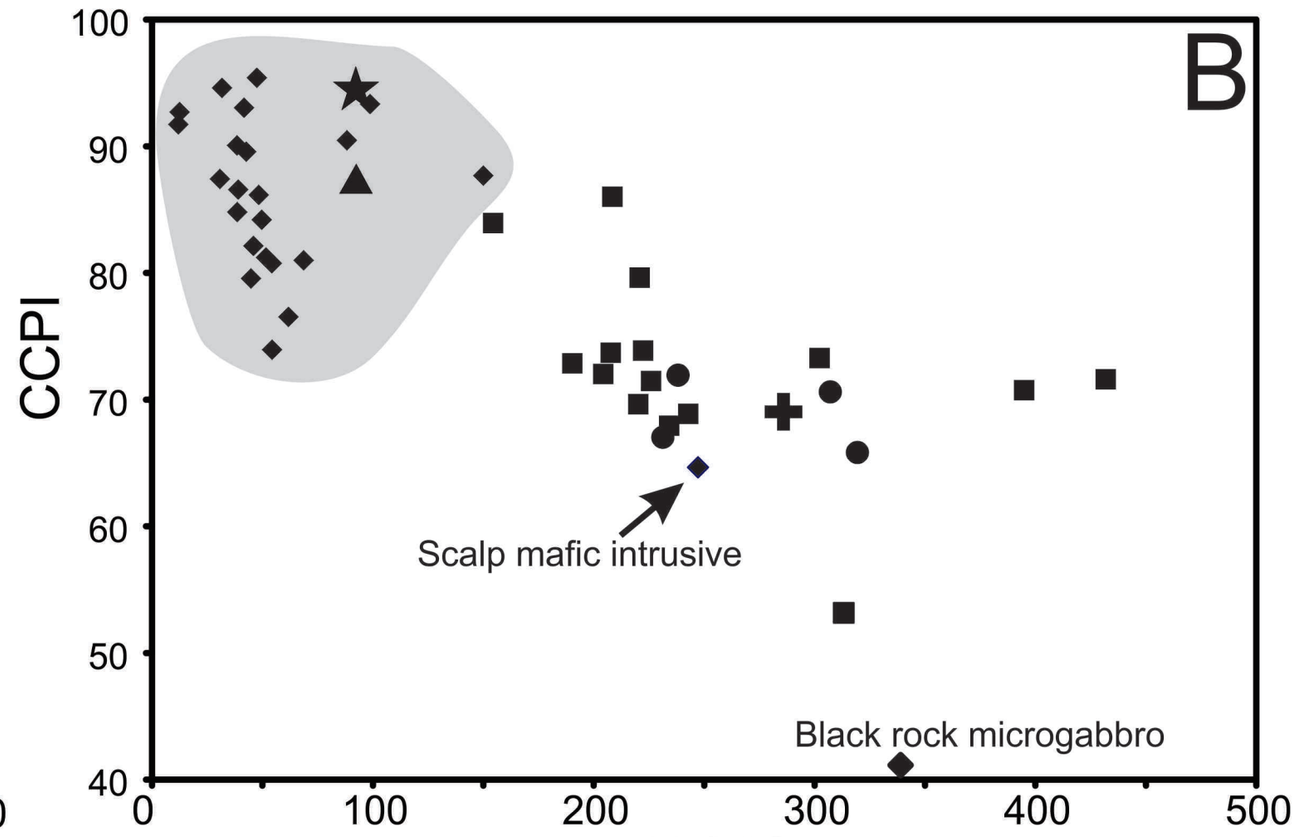
B
CCPI
Scalp mafic intrusive
Black rock microgabbro

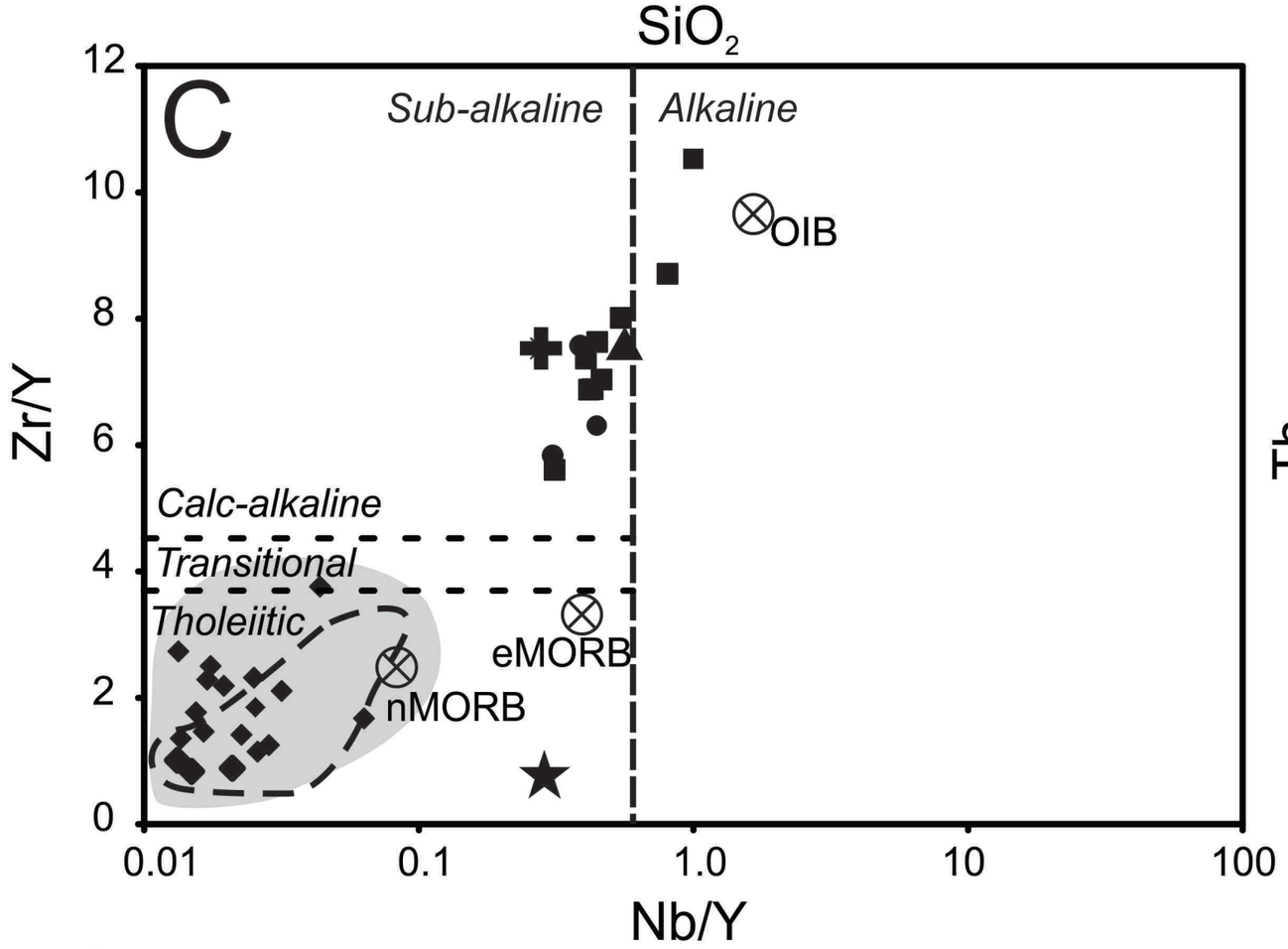
C
Sub-alkaline
Alkaline
Calc-alkaline
Transitional
Tholeiitic
OIB
eMORB
nMORB
Zr/Y
Nb/Y
SiO2

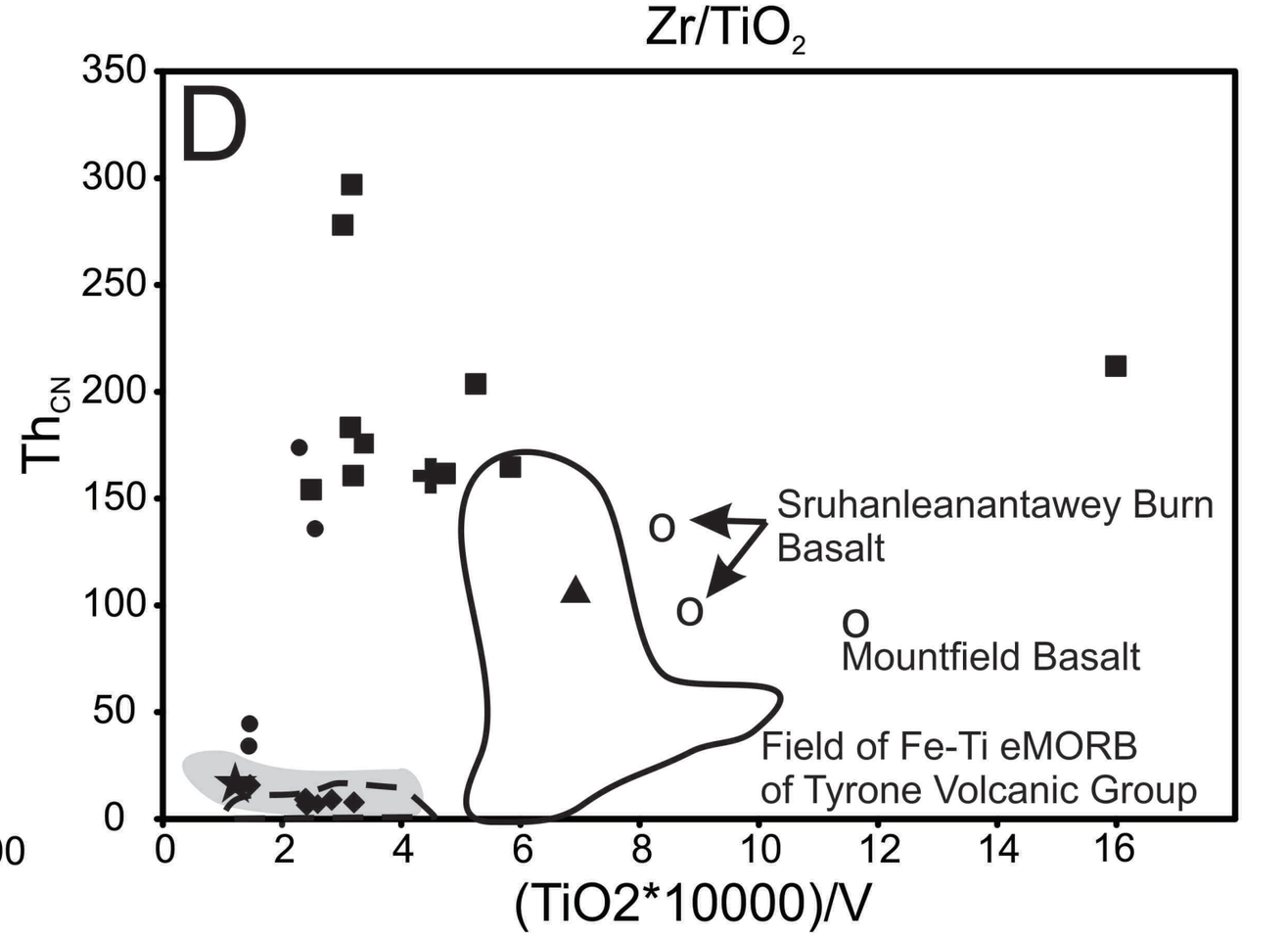
D
Sruhanleanantawey Burn Basalt
Mountfield Basalt
Field of Fe-Ti eMORB of Tyrone Volcanic Group
ThCN
(TiO2*10000)/V
Zr/TiO2

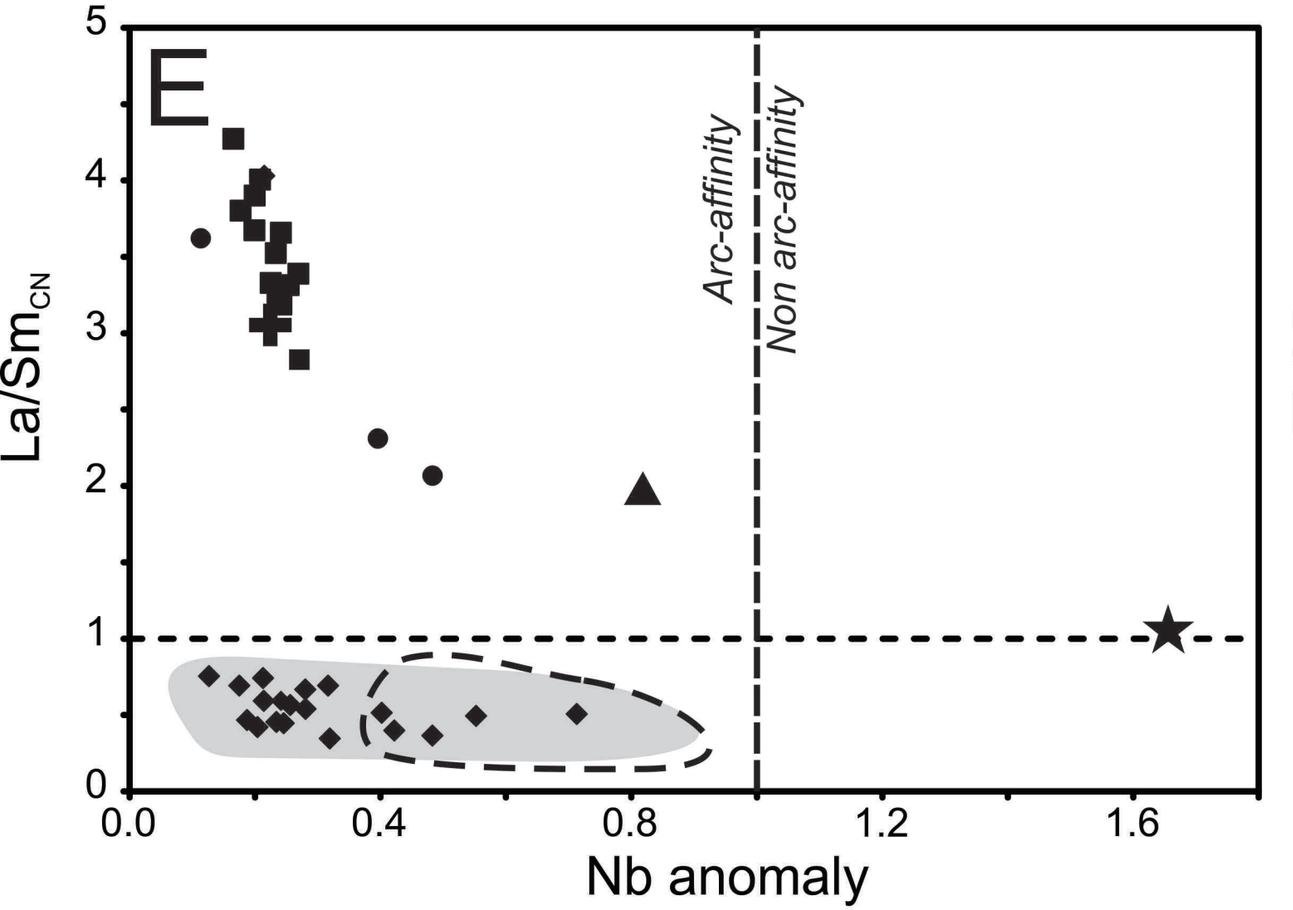
E
Arc-affinity
Non arc-affinity
La/SmCN
Nb anomaly

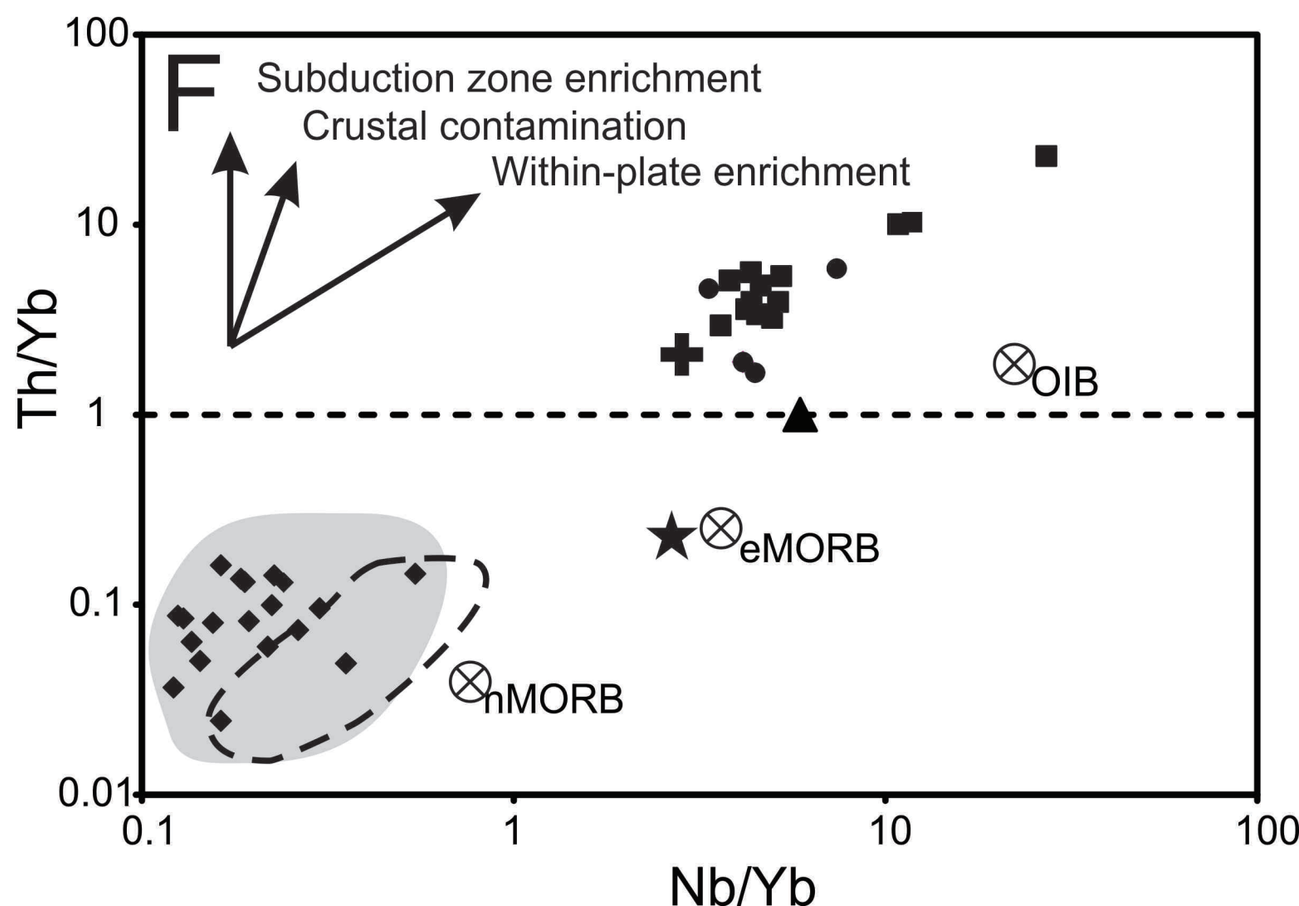
F
Subduction zone enrichment
Crustal contamination
Within-plate enrichment
OIB
eMORB
nMORB
Th/Yb
Nb/Yb

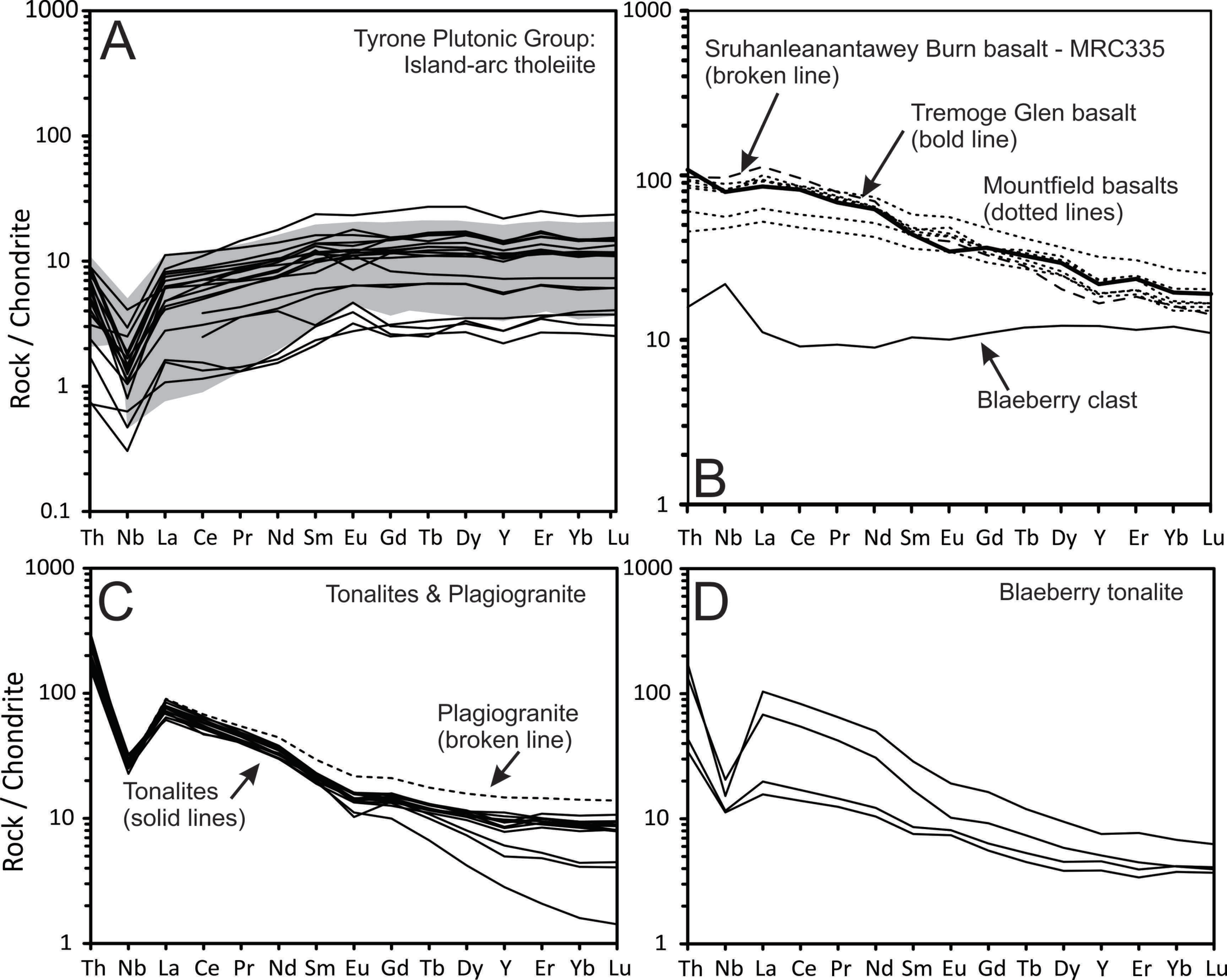
A
Tyrone Plutonic Group:
Island-arc tholeiite
Rock / Chondrite
1000
100
10
1
0.1
Th Nb La Ce Pr Nd Sm Eu Gd Tb Dy Y Er Yb Lu
B
Sruhanleanantawey Burn basalt - MRC335
(broken line)
Tremoge Glen basalt
(bold line)
Mountfield basalts
(dotted lines)
Blaeberry clast
C
Tonalites & Plagiogranite
Plagiogranite
(broken line)
Tonalites
(solid lines)
D
Blaeberry tonalite

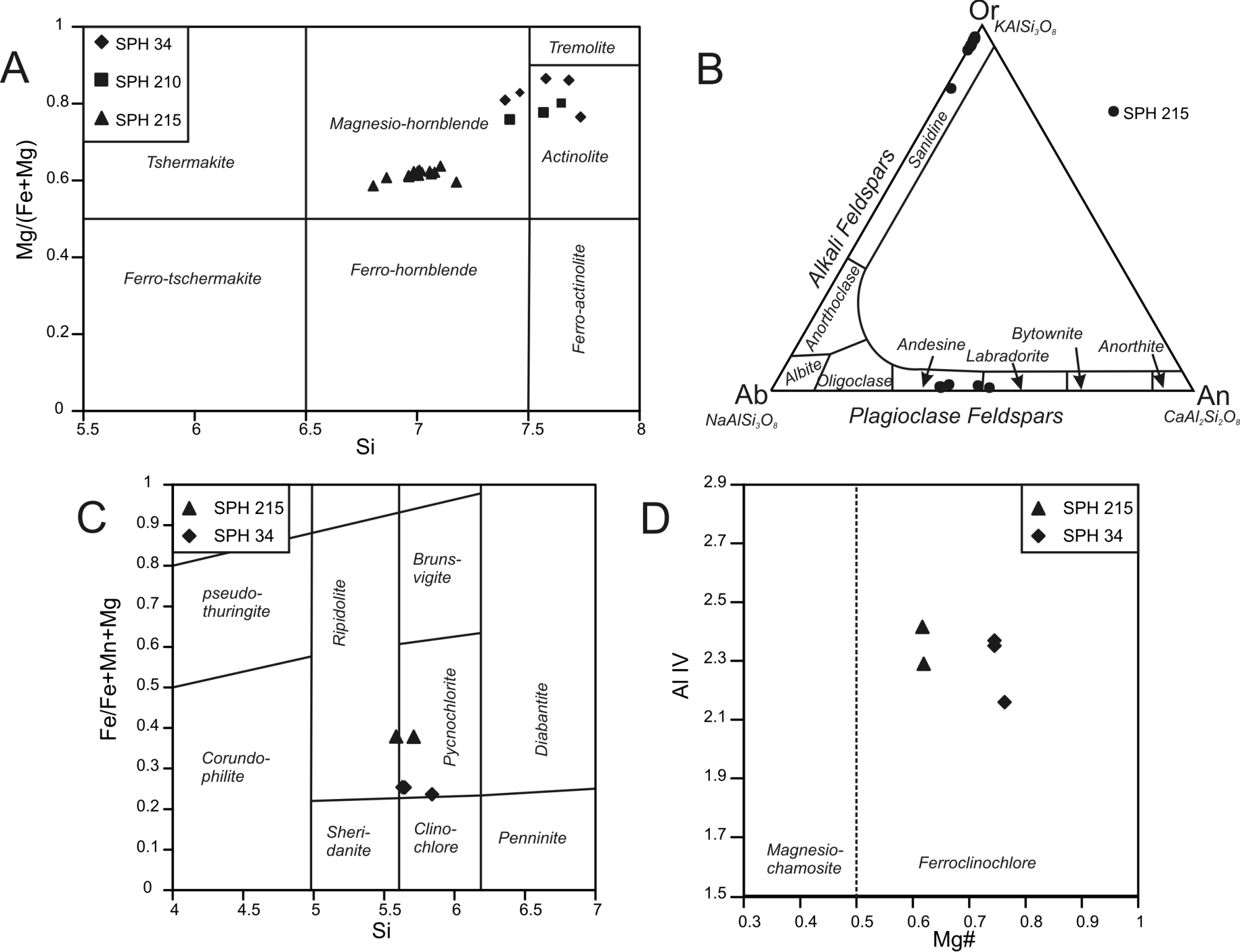
A
SPH 34
SPH 210
SPH 215
Tremolite
Magnesio-hornblende
Tshermakite
Actinolite
Ferro-tschermakite
Ferro-hornblende
Ferro-actinolite
Mg/(Fe+Mg)
Si
B
Or
KAlSi3O8
SPH 215
Alkali Feldspars
Sanidine
Anorthoclase
Albite
Oligoclase
Andesine
Labradorite
Bytownite
Anorthite
Ab
NaAlSi3O8
An
CaAl2Si2O8
Plagioclase Feldspars
C
SPH 215
SPH 34
pseudo-thuringite
Ripidolite
Bruns-vigite
Pycnochlorite
Diabantite
Corundo-philite
Sheri-danite
Clino-chlore
Penninite
Fe/Fe+Mn+Mg
Si
D
SPH 215
SPH 34
Al IV
Magnesio-chamosite
Ferroclinochlore
Mg#

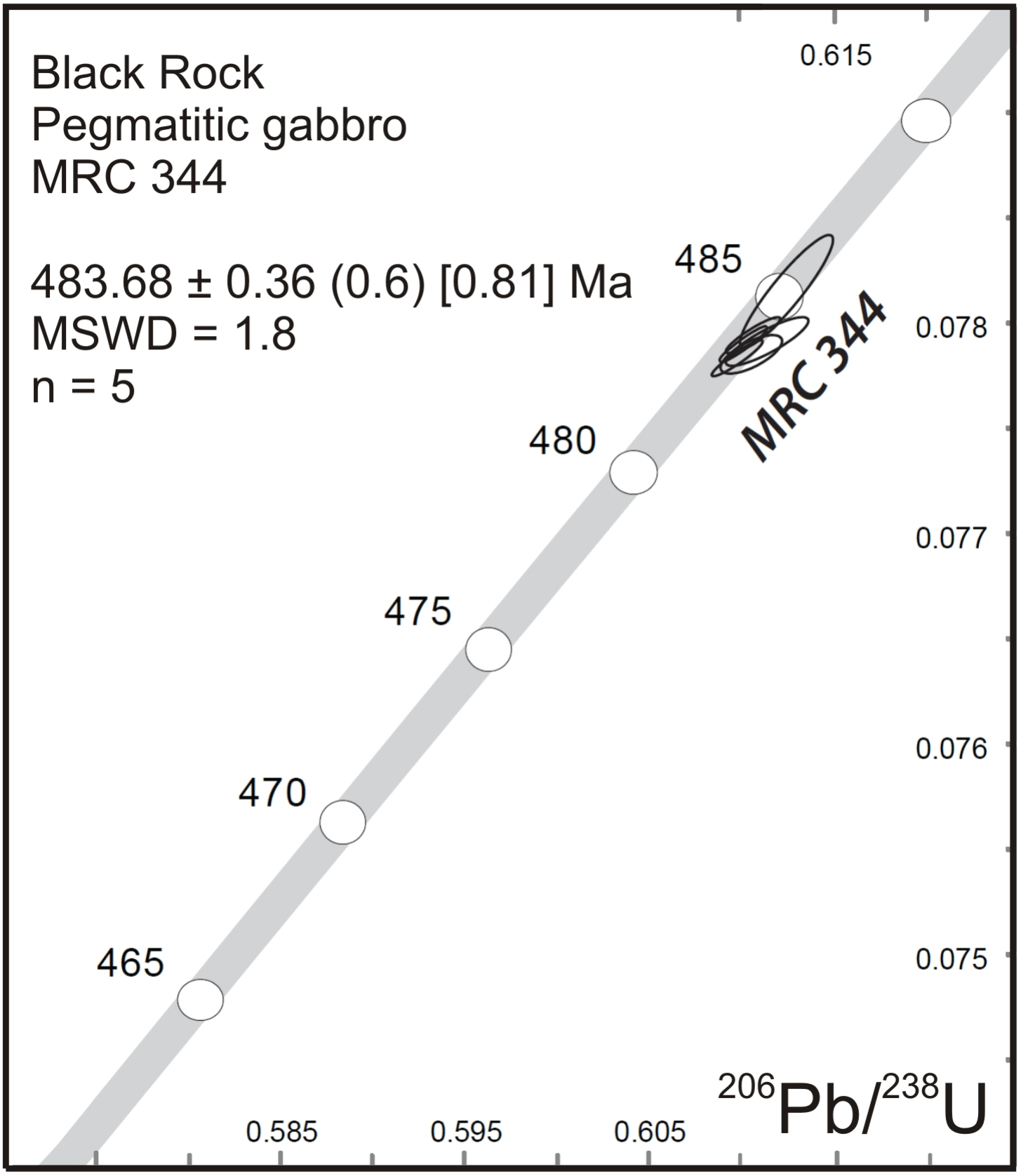
Black Rock
Pegmatitic gabbro
MRC 344
483.68 ± 0.36 (0.6) [0.81] Ma
MSWD = 1.8
n = 5
MRC 344
485
480
475
470
465
0.615
0.078
0.077
0.076
0.075
0.585
0.595
0.605
$^{207}Pb/^{235}U$
$^{206}Pb/^{238}U$

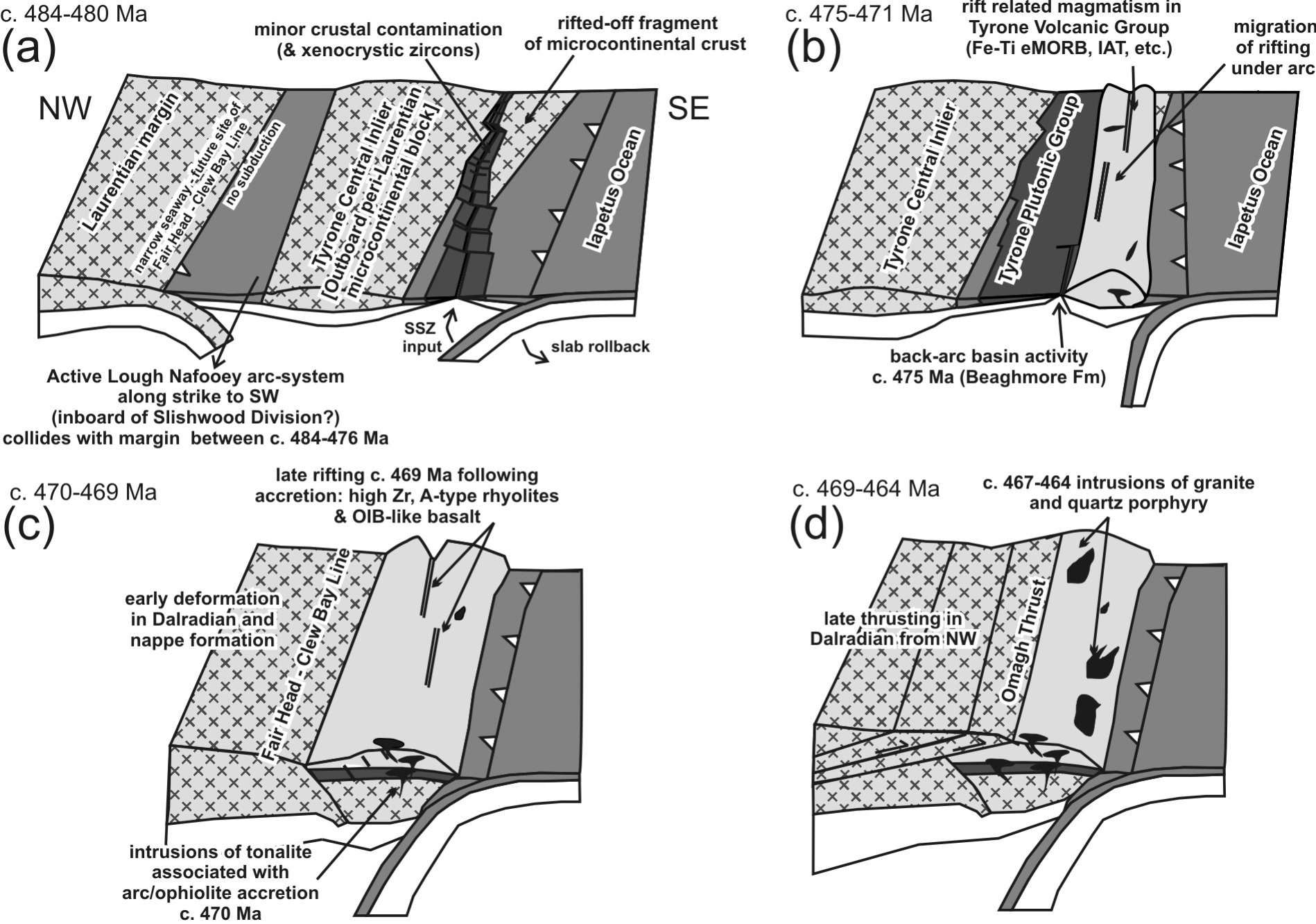
c. 484-480 Ma
(a)
minor crustal contamination
(& xenocrystic zircons)
rifted-off fragment
of microcontinental crust
NW
SE
Laurentian margin
narrow seaway - future site of
Fair Head - Clew Bay Line
no subduction
Tyrone Central Inlier
[Outboard peri-Laurentian
microcontinental block]
Iapetus Ocean
SSZ
input
slab rollback
Active Lough Nafooey arc-system
along strike to SW
(inboard of Slishwood Division?)
collides with margin between c. 484-476 Ma
c. 475-471 Ma
(b)
rift related magmatism in
Tyrone Volcanic Group
(Fe-Ti eMORB, IAT, etc.)
migration
of rifting
under arc
Tyrone Central Inlier
Tyrone Plutonic Group
Iapetus Ocean
back-arc basin activity
c. 475 Ma (Beaghmore Fm)
c. 470-469 Ma
(c)
late rifting c. 469 Ma following
accretion: high Zr, A-type rhyolites
& OIB-like basalt
early deformation
in Dalradian and
nappe formation
Fair Head - Clew Bay Line
intrusions of tonalite
associated with
arc/ophiolite accretion
c. 470 Ma
c. 469-464 Ma
(d)
c. 467-464 intrusions of granite
and quartz porphyry
late thrusting in
Dalradian from NW
Omagh Thrust

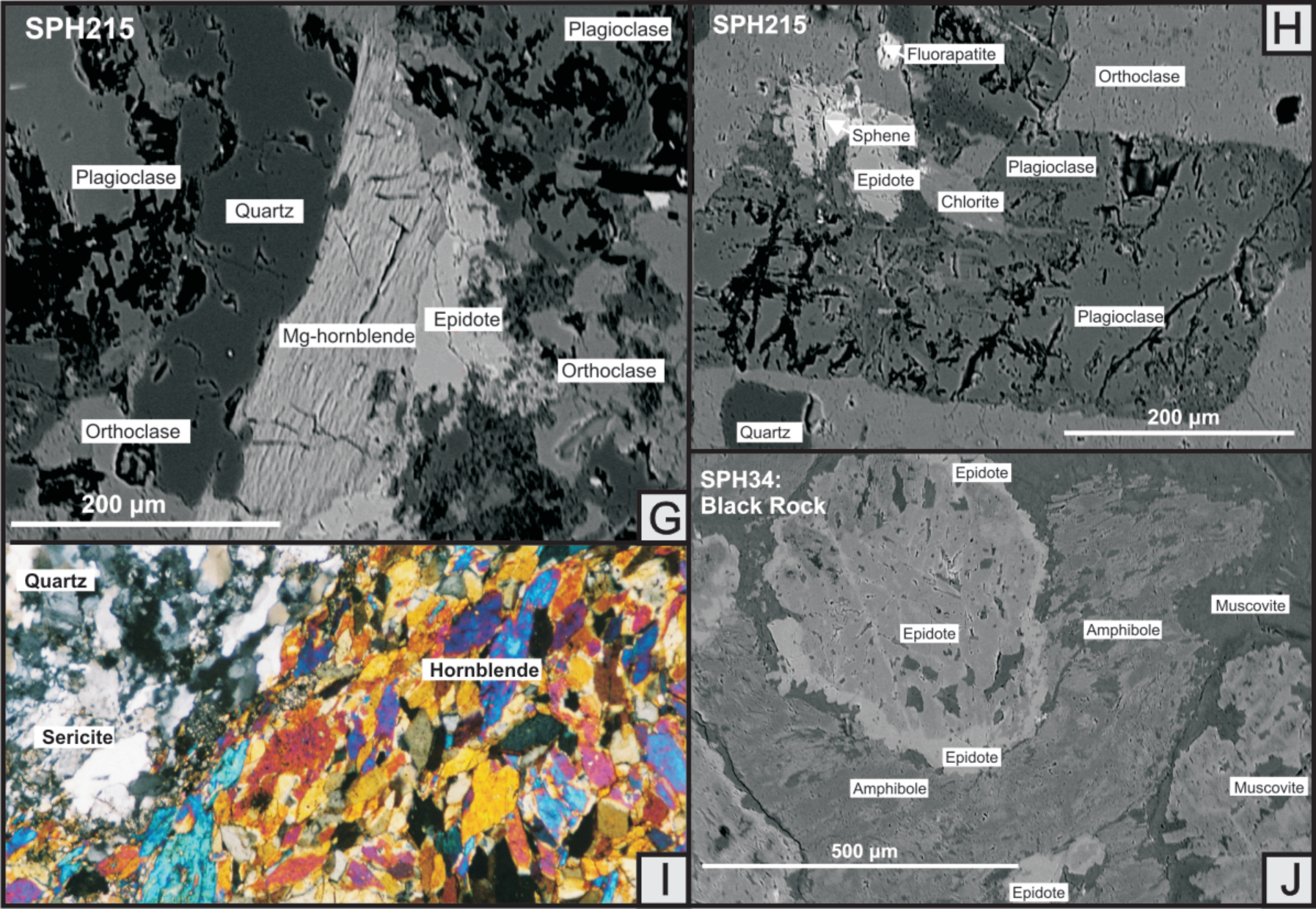
SPH215
Plagioclase
Plagioclase
Quartz
Epidote
Mg-hornblende
Orthoclase
Orthoclase
200 µm
G
SPH215
H
Fluorapatite
Orthoclase
Sphene
Plagioclase
Epidote
Chlorite
Plagioclase
Quartz
200 µm
Quartz
Hornblende
Sericite
I
SPH34:
Black Rock
Epidote
Muscovite
Epidote
Amphibole
Epidote
Amphibole
Muscovite
500 µm
Epidote
J

				Determined by (italics = isotope dilution):	XRF	XRF	XRF	XRF	XRF	XRF	XRF	XRF	XRF	XRF		
				Units:	wt.%	wt.%	wt.%	wt.%	wt.%	wt.%	wt.%	wt.%	wt.%	wt.%		
Sample	**Locality**	**Easting**	**Northing**	**Lithology (all meta-)**	**SiO2**	**TiO2**	**Al2O3**	**Fe2O3t**	**Mn3O4**	**MgO**	**CaO**	**K2O**	**Na2O**	**P2O5**	**LOI**	**Sample**
JTP 207	Scalp Hill	263900	374400	Layered gabbro	48.31	0.37	21.97	6.15	0.12	5.53	12.91	0.59	1.95	0.03	1.75	JTP 207
JTP 211	Black Rock	268350	383810	Gabbro	47.69	0.24	15.92	10.12	0.20	9.54	11.38	0.46	1.09	0.01	3.23	JTP 211
MRC 129	Tremoge Glen	262800	371250	Basaltic dyke	49.61	2.69	12.76	15.37	0.26	4.80	3.51	0.91	1.99	0.39	7.06	MRC 129
MRC 340	Craigballyharky	273360	375660	Basalt	52.15	0.58	14.51	8.58	0.18	7.73	11.84	0.24	3.95	0.04	0.96	MRC 340
MRC 343	Craigballyharky Quarry	273320	375650	Dolerite	49.41	0.91	15.60	9.81	0.19	8.95	9.67	0.41	3.93	0.08	1.61	MRC 343
MRC 344	Black Rock	268360	383430	Pegmatitic gabro	47.88	0.12	16.47	7.21	0.16	10.33	14.47	0.62	0.69	0.01	2.93	MRC 344
SPH 030	Craigballyharky	273360	375660	Basalt	51.15	0.63	15.45	9.87	0.15	7.93	11.29	0.29	3.80	0.06	1.19	SPH 030
SPH 034	Black Rock	268360	383430	Pegmatitic gabro	48.63	0.13	16.73	8.04	0.16	10.29	15.24	0.51	0.80	0.01	2.91	SPH 034
SPH 041	Scalp Hill	263000	374000	Mafic dyke	62.99	0.65	16.01	7.33	0.13	2.25	5.13	1.52	3.72	0.24	1.61	SPH 041
SPH 059	Craigballyharky Quarry			Dolerite	52.13	0.48	17.75	7.05	0.24	6.15	12.04	0.60	4.05	0.04	1.11	SPH 059
SPH 063	Black Rock			Dolerite	50.39	0.73	15.62	9.58	0.25	8.75	10.96	0.38	3.99	0.10	1.16	SPH 063
SPH 185	Bonnety Bush	272636	387449	Pegmatitic gabro	50.72	0.11	17.02	6.49	0.11	10.44	12.88	0.97	1.74	0.01	2.28	SPH 185
SPH 186	Bonnety Bush	272636	387449	Pegmatitic gabro	49.61	0.17	13.35	6.51	0.16	10.67	14.51	0.70	1.11	0.02	2.99	SPH 186
SPH 209	Blaeberry Rock	272995	385210	Tonalitic material	59.68	0.17	18.68	5.74	0.12	4.64	8.05	1.83	3.26	0.03	2.17	SPH 209
SPH 212	Blaeberry Rock	272995	385210	Tonalitic material	64.40	0.41	17.30	5.73	0.10	3.29	5.78	1.53	3.13	0.13	1.99	SPH 212
SPH 214	Blaeberry Rock	272995	385210	Tonalitic material	59.55	0.18	17.70	6.06	0.13	4.72	8.05	1.69	2.79	0.03	3.21	SPH 214
SPH 215	Blaeberry Rock	272995	385210	Tonalitic material	61.61	0.29	12.74	6.52	0.16	5.34	6.65	2.45	2.07	0.07	1.11	SPH 215
SPH 459	Black Rock			Dolerite	52.48	0.50	14.22	9.89	0.16	9.17	10.61	0.27	2.40	0.12		SPH 459
SPH 464	Black Rock	268508	383838	Microgabbro	67.88	0.35	15.64	2.95	0.08	2.18	2.65	0.57	6.78	0.10		SPH 464
SPH 538	Craigballyharky Quarry			Plagiogranite	61.63	0.61	16.19	7.35	0.12	2.14	6.94	1.20	3.06	0.14		SPH 538
SPH 541	Craigballyharky			Basalt	51.10	0.55	14.74	8.96	0.20	6.28	14.14	0.39	3.19	0.06		SPH 541
SPH 552	Black Rock			Volcaniclastics?	79.22	0.17	10.51	1.97	0.03	0.40	2.57	0.28	4.26	0.03		SPH 552
SPH-BR	Black Rock			Pegmatitic gabro	61.96	0.66	14.93	6.83	0.08	3.82	6.49	2.07	2.52	0.12		SPH-BR
SPH-CONT	Blaeberry Rock	272995	385210	Clast	52.51	0.20	8.01	9.88	0.26	14.14	12.51	0.77	0.62	0.03		SPH-CONT
9/83-1A	Carrickmore Quarry			Fine grained dolerite												9/83-1A
9/83-1B	Carrickmore Quarry			Coarse grained dolerite												9/83-1B
9/83-3	Scalp			Gabbro												9/83-3

Note samples with MRC and JTP prefixes are from Cooper et al. (2011)
Grid Reference is Irish Grid

Note samples
Grid Referen

XRF ppm	XRF ppm	XRF ppm	XRF ppm	XRF ppm	XRF ppm	XRF ppm	XRF ppm	XRF ppm	XRF ppm	XRF ppm	XRF ppm	XRF ppm	ICP-MS ppm	ICP-MS ppm	ICP-MS ppm	ICP-MS ppm	ICP-MS ppm	ICP-MS ppm	ICP-MS ppm	ICP-MS ppm	ICP-MS ppm	ICP-MS ppm	ICP-MS ppm	
Sc	**Zr**	**V**	**Cr**	**Co**	**Ni**	**Cu**	**Zn**	**Ga**	**Rb**	**Sr**	**Ba**	**Pb**	**Y**	**Nb**	**Cs**	**La**	**Ce**	**Pr**	**Nd**	**Sm**	**Eu**	**Gd**	**Tb**	**Sample**
29	17	142	98	21	58	587	38	16	12	201	95	1	8.53				2.35	0.40	2.32	0.88	0.36	1.29	0.24	JTP 207
36	3	163	37	48	29	35	48	14	13	120	89	2	4.35				1.52	0.33	1.82	0.45	0.26	0.60	0.10	JTP 211
36	247	389	53	50	14	41	142	20	31	88	142	22	34.25	19.00		20.29	50.12	6.36	28.39	6.48	1.93	7.23	1.17	MRC 129
35	26	240	343	40	151	1	59	13	2	192	49	3	15.53	0.98		1.43	4.35	0.66	3.75	1.81	0.48	2.31	0.40	MRC 340
40	47	283	231	43	116	1	73	16	7	180	84	5	22.30	0.71		2.64	7.26	1.19	6.41	2.38	0.90	3.07	0.52	MRC 343
48	5	134	74	43	65	59	41	9	19	127	188	2	4.35	0.11		0.38	0.95	0.12	0.83	0.44	0.22	0.52	0.09	MRC 344
42	39	264	425	42	191	13	59	15	3	145	38	2	16.83	0.42	0.05	1.77	5.05	0.81	4.25	1.49	0.59	2.11	0.40	SPH 030
45	13	152	103	47	63	37	41	12	15	128	141	2	3.46	0.15	0.19	0.26	0.70	0.12	0.70	0.31	0.18	0.50	0.10	SPH 034
21	161	138	27	16	21	25	51	18	27	397	636	4												SPH 041
36	26	197	521	37	145	16	168	13	12	388	207	9	11.32	0.19	0.33	1.45	3.95	0.64	3.43	1.20	0.62	1.65	0.28	SPH 059
	40	257	306	39	93	16	124	13	5	308	49	4	18.14	0.35	0.08	1.86	5.27	0.88	4.80	1.68	0.62	2.37	0.42	SPH 063
20	17.7	96	296	34	85	12	31	9	31	219	331	3	3.43	0.12	0.65	0.22	0.64	0.11	0.66	0.29	0.09	0.51	0.09	SPH 185
46	15	115	97	36	51	59	36	10	22	135	107	3	5.49	0.07	0.42	0.37	0.82	0.13	0.75	0.35	0.15	0.62	0.12	SPH 186
	38	116	27	16	24	13	51	15	53	199	328	8	6.06	2.70	0.59	3.71	8.55	1.16	4.76	1.12	0.41	1.11	0.16	SPH 209
14	129	157	56	18	23	83	51	17	41	239	330	10	7.98	4.94	0.32	16.10	33.47	3.92	14.08	2.49	0.57	1.83	0.27	SPH 212
	54	122	63	19	35	12	61	15	53	213	313	8	7.18	2.78	0.44	4.70	10.40	1.35	5.58	1.27	0.45	1.26	0.19	SPH 214
	69	127	252	20	62	13	65	15	57	166	532	13	11.88	3.65	0.50	24.61	50.72	6.03	22.89	4.24	1.07	3.25	0.43	SPH 215
	75	227	479	124	122	28	53	15	4	307	34	3												SPH 459
	117	72	86	33	15	8	34	15	13	199	195	6												SPH 464
30	174	136	92	71	11	28	54	16	43	228	367	9	23.11	6.44	2.22	21.42	41.55	5.04	20.28	4.36	1.21	4.18	0.64	SPH 538
34	38	230	511	109	158	23	54	15	*7.5*	*203.7*	63	4	18.36	0.40	0.27	1.48	4.13	0.70	*3.32*	*1.32*	0.59	2.36	0.45	SPH 541
43	93	13	136	19	16	17	5	10	4	147	68	2	33.12	4.37	0.08	5.14	10.59	1.45	6.41	2.14	0.99	3.19	0.63	SPH 552
22	178	173	192	83	48	33	30	16	43	391	763	4	16.45	8.09	0.43	24.59	52.45	5.97	22.45	4.16	1.04	3.41	0.49	SPH-BR
64	18	165	1672	129	142	18	121	11	20	47	143	5	19.09	5.24	0.34	2.64	5.59	0.87	4.10	1.53	0.56	2.18	0.43	SPH-CONT
									39.6	*276.3*									*3.42*	*1.27*				9/83-1A
									36.8	*282.7*									*3.43*	*1.29*				9/83-1B
									1.6	*99.3*									*3.06*	*0.97*				9/83-3

s with MRC and JTP prefixes are from Cooper et al. (2011)

ce is Irish Grid

Note samples

Grid Referen

ICP-MS ppm	ICP-MS ppm	ICP-MS ppm	ICP-MS ppm	ICP-MS ppm	ICP-MS ppm	ICP-MS ppm	ICP-MS ppm	ICP-MS ppm	ICP-MS ppm							
Dy	**Ho**	**Er**	**Tm**	**Yb**	**Lu**	**Hf**	**Ta**	**Th**	**U**	87Sr/86Sr (measured)	**2SE**	**Initital Sr ratios**	**147Sm/ 144Nd**	**143Nd/144 Nd**	**2SE**	**Ep Ndt 480 Ma**
1.61	0.35	1.04	0.15	0.99	0.15	0.57	0.50	0.20								
0.78	0.18	0.57	0.09	0.64	0.10	0.30	0.50	0.46								
7.22	1.42	3.76	0.50	3.12	0.47	5.81	1.03	3.13								
2.80	0.57	1.91	0.27	1.81	0.27	0.95	2.00	0.26								
3.94	0.86	2.77	0.36	2.35	0.36	1.71	2.00	0.23								
0.82	0.19	0.55	0.09	0.50	0.08	0.20	2.00	0.05								
2.68	0.61	1.82	0.28	1.86	0.29	0.89	0.04	0.27	0.10							
0.67	0.15	0.43	0.06	0.43	0.06	0.10	0.01	0.02	0.03							
1.88	0.40	1.17	0.17	1.18	0.18	0.51	0.04	0.19	0.14	0.710800	8	0.710192				
2.82	0.64	1.84	0.28	1.92	0.29	0.91	0.03	0.26	0.13	0.710958	7	0.710639				
0.63	0.14	0.42	0.07	0.43	0.07	0.20	0.02	0.03	0.02							
0.86	0.20	0.59	0.09	0.60	0.09	0.13	0.01	0.02	0.02							
0.94	0.19	0.54	0.09	0.61	0.09	0.52	0.41	1.01	0.46							
1.44	0.27	0.72	0.10	0.67	0.10	0.45	0.43	3.93	0.60							
1.11	0.22	0.63	0.10	0.67	0.10	0.47	0.43	1.27	0.74							
2.33	0.46	1.23	0.18	1.09	0.15	1.34	0.22	5.05	1.14							
3.89	0.82	2.32	0.35	2.27	0.34	2.11	0.13	4.71	1.78							
3.13	0.70	2.09	0.32	2.09	0.32	0.93	0.01	0.28	0.24	0.709807	5	0.709080	0.2400	0.513050	3	5.33
4.46	1.04	3.31	0.54	3.77	0.62	1.99	0.16	2.27	0.50							
2.81	0.56	1.60	0.24	1.61	0.24	3.97	0.22	7.28	1.59							
2.99	0.63	1.84	0.29	1.94	0.27	0.32	0.25	0.46	0.35							
										0.711583	4	0.708744	0.2257	0.513001	4	5.30
										0.711087	5	0.708507	0.2268	0.513006	4	5.33
										0.704223	5	0.703901	0.1910	0.512934	4	6.12

s with MRC and JTP prefixes are from Cooper et al. (2011)
ce is Irish Grid

Supplementary Data Table 2: Mineral chemical data
Chlorite

		Wt.% oxide:										
Sample	**Analysis**	**SiO2**	**TiO2**	**Al2O3**	**FeO**	**MnO**	**MgO**	**CaO**	**Na2O**	**K2O**	**BaO**	**F**
SPH34	PB-51	29.28	0.02	21.73	14.62	0.24	23.93	0.11	0.01	0.01	0.00	0.00
SPH34	PB-52	30.42	0.01	22.15	12.40	0.18	22.37	0.03	0.03	0.78	0.01	0.00
SPH34	PB-53	28.72	0.01	21.14	14.29	0.24	23.50	0.06	0.01	0.01	0.00	0.00
SPH215	PB-77	27.12	0.05	20.36	20.37	0.40	18.50	0.05	0.01	0.13	0.00	0.00
SPH215	PB-78	28.18	0.08	19.76	20.97	0.36	19.12	0.03	0.01	0.09	0.00	0.00

					Atoms based on 28 oxygens:								
Cr2O3	**NiO**	**V2O3**	**P2O5**	**CoO**	**Si**	**Al(IV)**	**Al(VI)**	**Mg**	**Ca**	**K**	**Mn**	**Fe**	**Fe/Fe+Mg**
0.01	0.04	0.00	0.00	0.02	5.63	2.37	2.57	6.86	0.02	0.00	0.04	2.35	0.26
0.00	0.03	0.00	0.00	0.01	5.84	2.16	2.90	6.40	0.01	0.38	0.03	1.99	0.24
0.00	0.06	0.02	0.00	0.03	5.65	2.35	2.55	6.89	0.01	0.01	0.04	2.35	0.25
0.15	0.08	0.04	0.01	0.04	5.59	2.41	2.54	5.68	0.01	0.07	0.07	3.51	0.38
0.02	0.04	0.06	0.02	0.00	5.71	2.29	2.44	5.77	0.01	0.05	0.06	3.55	0.38

Geothermometers:

Zhang & Fyfe (1995)	Kranidiotis & MacLean (1987)
234.64	596.41
232.95	591.30
234.56	596.16
246.47	632.28
246.38	632.02

Supplementary Data Table 2: Mineral chemical data

Epidote		Weight % oxide											
Sample	**Analysis number**	**SiO2**	**TiO2**	**Al2O3**	**FeO**	**MnO**	**MgO**	**CaO**	**Na2O**	**K2O**	**P2O5**	**Cr2O3**	**CoO**
SPH34	PB-84	38.64	0.00	28.42	6.25	0.14	0.02	23.81	0.02	0.00	0.01	0.00	0.00
SPH34	PB-89	40.83	0.00	31.29	2.12	0.06	0.03	22.95	0.60	0.04	0.02	0.00	0.00
SPH34	PB-91	39.15	0.03	29.39	5.17	0.03	0.01	23.98	0.02	0.04	0.02	0.00	0.00
SPH34	PB-79	39.07	0.01	28.69	5.95	0.04	0.03	24.07	0.06	0.05	0.01	0.00	0.00
SPH34	PB-81	38.78	0.09	26.22	9.07	0.15	0.03	23.49	0.01	0.00	0.03	0.00	0.00
SPH34	PB-90	39.51	0.04	29.00	5.55	0.05	0.02	23.47	0.19	0.08	0.06	0.01	0.00
SPH34	PB-82	39.20	0.00	29.33	5.64	0.03	0.01	24.14	0.00	0.01	0.03	0.01	0.00
SPH34	PB-85	38.95	0.01	29.46	5.19	0.06	0.03	24.38	0.00	0.02	0.03	0.00	0.00
SPH34	PB-88	41.78	0.01	31.16	1.78	0.10	0.03	22.40	0.96	0.01	0.02	0.00	0.00
SPH34	PB-80	38.09	0.16	24.98	10.09	0.09	0.03	23.65	0.03	0.00	0.01	0.00	0.02
SPH34	PB-83	38.76	0.02	26.19	9.29	0.07	0.02	23.78	0.00	0.01	0.02	0.00	0.00
SPH34	PB-86	34.53	0.04	25.64	8.30	0.08	3.49	18.97	0.03	0.00	0.00	0.01	0.00
SPH34	PB-87	39.09	0.01	29.99	4.64	0.09	0.04	24.05	0.00	0.00	0.04	0.00	0.00
SPH210	PB-109	38.26	0.06	24.38	11.18	0.10	0.08	23.67	0.00	0.00	0.01	0.02	0.00
SPH210	PB-110	38.15	0.04	24.75	10.85	0.14	0.03	23.64	0.01	0.00	0.02	0.02	0.01
SPH210	PB-111	37.63	0.23	22.94	12.49	0.27	0.04	23.30	0.02	0.01	0.03	0.01	0.00
SPH215	PB-112	42.16	0.06	25.89	8.61	0.10	0.53	18.94	0.04	1.95	0.01	0.07	0.01
SPH215	PB-115	36.62	0.11	23.10	10.98	0.11	0.01	23.00	0.00	0.00	0.02	0.26	0.00
SPH215	PB-117	38.15	1.67	22.08	12.65	0.08	0.03	23.31	0.02	0.02	0.03	0.05	0.00
SPH215	PB-113	38.24	0.04	25.40	9.72	0.11	0.03	23.38	0.00	0.00	0.05	0.03	0.00
SPH215	PB-114	38.00	0.04	23.51	11.89	0.18	0.16	22.72	0.01	0.00	0.03	0.10	0.01
SPH215	PB-116	37.91	0.04	23.75	11.56	0.15	0.08	22.94	0.01	0.00	0.01	0.10	0.01

					Atoms (after 12.5 oxygens)								
NiO	**F**	**Ce2O3**	**BaO**	**V2O3**	**Si**	**Ti**	**Al**	**Fe3+**	**Mn**	**Mg**	**Ca**	**Na**	**K**
0.02	0.00	0.00	0.00	0.01	3.00	0.00	2.60	0.41	0.01	0.00	1.98	0.00	0.00
0.00	0.00	0.02	0.01	0.00	3.09	0.00	2.79	0.13	0.00	0.00	1.86	0.09	0.00
0.02	0.00	0.00	0.00	0.01	3.01	0.00	2.66	0.33	0.00	0.00	1.98	0.00	0.00
0.02	0.00	0.00	0.00	0.00	3.01	0.00	2.60	0.38	0.00	0.00	1.99	0.01	0.00
0.01	0.00	0.00	0.00	0.02	3.02	0.01	2.40	0.59	0.01	0.00	1.96	0.00	0.00
0.00	0.00	0.00	0.00	0.02	3.03	0.00	2.62	0.36	0.00	0.00	1.93	0.03	0.01
0.01	0.00	0.00	0.00	0.00	3.00	0.00	2.65	0.36	0.00	0.00	1.98	0.00	0.00
0.01	0.00	0.00	0.00	0.00	2.99	0.00	2.67	0.33	0.00	0.00	2.01	0.00	0.00
0.01	0.00	0.01	0.00	0.00	3.15	0.00	2.77	0.11	0.01	0.00	1.81	0.14	0.00
0.01	0.00	0.00	0.00	0.01	3.00	0.01	2.32	0.66	0.01	0.00	2.00	0.00	0.00
0.00	0.00	0.00	0.00	0.01	3.01	0.00	2.40	0.60	0.00	0.00	1.98	0.00	0.00
0.03	0.00	0.00	0.00	0.03	2.87	0.00	2.51	0.58	0.01	0.43	1.69	0.00	0.00
0.02	0.00	0.01	0.00	0.00	3.00	0.00	2.71	0.30	0.01	0.00	1.98	0.00	0.00
0.00	0.00	0.00	0.00	0.05	3.00	0.00	2.25	0.73	0.01	0.01	1.99	0.00	0.00
0.01	0.00	0.00	0.00	0.03	2.99	0.00	2.29	0.71	0.01	0.00	1.99	0.00	0.00
0.03	0.00	0.00	0.00	0.04	2.99	0.01	2.15	0.83	0.02	0.00	1.99	0.00	0.00
0.00	0.00	0.00	0.00	0.08	3.22	0.00	2.33	0.55	0.01	0.06	1.55	0.01	0.19
0.02	0.00	0.00	0.00	0.03	3.00	0.01	2.23	0.75	0.01	0.00	2.02	0.00	0.00
0.01	0.00	0.00	0.00	0.07	3.00	0.10	2.05	0.83	0.01	0.00	1.97	0.00	0.00
0.01	0.00	0.00	0.00	0.06	3.01	0.00	2.36	0.64	0.01	0.00	1.97	0.00	0.00
0.00	0.00	0.00	0.00	0.04	3.02	0.00	2.20	0.79	0.01	0.02	1.93	0.00	0.00
0.00	0.00	0.00	0.00	0.04	3.01	0.00	2.23	0.77	0.01	0.01	1.95	0.00	0.00

Supplementary Data Table 2: Mineral chemical data

Amphibole		Wt.% oxide												
Sample	**Analysis**	**SiO2**	**TiO2**	**Al2O3**	**FeO**	**MnO**	**MgO**	**CaO**	**Na2O**	**K2O**	**P2O5**	**BaO**	**NiO**	**CoO**
SPH34	PB-125	53.68	0.05	4.10	7.12	0.18	19.35	12.29	0.47	0.06	0.02	0.00	0.01	0.02
SPH34	PB-126	56.02	0.06	2.23	5.96	0.19	20.75	12.38	0.26	0.05	0.00	0.00	0.03	0.01
SPH34	PB-127	55.39	0.03	2.92	5.79	0.20	20.89	12.37	0.41	0.01	0.02	0.00	0.01	0.02
SPH34	PB-129	52.96	0.45	4.54	7.81	0.18	18.61	12.51	0.55	0.07	0.00	0.00	0.01	0.02
SPH34	PB-130	55.13	0.08	1.74	9.88	0.27	18.05	11.82	0.26	0.03	0.02	0.00	0.02	0.00
SPH210	PB-131	54.61	0.00	3.02	8.16	0.35	18.44	12.82	0.35	0.09	0.02	0.00	0.07	0.00
SPH210	PB-132	54.03	0.08	3.93	9.00	0.33	17.58	12.52	0.43	0.23	0.02	0.00	0.09	0.00
SPH210	PB-133	52.70	0.03	4.79	9.71	0.35	17.11	12.44	0.54	0.33	0.02	0.01	0.07	0.00
SPH215	PB-134	48.38	0.42	6.91	14.53	0.46	13.51	12.10	0.77	0.57	0.01	0.00	0.02	0.01
SPH215	PB-135	48.43	0.35	8.14	14.05	0.41	11.61	11.06	0.74	1.67	0.04	0.03	0.04	0.00
SPH215	PB-136	48.63	0.38	7.20	14.46	0.44	13.61	12.01	0.80	0.55	0.02	0.00	0.03	0.01
SPH215	PB-137	49.29	0.37	6.51	14.11	0.42	13.89	12.20	0.79	0.47	0.02	0.00	0.02	0.02
SPH215	PB-138	49.26	0.38	6.97	14.60	0.42	13.43	11.99	0.79	0.58	0.00	0.00	0.02	0.00
SPH215	PB-139	46.77	0.35	6.81	14.12	0.40	13.09	11.89	0.74	0.57	0.00	0.00	0.01	0.00
SPH215	PB-140	48.64	0.37	7.03	14.59	0.42	13.18	12.20	0.91	0.51	0.03	0.00	0.00	0.00
SPH215	PB-141	48.64	0.40	6.86	14.48	0.41	13.46	12.20	0.86	0.52	0.02	0.00	0.01	0.00
SPH215	PB-142	48.35	0.37	7.39	14.52	0.44	13.48	12.02	0.86	0.62	0.01	0.00	0.02	0.01
SPH215	PB-118	47.30	0.41	7.31	14.65	0.43	13.00	12.07	0.82	0.63	0.03	0.00	0.00	0.01
SPH215	PB-119	46.73	0.65	8.00	14.80	0.41	12.83	11.97	0.81	0.62	0.02	0.01	0.01	0.00
SPH215	PB-120	47.75	0.40	7.48	14.84	0.43	13.02	12.02	0.84	0.66	0.02	0.00	0.02	0.00
SPH215	PB-121	47.87	0.39	7.10	14.72	0.44	13.10	12.06	0.79	0.61	0.02	0.00	0.02	0.00
SPH215	PB-122	48.11	0.41	7.23	14.80	0.44	13.19	12.09	0.81	0.62	0.01	0.00	0.03	0.01
SPH215	PB-123	46.38	0.49	8.54	15.55	0.40	12.35	11.91	0.98	0.78	0.03	0.02	0.02	0.00

V2O3	Cr2O3	Ce2O3	F	Atoms after 23 oxygens Si	Al iv	Al vi	Ti	Cr	Fe3+	Fe2+	Mn	Mg	Ca	Na
0.02	0.01	0.00	0.00	7.46	0.54	0.13	0.01	0.00	0.60	0.23	0.02	4.01	1.83	0.13
0.01	0.01	0.00	0.03	7.68	0.32	0.04	0.01	0.00	0.55	0.14	0.02	4.24	1.82	0.07
0.01	0.00	0.02	0.00	7.58	0.42	0.05	0.00	0.00	0.63	0.03	0.02	4.26	1.81	0.11
0.03	0.02	0.00	0.02	7.40	0.60	0.14	0.05	0.00	0.46	0.45	0.02	3.87	1.87	0.15
0.05	0.01	0.00	0.01	7.73	0.27	0.02	0.01	0.00	0.60	0.56	0.03	3.77	1.78	0.07
0.00	0.00	0.00	0.07	7.65	0.35	0.15	0.00	0.00	0.25	0.71	0.04	3.85	1.92	0.10
0.02	0.00	0.00	0.14	7.57	0.43	0.22	0.01	0.00	0.28	0.77	0.04	3.67	1.88	0.12
0.01	0.03	0.00	0.12	7.42	0.58	0.21	0.00	0.00	0.40	0.74	0.04	3.59	1.88	0.15
0.08	0.03	0.00	0.07	7.02	0.98	0.20	0.05	0.00	0.59	1.17	0.06	2.92	1.88	0.22
0.04	0.01	0.00	0.01	7.18	0.82	0.60	0.04	0.00	0.10	1.64	0.05	2.56	1.76	0.21
0.05	0.01	0.01	0.07	7.01	0.99	0.23	0.04	0.00	0.64	1.10	0.05	2.92	1.85	0.22
0.05	0.08	0.00	0.04	7.11	0.89	0.21	0.04	0.01	0.52	1.18	0.05	2.98	1.88	0.22
0.06	0.13	0.00	0.07	7.08	0.92	0.26	0.04	0.01	0.55	1.21	0.05	2.88	1.85	0.22
0.06	0.14	0.00	0.07	7.00	1.00	0.20	0.04	0.02	0.56	1.20	0.05	2.92	1.91	0.21
0.06	0.13	0.00	0.07	7.06	0.94	0.27	0.04	0.01	0.43	1.34	0.05	2.85	1.90	0.26
0.06	0.06	0.01	0.05	7.06	0.94	0.23	0.04	0.01	0.49	1.27	0.05	2.91	1.90	0.24
0.06	0.03	0.00	0.07	6.98	1.02	0.24	0.04	0.00	0.61	1.14	0.05	2.90	1.86	0.24
0.05	0.14	0.00	0.07	6.96	1.04	0.23	0.05	0.02	0.55	1.26	0.05	2.85	1.90	0.23
0.05	0.02	0.01	0.10	6.86	1.14	0.25	0.07	0.00	0.63	1.19	0.05	2.81	1.88	0.23
0.06	0.11	0.00	0.03	6.96	1.04	0.25	0.04	0.01	0.58	1.23	0.05	2.83	1.88	0.24
0.06	0.07	0.01	0.05	7.01	0.99	0.23	0.04	0.01	0.55	1.25	0.05	2.86	1.89	0.22
0.05	0.12	0.00	0.09	6.99	1.01	0.23	0.04	0.01	0.57	1.23	0.05	2.86	1.88	0.23
0.05	0.06	0.00	0.07	6.80	1.20	0.28	0.05	0.01	0.63	1.27	0.05	2.70	1.87	0.28

K	Ba	F	OH*	Total
0.01	0.00	0.00	2.00	16.97
0.01	0.00	0.01	1.99	16.90
0.00	0.00	0.00	2.00	16.92
0.01	0.00	0.01	1.99	17.03
0.01	0.00	0.00	2.00	16.85
0.02	0.00	0.03	1.97	17.03
0.04	0.00	0.06	1.94	17.04
0.06	0.00	0.05	1.95	17.08
0.11	0.00	0.03	1.97	17.20
0.32	0.00	0.00	2.00	17.29
0.10	0.00	0.03	1.97	17.18
0.09	0.00	0.02	1.98	17.19
0.11	0.00	0.03	1.97	17.17
0.11	0.00	0.03	1.97	17.23
0.09	0.00	0.03	1.97	17.25
0.10	0.00	0.02	1.98	17.23
0.11	0.00	0.03	1.97	17.21
0.12	0.00	0.03	1.97	17.25
0.12	0.00	0.05	1.95	17.23
0.12	0.00	0.01	1.99	17.24
0.11	0.00	0.02	1.98	17.23
0.11	0.00	0.04	1.96	17.23
0.15	0.00	0.03	1.97	17.30

Supplementary Data Table 2: Mineral chemical data

Feldspar		Wt.% Oxide:											
Sample	**Analysis**	**SiO2**	**TiO2**	**Al2O3**	**FeO**	**MnO**	**MgO**	**CaO**	**BaO**	**Na2O**	**K2O**	**Ce2O3**	**P2O5**
SPH215	PB-153	64.79	0.00	18.74	0.20	0.01	0.02	0.00	0.46	0.46	16.57	0.17	0.00
SPH215	PB-154	64.30	0.01	18.58	0.06	0.01	0.00	0.00	0.61	0.38	16.63	0.21	0.00
SPH215	PB-155	64.45	0.00	19.18	0.06	0.00	0.00	0.25	0.71	1.76	13.73	0.25	0.00
SPH215	PB-156	63.76	0.02	19.09	0.07	0.00	0.00	0.00	1.42	0.57	16.04	0.53	0.00
SPH215	PB-157	64.27	0.00	18.76	0.06	0.01	0.01	0.02	0.65	0.61	16.33	0.21	0.00
SPH215	PB-158	64.50	0.00	18.70	0.03	0.00	0.00	0.00	0.68	0.64	16.36	0.26	0.00
SPH215	PB-159	62.99	0.03	19.98	0.43	0.01	0.37	0.00	0.58	0.35	15.74	0.22	0.00
SPH215	PB-160	64.06	0.01	18.47	0.05	0.00	0.00	0.00	0.49	0.40	16.59	0.18	0.01
SPH215	PB-161	64.81	0.00	18.92	0.05	0.01	0.00	0.00	0.71	0.78	16.05	0.23	0.03
SPH215	PB-162	64.15	0.02	19.07	0.03	0.00	0.01	0.00	1.25	0.65	15.80	0.47	0.00
SPH215	PB-163	64.66	0.00	18.63	0.06	0.00	0.00	0.00	0.50	0.43	16.44	0.20	0.00
SPH215	PB-164	64.74	0.00	18.69	0.16	0.00	0.00	0.00	0.55	0.43	16.64	0.19	0.00
SPH215	PB-165	64.55	0.00	18.76	0.04	0.00	0.01	0.00	0.80	0.37	16.43	0.27	0.01
SPH215	PB-166	64.82	0.00	18.82	0.04	0.00	0.00	0.00	0.55	0.64	16.36	0.18	0.01
SPH215	PB-167	63.86	0.01	18.88	0.07	0.00	0.00	0.01	1.23	0.58	16.08	0.44	0.01
SPH215	PB-168	65.10	0.00	18.88	0.06	0.00	0.01	0.00	0.62	0.41	16.30	0.20	0.01
SPH215	PB-169	63.28	0.02	18.44	0.07	0.00	0.01	0.00	0.47	0.46	16.44	0.19	0.00
SPH215	PB-170	64.79	0.01	18.75	0.04	0.01	0.00	0.00	0.51	0.48	16.48	0.17	0.02
SPH215	PB-242	54.71	0.00	29.05	0.14	0.00	0.00	10.85	0.00	5.61	0.12	0.00	0.03
SPH215	PB-243	58.18	0.00	27.08	0.17	0.00	0.00	8.53	0.00	7.13	0.17	0.00	0.04
SPH215	PB-244	55.73	0.01	28.50	0.16	0.00	0.00	10.24	0.02	5.87	0.21	0.00	0.01
SPH215	PB-245	57.43	0.00	26.69	0.14	0.00	0.01	8.44	0.01	6.99	0.19	0.00	0.02
SPH215	PB-246	57.60	0.00	26.89	0.16	0.01	0.00	8.75	0.00	6.67	0.30	0.02	0.01
SPH215	PB-247	58.26	0.00	26.95	0.11	0.00	0.00	8.46	0.00	6.97	0.15	0.00	0.00

Atoms:													End Member	
Si	**Ti**	**Al**	**Cr**	**Fe3**	**Fe2**	**Mn**	**Mg**	**Ca**	**Ba**	**Na**	**K**	**Total Oxy**	**An**	**Ab**
2.96	0.00	1.01	0.00	0.00	0.01	0.00	0.00	0.00	0.01	0.04	0.97	7.97	0.00	4.05
2.96	0.00	1.01	0.00	0.00	0.00	0.00	0.00	0.00	0.01	0.03	0.98	7.96	0.00	3.36
2.97	0.00	1.04	0.00	0.00	0.00	0.00	0.00	0.01	0.01	0.16	0.81	8.01	1.26	16.10
2.94	0.00	1.04	0.00	0.00	0.00	0.00	0.00	0.00	0.03	0.05	0.94	7.96	0.00	5.12
2.96	0.00	1.02	0.00	0.00	0.00	0.00	0.00	0.00	0.01	0.05	0.96	7.96	0.10	5.37
2.96	0.00	1.01	0.00	0.00	0.00	0.00	0.00	0.00	0.01	0.06	0.96	7.96	0.00	5.61
2.90	0.00	1.09	0.00	0.00	0.02	0.00	0.03	0.00	0.01	0.03	0.93	7.97	0.00	3.27
2.97	0.00	1.01	0.00	0.00	0.00	0.00	0.00	0.00	0.01	0.04	0.98	7.96	0.00	3.53
2.96	0.00	1.02	0.00	0.00	0.00	0.00	0.00	0.00	0.01	0.07	0.94	7.97	0.00	6.88
2.95	0.00	1.03	0.00	0.00	0.00	0.00	0.00	0.00	0.02	0.06	0.93	7.98	0.00	5.88
2.98	0.00	1.01	0.00	0.00	0.00	0.00	0.00	0.00	0.01	0.04	0.96	7.98	0.00	3.82
2.96	0.00	1.01	0.00	0.00	0.01	0.00	0.00	0.00	0.01	0.04	0.97	7.96	0.00	3.78
2.97	0.00	1.02	0.00	0.00	0.00	0.00	0.00	0.00	0.01	0.03	0.96	7.98	0.00	3.31
2.96	0.00	1.01	0.00	0.00	0.00	0.00	0.00	0.00	0.01	0.06	0.95	7.97	0.00	5.61
2.95	0.00	1.03	0.00	0.00	0.00	0.00	0.00	0.00	0.02	0.05	0.95	7.96	0.05	5.19
2.98	0.00	1.02	0.00	0.00	0.00	0.00	0.00	0.00	0.01	0.04	0.95	7.99	0.00	3.68
2.95	0.00	1.01	0.00	0.00	0.00	0.00	0.00	0.00	0.01	0.04	0.98	7.95	0.00	4.08
2.97	0.00	1.01	0.00	0.00	0.00	0.00	0.00	0.00	0.01	0.04	0.96	7.97	0.00	4.24
2.45	0.00	1.53	0.00	0.00	0.01	0.00	0.00	0.52	0.00	0.49	0.01	7.97	51.31	48.01
2.56	0.00	1.41	0.00	0.00	0.01	0.00	0.00	0.40	0.00	0.61	0.01	7.96	39.43	59.64
2.49	0.00	1.50	0.00	0.00	0.01	0.00	0.00	0.49	0.00	0.51	0.01	7.98	48.50	50.31
2.57	0.00	1.41	0.00	0.00	0.01	0.00	0.00	0.40	0.00	0.61	0.01	7.96	39.60	59.34
2.57	0.00	1.41	0.00	0.00	0.01	0.00	0.00	0.42	0.00	0.58	0.02	7.98	41.32	57.00
2.58	0.00	1.41	0.00	0.00	0.00	0.00	0.00	0.40	0.00	0.60	0.01	7.98	39.81	59.35

s:

Or

95.95
96.64
82.64
94.88
94.54
94.39
96.73
96.47
93.12
94.12
96.18
96.22
96.69
94.39
94.76
96.32
95.92
95.76
0.68
0.94
1.18
1.06
1.69
0.84

Table 3. *U-Th-Pb isotopic data for sample MRC344.*

	Compositional Parameters						Radiogenic Isotope Ratios								Isotopic Ages					
Sample *	$\frac{Th}{U}$ †	$^{206}Pb^*$ x10-13 mol §	mol % $^{206}Pb^*$ §	$\frac{Pb^*}{Pbc}$ §	Pbc (pg) §	$\frac{^{206}Pb}{^{204}Pb}$ #	$\frac{^{208}Pb}{^{206}Pb}$ **	$\frac{^{207}Pb}{^{206}Pb}$ **	% err ††	$\frac{^{207}Pb}{^{235}U}$ **	% err ††	$\frac{^{206}Pb}{^{238}U}$ **	% err ††	corr. coef.	$\frac{^{207}Pb}{^{206}Pb}$ §§	± ††	$\frac{^{207}Pb}{^{235}U}$ §§	± ††	$\frac{^{206}Pb}{^{238}U}$ §§	± ††
z1	0.627	8.4572	99.92%	380	0.58	22342	0.197	0.05689	0.17	0.6108	0.22	0.077865	0.100	0.694	486.91	3.76	484.05	0.86	**483.44**	**0.47**
z2	0.353	2.8468	99.76%	120	0.57	7597	0.111	0.05683	0.11	0.6100	0.19	0.077845	0.090	0.932	484.54	2.41	483.55	0.72	**483.34**	**0.42**
z3	0.407	2.0402	99.71%	103	0.48	6432	0.127	0.05683	0.12	0.6109	0.20	0.077961	0.088	0.909	484.52	2.70	484.12	0.76	**484.03**	**0.41**
z5	0.423	1.8008	98.47%	19	2.38	1118	0.133	0.05692	0.21	0.6116	0.30	0.077926	0.117	0.852	488.01	4.62	484.55	1.16	**483.82**	**0.54**
z6	0.787	3.7671	99.63%	88	1.15	4969	0.246	0.05685	0.14	0.6126	0.34	0.078162	0.277	0.915	485.25	3.06	485.22	1.30	485.22	1.30
z7	0.416	3.1163	99.92%	388	0.20	24071	0.130	0.05681	0.09	0.6103	0.17	0.077916	0.087	0.959	483.75	2.00	483.76	0.66	**483.76**	**0.40**

* z1, z2 etc. are labels for fractions composed of single zircon grains or fragments; all fractions annealed and chemically abraded after Mattinson (2005).
† Model Th/U ratio calculated from radiogenic $^{208}Pb/^{206}Pb$ ratio and $^{207}Pb/^{235}U$ age.
§ Pb* and Pbc represent radiogenic and common Pb, respectively; mol % $^{206}Pb^*$ with respect to radiogenic, blank and initial common Pb.
# Measured ratio corrected for spike and fractionation only.
** Corrected for fractionation, spike, and common Pb; up to 2 pg of common Pb was assumed to be procedural blank: $^{206}Pb/^{204}Pb = 18.60 \pm 0.80\%$; $^{207}Pb/^{204}Pb = 15.69 \pm 0.32\%$; $^{208}Pb/^{204}Pb = 38.51 \pm 0.74\%$ (all uncertainties 1-sigma). Excess over blank was assigned to initial common Pb.
†† Errors are 2-sigma, propagated using the algorithms of Schmitz and Schoene (2007).
§§ Calculations are based on the decay constants of Jaffey et al. (1971). $^{206}Pb/^{238}U$ and $^{207}Pb/^{206}Pb$ ages corrected for initial disequilibrium in $^{230}Th/^{238}U$ using Th/U [magma] = 3 using the algorithms of Schärer (1984).
Dates in bold are those included in weighted mean calculations. See text for discussion.